

The Propulsion Committee

Final Report and Recommendations to the 22nd ITTC

1. GENERAL

1.1 Membership and Meetings

The members of the Propulsion Committee of the 22nd ITTC are as follows:

B. Gindroz
T. Hoshino
J. Holtrop (from September 1997)
S. D. Jessup
J. T. Ligtelijn (to June 1997)
F. Mewis
A. Poustoshniy
J. V. Pylkkanen
G.-Q. Wang

J. T. Ligtelijn was elected Chairman by the conference. J. T. Ligtelijn moved from MARIN and resigned from the committee. J. V. Pylkkanen was elected Chairman by the Executive Committee. S. D. Jessup was elected Secretary by the Committee.

The meetings of the committee were held as follows:

Shanghai, China, January, 1997 (7)
Val de Reuil, France, September, 1997 (8)
Grenoble, France, April, 1998 (8)
San Diego, USA, November, 1998 (8)

A workshop on Panel methods and RANS computations was held in conjunction with the third meeting in Grenoble, France.

1.2 Recommendations of the 21st ITTC

The recommendations for the work of the propulsion Committee as given by the 21st ITTC were as follows:

1. Review the state of the art, comment on the potential impact of new developments on ITTC, and identify the need for research and development in the areas of propulsors, cavitation and powering performance. Monitor and follow the development of new experimental techniques and extrapolation methods.
2. Review the ITTC recommended procedures, benchmark data, and test cases for validation and uncertainty analyses and update as required. Pass the information to the quality systems group for publication in 1999.
3. Identify the requirements for new procedures, benchmark data, validation, uncertainty analysis and stimulate the necessary research for their preparation.
4. Prepare an up-to-date bibliography of relevant technical papers and reports.
5. Review the development of the design and analysis methods for propulsors with special emphasis on modeling of the vortex wake. The committee should consider repeating the 18th ITTC comparative exercise.
6. Review research on the performance of propellers in various conditions such as for ships when turning, accelerating,



decelerating, backing, or operating in waves.

7. Review available LDV data for propulsors.
8. Review the correlation of water quality (liquid tension and nuclei distribution) with cavitation inception and the stability of cavitation patterns. Cavitation experimental techniques should be reviewed to predict cavitation behavior more accurately. The effects of turbulence and propeller blade roughness should be taken into account.

1.3 General Remarks

The present Propulsion Committee was formed by combining the previous Propulsor, Cavitation, and Powering Performance Committees. This change is reflected in the tasks given to the 22nd ITTC Propulsion Committee.

The formulation of Tasks 1 and 3 left some freedom in selecting the topics to be dealt with in these tasks. New developments in extrapolation methods are reviewed in Task 1, whilst Task 3 focuses on the fact that the diversity in powering performance procedures has widened instead of converging to one or two high quality standard methods. A component-wise improvement of scaling procedures is outlined.

The bibliography of relevant technical paper and reports was updated. Because of the page allowance and the wide interest area of the Propulsion Committee, the list of recent relevant symposia is not included in this report. Similarly the tables depicting the frequency of the keywords are not included.

In addition to the customary review of the development and analysis methods for propulsors, the Propulsion Committee organised a workshop on RANS/Panel methods. Because of the abundance of the material in the workshop papers, the results of the workshop are presented in a separate section.

The application of LDV to propeller flows has continued. A review of particle image velocimetry (PIV) measurement techniques is included in this section. In the future the review of LDV and PIV applications to propulsor and propulsion related flows can possibly be included in the general Task 1.

2. REVIEW THE STATE OF THE ART, COMMENT ON THE POTENTIAL IMPACT OF NEW DEVELOPMENTS ON ITTC, AND IDENTIFY THE NEED FOR RESEARCH AND DEVELOPMENT IN THE AREAS OF PROPULSORS, CAVITATION AND POWERING PERFORMANCE. MONITOR AND FOLLOW THE DEVELOPMENT OF NEW EXPERIMENTAL TECHNIQUES AND EXTRAPOLATION METHODS.

2.1 Introduction

The formulation of Tasks 1 left some freedom in selecting the topics to be dealt with in these tasks. The Propulsion Committee decided to review the developments in new blade sections, optimisation techniques for propulsor design, powering performance prediction, and interpretation of model tests for azimuthing thrusters in Task 1. Additionally a draft on uncertainty analysis was prepared, but had to be left out of the report because of the page allowance specified for committee reports.

2.2 New Blade Sections

New blade section design was reviewed in considerable detail by the 19th ITTC Propulsor Committee (1990). Most approaches were based around the method of Eppler (1980). Since that time a number of papers have demonstrated the application of new blade sections including full scale demonstrations. Also, alternative methods to Eppler have been developed. The primary application is in the delay of cavitation inception, but some efforts to reduce cavitation induced hull pressures have been pursued.

Jessup et al. (1994) presented application and full scale demonstration of Eppler type sections to a naval CP propeller for the increase of cavitation inception speed. Using the procedure of Shen and Eppler (1981) ten individual two-dimensional sections were designed and incorporated into the propeller by specifying the chordwise 2-D loading distribution into lifting surface calculations. The 2-D thickness forms were used directly into the propeller geometry. Numerous 2-D sections designed across the blade span required careful cross fairing of lifting surface input parameters. Panel methods were used to analyse the final blade pressure distributions. At the maximum blade loading condition, the suction side

pressure distribution was designed to be flat with the steepest pressure recovery allowable to avoid trailing edge separation. Model and full scale results showed significant improvements in blade surface cavitation inception and reduction in thrust breakdown over the original propeller with standard NACA blade sections.

Jessup et al. (1997) incorporated similar new blade sections into a high speed patrol boat propeller. Again, flat Eppler-type pressure distributions were obtained at maximum loading. Blade sections were significantly modified using iterative analysis with panel methods. Model and full scale tests were conducted showing predominance of small bubble cavitation, associated with the leading edge unloading and designed flat pressure distributions. Testing showed that the small bubble blade surface cavitation was not inherently noisy or erosive, as has previously been thought.

Scherer and Stairs (1994) presented a new method of section design for the increase of cavitation inception speeds. Linear theory with modifications for second order accuracy were used to calculate section pressure distributions. By parameterizing various loading and thickness distributions along the chord, a family of sections was generated and tabulated in the paper. By combining the thickness and camber forms, a variety of sections can be created with specified favorable performance. Section comparisons were made with the classical Shen and Eppler sections showing similar performance. An advantage of this approach was the ability to easily cross fair sections by interpolating the original foil parameters. Also, the procedure is adaptable to blunt base section design.

Cox et al. (1997) presented a 2-D foil design and evaluation of blunt based sections. Using Scherer and Stairs (1994) approach, blunt base sections were designed to improve cavitation performance over sections with sharp trailing edges. 2-D water tunnel tests were performed to validate the blunt base section design approach and determine the performance comparison to sharp trailing edge foils. Tests showed improvements in cavitation performance over the sharp edged foils, with a drag increase consistent with previous test results. The measured lift using LDV was lower than predictions. The cause was thought to be due to the tunnel blockage effects from a relatively large foil mounted in a closed jet square cross-sectional water tunnel.

Praefke (1997) presented a design exercise to develop a new section propeller to reduce propeller induced hull pressures. Eppler method was used to design alternative thickness and camber forms incorporated into two new designs. The new camber was reduced near the leading edge and increased aft of mid-chord. The new thickness form was thinner at the nose and thicker aft of mid chord. To compensate for the changes in the blade sections, the new propellers incorporated reduced pitch and increased maximum sectional camber. One new model propeller was built with only the new camber form and the second new propeller was built with both the new camber and thickness form. Open water and cavitation tests were performed on the original standard section propeller and the two new propellers. Also, load and cavitation predictions were made with PUF3. Predictions and test results showed 1.5% decrease in efficiency. Propeller induced hull pressures were decreased with the new designs, but the increased aft chord camber appeared to create an unusual midchord cavitation near the tip, that was somewhat predicted with the PUF3.

Alexandrov (1981) developed a cavitating hydrofoil analysis procedure which later became the basis for a section design method. The constant pressure cavity boundary condition inherently resulted in smooth sectional pressure distributions. Cavitation around a foil section was calculated using the surface singularity method for non-linear potential flow. An iterative scheme was developed to generate the coordinates of the cavity shape. A vortex distribution was used to satisfy the kinematic boundary condition, initially as a fully wetted hydrofoil. The dynamic boundary condition of constant velocity along the cavity was satisfied by a source distribution on the foil profile including the surface of cavity. The boundary of cavity was determined by iterative method. An inclined flat plate cavity closure model was incorporated by a method of Ivanov (1980). Later the method was modified for the cascade profiles by Semionicheva (1986) and supercavitating profiles by Pozharsky (1986).

Further development were made by Aleksandrov (1994) presenting an iterative decoupled solution method, based on the solution of the mixed-inverse problem. This permitted optimisation of profiles over a range of operational angles of attack. Design examples demonstrated that small changes of the leading edge resulted in considerable

change in cavity performance. Also, the design cycle was short enough to permit custom section design for each application.

An application of Alexandrov's method was described by Poustoushniy (1996), experimentally verifying improvements in cavitation characteristics of propulsors of different types at bollard pull and positioning mode. Two series of profiles were developed for symmetrical (-8° $+8^\circ$) and non-symmetrical (-12° $+4^\circ$) range of the angle of attack. The experiments were carried out in a special cavitation tunnel set-up for a Voith-Schneider model propeller at various advance ratios including bollard pull. The application of optimised profiles resulted in a 10% reduction of critical cavitation number.

Another example of the method above was described by Denisov (1996) presenting the results of computational optimisation the blade sections with improved cavitation characteristics for CPP of the Arctic nuclear-power lighter carrier "Sevmorput". New section profiles showed a significant increase in the width of cavitation diagrams and also showed a 40-50% reduction in cavity volume at cavitating conditions. A design compromise was performed for the extremes of packed ice and full power open water conditions for the avoidance of cavitation erosion damage.

Biskoup (1998) investigated blunt based profile sections having non-linear lift characteristics. The advantage of such profiles was increased efficiency in non-uniform inflow. To determine the profile geometry, a modification of Alexandrov method was applied considering local separation at the trailing edge. The new profiles were characterised with increased camber and maximum thickness aft of mid chord.

2.3 Application of Optimisation Techniques to Propulsor Design

Mishima (1996) investigated the design of cavitating propeller blades using a lifting-surface analysis code. The blade geometry was defined as a B-spline surface, which was optimised using a non-linear algorithm. Unsteady cavitation was computed and used as one of several design criteria. The design of two-dimensional cavitating blade sections was also studied with the goal of maximizing the lift to drag ratio of the sections.

Black (1995) presented a section design approach utilizing a B-spline 2-D panel method in conjunction with a genetic algorithm optimizing code. The method of feasible directions was also used and was found to handle the problems with a great deal fewer functional evaluations than genetic algorithms.

The foil camber was represented with 3 fourth order B-spline vertices at x/c values of 0.15, 0.50, and 0.85. The thickness was represented with three parameters, the leading edge radius, maximum thickness, and chordwise location of maximum thickness. A foil was created to be equivalent to the Shen, Eppler (1981) P1127 foil. Also, a 2-D section viscous flow solver was coupled with the parametrically defined foil to obtain a section with a specified cavitation bucket, but with reduced drag over the specified section. The program used for viscous analysis was XFOIL developed by Drela (1989). The advantages of this foil design approach was its relative simplicity over the other approaches discussed, which generally require more expertise to execute.

Kawakita and Hoshino (1998) presented a new blade section design method using optimisation techniques. The procedure performed optimised calculations of the blade pressure distributions using the Quasi-Continuous Method (QCM), a modified vortex lattice method. A specified blade pressure distribution was determined using the Sequential Unconstrained Minimisation Technique (SUMT). Two example cases were presented to improve both propeller efficiency and reduce hull pressure excitation due to unsteady propeller cavitation. Model test verification showed successful results. Blade sections designed at the circumferential average conditions with flat pressure distributions, with higher pressure at the leading edge had lowest hull pressure excitation and the best overall efficiency.

Thomas (1998) investigated the use of genetic algorithms for study the optimisation of underwater vehicle propulsion characteristics. A multiple component lifting line program which included an axisymmetric body and duct was modeled with the propulsor. The genetic algorithm was used to minimise the power required to propel a vehicle with variable afterbody shape, propulsor/duct loading and propulsor type. A genetic algorithm was utilised since the author considered the solution

space to have too many independent variables to solve the problem using differential methods.

A generic optimisation program was used by Dai et al. (1994) to perform automated propeller design. A series of propeller design/analysis programs which compute blade loading, stress, cavitation, unsteady reactions and acoustics were tied together to optimise propeller performance. A sample design was performed by a human designer and compared with designs developed using different numerical optimisation methods.

2.4 Extrapolation and Powering Performance

The methods used for extrapolation from model to full scale still differ between towing tanks. The extrapolation method proposed by the 15th ITTC (1978) is used with some modifications by about 50% of the model basins. The differences in extrapolation methods lead to great difficulties in comparing the test results of different model basins. The model-ship correlation line recommended by the 7th ITTC (1957) is used by most basins. The use of a form factor for taking into account the three-dimensional flow is not used at all model basins, partially due to the difficulties in determining the form factor in a model test. Most model basins use their own correlation allowance C_A based on their own rules and experience. Differences exist between the different methods used for extrapolating the propeller open water characteristic for full scale. The same holds for the wake fraction. There are differences in the methods used for calculating the wind resistance, the added resistance due to openings in the hull and of appendages, and for the scaling of appendage resistance. In general the method used by any model basin yields a consistent set of data which can be utilised by those acquainted with the method. However the direct comparison of individual propulsive coefficients derived by different model basins is not always possible.

2.5 New Developments in Extrapolation Methods

Karafiath (1997) presented a comprehensive evaluation of sea trials performed by the US Navy. The ships in the database are navy combatants, navy auxiliaries, and large commercial tankers.

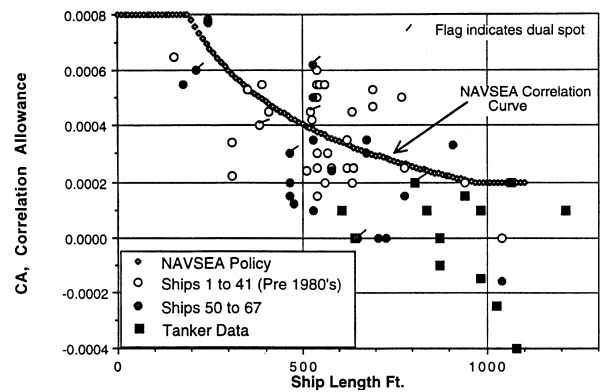


Figure 2.1 NAVSEA correlation curve: Ship-model correlation for all the data (Karafiath, 1997).

Karafiath used only a single parameter correlation allowance, C_A . It is stated in the analysis that: “Once the correlation allowance is determined, a common method for comparing the prediction relative to the ship trial data is through the correlation coefficient, C_P , for power and C_N , for shaft rotational speeds as defined by

$$C_P = P_D \text{ trial} / P_D \text{ prediction} \quad (1)$$

$$C_N = N \text{ trial} / N \text{ prediction} \quad (2)$$

It is important to note that the single parameter correlation allowance, C_A , affects both delivered power and RPM. Thus a key measure of the validity of the DTMB powering extrapolation method for model test data is to see how well the propeller RPM is predicted for C_A values that are selected to match the predicted power with the trials power, i.e. $C_P = 1.0$.”

Figure 2.1 shows the entire range in which the C_A value must be varied in order to bring the prediction in line with the full scale results. The error which occurs is up to 10% of the delivered power. The author makes a clear connection between the required C_A value and the roughness of the hull and the propeller which have been measured since 1980. He has also found that the ships which have been put into service since 1982 require a 0.0002 smaller C_A value than the ships before this date. The use of self-polishing antifouling paints account for only a part of this difference.

Pylkkänen (1998) developed a method for converting model resistance to ship resistance for three groups of large, high speed ships (Multi-screw ships: $L = 103\text{...}286$ m, $V =$

24...36 kt; single screw ships: $L = 94...171$ m, $V = 20...30$ kt; fast attack craft type vessels: $L = 47...59$ m, $V = 32...50$ kt). He reviewed those parts of ITTC work on powering performance that are of relevance to resistance conversion. Some problem areas in the prediction methods now in use are also pointed out. The ITTC-57 method was selected to be used for converting model resistance into ship resistance. A set of formulae were proposed for calculating the incremental resistance coefficient. The formulae model the effects of transom width, hull form in front of the transom, length of hard chine and length of skegs. The coefficients of the formulae were determined on the basis of published analyses of trial trip test data for 12 ships. Pylkkänen also presented validation calculations for five additional ships.

Iannone (1997) introduced a new correlation method which allows performance prediction for screw propeller ships without resistance tests. According to that method, the true load at which the ship propeller will operate is assessed by separating and analyzing the viscous and potential flow components via a new form factor concept applied in self-propulsion conditions. The author proposed to estimate a form factor k_{AP} from propulsion tests for low speeds which is different from the k of the ITTC-78 method. The self-propulsion model tests are to be carried out as load-varied tests for each speed using a wide range of propeller loadings to include all possible full scale ship self-propulsion points. The results and the comparison of results with the ITTC-78 method show differences. An accurate form factor (k_{AP}) determination for very low speeds in the self-propulsion condition could be very difficult.

2.6 Form Factor

Bruzzone et al. (1997) published results of model tests with three geosim model series. The form factors have been estimated using different methods. The form factors found using Prohaska's method are shown in Table 2.1.

Table 2.1 Form factors k determined using Prohaska's method (Bruzzone, 1997).

C_B	Model Size		
L_{PP} [m]	1.6-1.9	3.4-4.0	5.2-6.0
0.6	0.011	0.019	0.014
0.7	0.029	0.073	0.059
0.8	0.101	0.114	0.109

These results show the difficulties in form factor determination in general. The author indicated that the reasons for the uncertainty lie in the low Reynolds number, small size of models, the Froude number and the hull form.

A new extrapolation method has been developed by Grigson (1994). This method is based on a new formulation of the flat plate friction, the behind-ship propeller characteristics, and several other new features. Greater prediction accuracy is claimed. Grigson (1995) presented a reanalysis of the resistance tests of the Lucy Ashton and Victory geosims. The resistance tests of both were analysed using his own flat-plate friction formulation. Grigson's (1993) formulation has been expressed as a correction on the 1957 ITTC correlation line:

$$C_{FM} = [0.93 + 0.1377 (\text{Log } R_n - 6.3)^2 - 0.06334 (\text{Log } R_n - 6.3)^4] \cdot C_{F \text{ ITTC } 1957} \quad (3)$$

valid between $1.5 \cdot 10^6 < R_n < 2 \cdot 10^7$

$$C_{FS} = [1.032 + 0.02816 (\text{Log } R_n - 8) - 0.006273 (\text{Log } R_n - 8)^2] \cdot C_{F \text{ ITTC } 1957} \quad (4)$$

valid between $10^8 < R_n < 4 \cdot 10^9$.

These factors represent lower C_F -values for model scale and higher values for full scale than $C_{F \text{ ITTC } 1957}$.

By using Grigson's flat-plate friction formulation, no scale effect could be detected for the Victory design, but possibly a small one for the Lucy Ashton, see Tables 2 and 3.

Table 2.2 Form factors k determined using the Grigson friction formulation (Grigson, 1995).

	Lucy Ashton	Victory (Ballast)	Victory (Loaded)
k_M	0.089	0.210	0.211
k_S, k_{GS} full scale	0.081	0.220	0.225

Table 2.3 Estimated form factors k relative to the 1957 ITTC line (Grigson, 1995).

	Lucy Ashton	Victory (Ballast)	Victory (Loaded)
k_M	0.044	0.150	0.150
k_S, k_{GS} full scale	0.186	0.244	0.262

2.7 Azimuthing Propulsors

In case of a “tractor” version of the thruster (the propeller is in the pulling mode in front of the pod) the interaction effects between the thruster body and the propeller are pronounced, as Kurimo et al. (1997) and Heinke (1998) have pointed out. The local high pressure behind the working propeller leads to inner forces between the pulling propeller and the pod-body which influences the propeller thrust. The interaction of the hull and an azimuthing thruster at the bow of a double ended ferry is of similar type (Kristensen, 1998).

In testing pods, two objectives should be met: (1) The institution should provide the total propeller thrust, and the total unit thrust (= pod thrust), including scale effects leading to an accurate power prediction. (2) For the propeller designer the test institution should provide the blade thrust, the effective wake fraction, and the propeller on-set wake distribution.

Mewis (1998) published the results of open water tests for the propeller of an azimuth drive which have been carried out for different configurations of propeller and pod (Figure 2.2). It can be seen in the open water diagram that the manner in which the test has been performed has a direct influence on the results of the test. Depending on whether the curves from configuration A, B or C are used, the resulting wake fractions and relative rotative efficiencies will differ. Also, the value of the thrust deduction fraction will depend on whether the propeller thrust or the net system thrust has been used for its determination. The open water characteristics based on net system thrust (curve A) are least affected by errors. Care must be taken when comparing the efficiencies of different podded drives. It should also be mentioned that scale effects for the thruster housings and struts depend on the propeller loadings. Load variation tests can be an aid in judging these scale effects.

Poustoshniy et al. (1998) investigated the scaling problems for azimuthing propulsors in the pushing mode. He describes model investigations of the flow around the strut and pod of a pushing thruster in the absence of the propeller. The impact of turbulence stimulation on resistance and wake distribution of the pod and the strut configuration are considered. Poustoshniy concluded that for the resistance and self-propulsion tests using azimuthing thrusters in the pushing mode attention should be paid to the stimulation of turbulent flow around the thruster elements. This is extremely important for poorly streamlined thrusters where the errors in determination of their own resistance may be in the range of 50%. For well streamlined thrusters these errors may be about 20%. The experience of Bussemaker (1987) is that turbulence stimulators control scale effects by preventing separation as a result of excessive laminar flow.

2.8 Conclusions

Significant advancement has been made in the application of new blade sections for propeller design. The method of Eppler (1981) along with various optimisation procedures have been used to design new section shapes. Applications have included both the extending of cavitation inception speed, and the improvement of propeller performance with cavitation.

Optimisation techniques have been applied to relatively simple, multiple design trade-offs, and for specific, detailed design procedures. Studies have shown the capability to arrive at an optimum with little design expertise. Further advances will be expected utilizing more advanced calculations and consideration of more design parameters.

The ITTC-78 method is well suited as a standard model test evaluation method for single screw ships, especially for the purpose of comparison of model test results from different testing facilities. Working with form factors in a successful manner is very difficult for small ship models and small model basins.

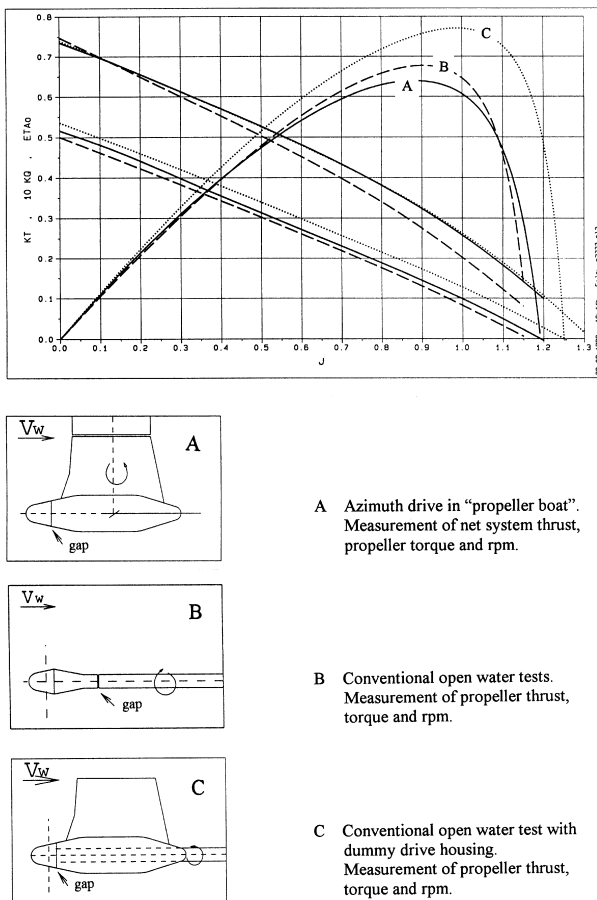


Figure 2.2 Open water characteristics of azimuth drive propellers for different open water tests configurations, HSVA-propeller 2333. The ranges of the variables are, $0.0 < \eta < 0.8$, $0.0 < J < 1.3$, (Mewis, 1998).

A power prediction method should be established for ships with azimuthing propulsors. Special attention must be paid to thrust measurements on thrusters with pulling propellers. Turbulence stimulation on the housing models of azimuthing thrusters is a requirement.

3. REVIEW THE ITTC RECOMMENDED PROCEDURES, BENCHMARK DATA, AND TEST CASES FOR VALIDATION AND UNCERTAINTY ANALYSES AND UPDATE AS REQUIRED. PASS THE INFORMATION TO THE QUALITY SYSTEMS GROUP FOR PUBLICATION IN 1999.

On the instructions of the 22nd ITTC Advisory Council the 22nd ITTC Quality Systems Group has collected and collated the existing ITTC adopted procedures and sent them to the technical committees for checking. The primary task of the committees was to check that the procedures in their present form are complete, up-to-date, correct, and that the symbols and terminology are up-to-date. Eleven ITTC adopted procedures were assigned to the Propulsion Committee for checking. Corrected procedures were returned to the Quality Systems Group for publication. The 22nd ITTC Propulsion Committee recommends that some of the procedures should be supplemented or rewritten.

The 22nd ITTC Propulsion Committee recommends to the Conference that the Procedure "Density and Viscosity of Water" (4.9-03-01-03) be supplemented as follows. Salt water data with salinity of 3.5 per cent are to be derived from Hardy's formula. For intermediate values of salinity the viscosity is to be found by linear interpolation between fresh water and the (standard 3.5 per cent) salt water viscosity data. (The recommendation is given as APPENDIX 1: INTERPOLATION OF VISCOSITY at the end of this report.)

4. IDENTIFY THE REQUIREMENTS FOR NEW PROCEDURES, BENCHMARK DATA, VALIDATION, UNCERTAINTY ANALYSIS AND STIMULATE THE NECESSARY RESEARCH FOR THEIR PREPARATION

4.1 Introduction

This task will focus on the prediction of powering performance, with particular emphasis on the extrapolation of model test results to full-scale values. In the most traditional field of ITTC activities, over time, prediction methods have become more dissimilar amongst the various towing tanks. This contrasts a more desirable goal to adopt a standardised procedure supported by the ITTC and used by a majority of towing tanks.

In this section problem areas are pointed out. Some alternative solutions are sketched. The solution options range from addressing short term specific problems with further

refinements of simple methods to long term approaches using CFD.

4.2 The ITTC 1978 Method

The development of the 1978 method was initially intended to bring more unity and to offer a sound theoretical basis in the various approaches. At the time of introduction and implementation of this method, theory used so that empiricism could be reduced a minimum. Statistical analyses of collective correlation data, was brought together in a cooperation of several institutions and demonstrated the superiority of the 1978 method.

When this method was accepted in 1978 for making standard predictions it did not actually substitute existing methods in use at most of the various model testing institutions for several reasons. Reluctance to incorporate the method related almost everywhere to practical issues as lack of experience, problems to determine form factors, lack of flexibility of the method to handle ships with appendages and complex propulsors, and, to a lesser extent, several theoretical objections. Adaptations of the method presented in 1984 and 1987 did not change the situation significantly. These modifications concerned limitations to the wake scaling for slender ships and rudder effects, the recognition of separate hull roughness effects and, further, the introduction of the rotation rate correlation coefficient C_{NP} through which both power and speed identity are preserved. Here C_{NP} is trial correction for propeller rate of revolution at power identity.

Nevertheless, in several institutions, elements of the ITTC-78 have been incorporated in daily practice and in other towing tanks modified versions of the method are being used every day.

4.3 The Need for Improved Performance Prediction Methods

In present day towing tank experiments there is a growing need for more sophisticated methods than the ITTC-78 procedure. There is a need to make accurate predictions for a variety of hull forms, sizes, appendage configurations and the ever-widening spectrum of propulsor types. This requires that a rational model test procedure and analysis method be defined. It is expected that when the relative

merits of various configurations and different types of propulsors are to be assessed by model experiments, this can be done with some chance of success only through a component-wise treatment of the various scale effects involved. A general procedure for the treatment of appendages is required, along with procedures to address passive propulsive components, for example, ducts and thruster housings. Next to this are the implementation of a better flat-plate drag formulation, an upgrading of the wake-scale effect assessment taking into account the loading dependency of the propulsion factors and the handling of the problem of unknown extent of laminar flow on model propellers. Further, attention should be paid to testing hull forms with severe flow separation.

In the appendix of this section the ITTC-78 method is compared to the standard DTMB performance prediction method in the case of the AOJ-179, a slender single-screw, centerline skeg ship with few appendages, of which standardization/correlation trials and model experiments are available.

The standard performance prediction method of DTMB is a comparatively simple procedure without the use of form factor, but utilizing a model-ship correlation allowance (see Section 2.3) which applies to Navy-type, slender hull forms with a multitude of appendages, typical for tests at DTMB. The study concluded that the ITTC-78 method predicts 7.5 per cent lower delivered power, without the use of the correlation factors C_P , C_N and C_{NP} . This is chiefly in line with earlier conclusions drawn in the correlation studies presented in the report of the Powering Performance Committee of the ITTC in 1984 where for the DTMB towing tank an average C_P value of 1.067 was found (17th ITTC, 1984). The difference in power prediction in the case of the AOJ-179 was shown to be almost fully due to the form factor and only to a minor extent due to the propeller blade friction scale effects. Uncertainty in the measurement of the form factor is the primary factor for use of simple Froude method over the ITTC-78 method or its derivatives. As the other elements of the ITTC-78 method causes only small deviations, at least in this particular correlation case, the principal item is the form factor. This emphasises the on-going need for a reliable experimental determination of the form factor.

4.4 Appendage Scaling

There has been a continuous problem in accounting for the influence of “normal” appendages on propulsion performance derived from model tests. Though effects of individual appendages may be relatively small and of second order, comparable to measurement uncertainty, their cumulative effect can be substantial. Interaction with the hull and/or other appendages can cause significant deviations from generalised prediction methods. Also the accuracy and quality of the model appendages can introduce uncertainty in the model test results. A breakdown of the contribution of appendages for a typical twin-shaft naval ship at a Froude number of 0.28 is shown below in Figure 4.1. The contribution of the shafts and struts is relatively large and for reference, a typical uncertainty in propulsion testing and full scale predictions of speed and rotation rate has been added.

The use of the methods of appendage drag scaling depends on the size of the test facility, the size and quality of the models and appendages, the types of appendages and requirements of the customer. Most current concepts use corrections on the measured difference between the bare hull and appended resistance. The most frequently used method is the Beta correction method.

4.5 Application of CFD

Since the work of the previous committees, advancements in CFD and experimental methods have been made. Beyond the use of purely empirical methods in treating the appendage drag scaling problem is the CFD approach. Cordier et al. (1997) investigated open shaft and strut flows using LDV and RANS solutions. Progress was made but gridding the combined hull, shaft and strut configuration created difficulty. It is expected that further progress in CFD will eventually assist in assessing scale effects, but a more practical solution is desirable in the near term, to improve prediction methods derived from towing tank tests.

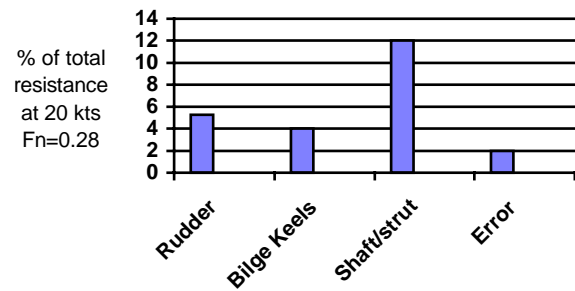


Figure 4.1 Contribution of appendages to resistance of a typical twin-shaft naval ship at $F_n = 0.28$ (courtesy DTMB).

4.6 Streamlined Appendages

Scaling of streamlined, flow oriented appendages is performed using the Beta factor method (Beta is in the range 0.4-0.7) or the form factor concept. Alternatively, the scaling of the appendage drag is carried out by using $\text{Beta} = C_{FM}/C_{FS}$ or by calculating the appendage friction coefficients from an equivalent appendage length as the square root from the appendage wetted surface area. Some institutions maintain consistent predictions by accounting for the wetted surface areas of the appendages and an appropriate choice of the model-to-ship correlation allowance. In other methods the form factor is used and form factors of appended hulls, needed to scale the appendage drag, can be found under the assumption that the wave resistance is the same for the bare hull and the appended form. In this way, testing the appendages at extremely low Reynolds numbers is avoided.

The form factor approach for appendage drag scaling is reflected by an increased $1+k$ for appended hull. The increase of the form factor due to the appendages can easily be derived from:

$$\Delta k = C_{APP}/C_{FM}, \quad (5)$$

where Δk is the form factor increase, C_{APP} is the appendage drag coefficient based on the bare hull wetted surface area and C_{FM} is the flat-plate friction coefficient of the ship model. In this approach the wetted surface areas of the appendages are not used in the extrapolation and their effect is expressed only by the changed form factor:

$$1+k(\text{appended}) = 1+k(\text{bare hull}) + \Delta k. \quad (6)$$

4.7 Non-Streamlined Appendages

For a mixture of streamlined and non-streamlined appendages the increase of the form factor should be selected between 0 and Δk , with the possibility of deriving the increase in form factor from $\Delta C_{TM}/\Delta C_{FM}$. Here, ΔC_{FM} is the change in appendage drag coefficient over the tested speed range when the model frictional coefficient varies by ΔC_{FM} . Experimental uncertainty will often hamper an appropriate choice of the appended form factor using this approach (Holtrop, 1989). Apparently, it appears practically impossible to discern from the test results the fraction of the appendage drag which is scale effect dependent. As in assessing the experimental form factors from experiments, the choice of the appendage drag scale effects in those cases where a combination of streamlined and non-streamlined appendages is dealt with, requires careful judgement of the experimenter.

4.8 Passive Propulsor Components

Some classes of appendages, such as rudders behind propellers, nozzles, engine housings, gear housings, pods struts and azimuthing thrusters, the local flow velocity depends not only on the upstream velocity but also the propeller-induced flow. Traditional appendage scale effects are augmented by model to full scale changes in entrance velocity and propulsor loading. Effects of model streamlining and flow orientation will also be important. When considering the effect of propeller loading on the scale effects, an appropriate numerical model should be used to take into account the induced velocity effects. Propulsor loading effects are absent in the ITTC-78 method. It is likely that a simple procedure is sufficient to make significant progress, as the coarse methods followed now render already an almost acceptable procedure for many customers. The drag of thruster and pod housings should preferably be measured and followed with simple drag corrections. To avoid measurements at low speeds and loading, a suitable numerical model, can be expressed with sufficient accuracy, as a simple function of a combination of both the square of the model forward speed, V_M , and the square of an equivalent "slipstream velocity", nP . Here, n is the rotative speed and P is the average pitch of the propeller. A scale effect correction now based on these simple speed and loading parameters can then easily be defined, whereas

its accuracy can substantially be improved by tuning to results of dedicated force measurements on the passive propulsor elements. With some code development, CFD is a potential tool for investigating propulsor scale effects.

4.9 Other Elements

Under renewed debate is the appropriate slope of the model-to-ship correlation line (Grigson, 1993, 1995; Kodama, 1998; Schweighofer, 1997). A proper validation by a statistical analysis of independent correlation data is needed to prove the superiority of a new friction formulation.

The propeller scale effects require renewed attention, as unexpected scale effects emerge from updated correlation. The advent of new blade sections with extensive laminar flow in model propulsion and open water tests, the use of large skew, the use of low rotative speeds in special propulsors such as contra-rotating propellers, require that the propeller scale effects be properly treated. Effects of pitch reduction of high skew, fixed-pitch propellers under their thrust load should be included. New procedures, both as regards experiments and the extrapolation procedure should be developed. In this respect it could be worthwhile to relate the scale effects, both lift and drag, to the difference in thrust and torque coefficients between the smooth and leading-edge roughened propeller models. Propeller and profile section scale effects were dealt with in the two previous Propulsor Committee Reports (20th & 21st ITTC Propulsor Committee Reports, 1993 & 1996). It was not possible to generalise the sample cases reviewed in these two reports into guidelines.

As the use of individual experimental form factors is often hampered by its determination in practice in a reliable and consistent manner, there appears to be a need for an improved method to determine $1+k$ and an updated guide to assist in assessing its value from the experimental results. In such a guide the most useful recommendations given in past ITTC proceedings should be brought together in an upgraded form. Such a guide for form factor determination should become a part of the ITTC Quality Manual.

A similar issue is the treatment of models with separated flow. Not only the detection of flow separation, also the assessment of the

form factor and the wake scale effect should be considered with care. Severe effects of the propeller loading on the propulsion factors occur here. There is an obvious need to improve the scale effect corrections for this class of ships.

4.10 Conclusions and Recommendations

Items for Improvement.

1. Scale effect procedures for appendage drag should be improved and validated.
2. A method for the scale effect on the passive components of propulsors should be developed.
3. New formulations of the flat plate friction should be validated.
4. A method should be developed by which propeller scale effects, both lift and drag, should be assessed with emphasis on the occurrence of excessive laminar flow. Tests on turbulence tripped propeller models should be contemplated.
5. A guide for the assessment of experimental form factors and their use in extrapolation should be compiled and made part of the ITTC Quality Manual .
6. Guidelines for testing separation prone forms, detection of separation and the choice of scale effect corrections should be developed.

Solution Strategy.

7. The use of CFD in predicting appendage scaling effects should be encouraged, including the planning and execution of CFD validation experiments.
8. Distribution of a questionnaire to the ITTC member towing tanks to collect information on appendage types, scaling methods used, model appendage detail quality, types of tests performed, availability of test data and identified problem areas. Knowing specifically what type of appendages are of interest to the ITTC as a whole is very important. Each appendage type potentially requires a different plan for improvement. Also, ITTC members should be asked how they would like to improve their scaling methods. The options could range from addressing short term specific problems with further refinements of simple methods to a long term approach using CFD.

4.11 APPENDIX: COMPARISON OF ITTC-78 AND DTMB STANDARD SHIP PERFORMANCE PREDICTION METHODS FOR AOJ-179

Introduction. Model data, from tests conducted during the AOJ-179 standardization-correlation experiments, was analysed and extrapolated to ship scale using the two methods (Forgach, 1999). This particular data set was selected because the AOJ-179 is the only Navy ship with single screw centerline skeg configuration to be correlated since 1980 (Figure A.1). Using correlation data provides the opportunity to compare the results of each of the extrapolation methods to high quality full scale trials data.

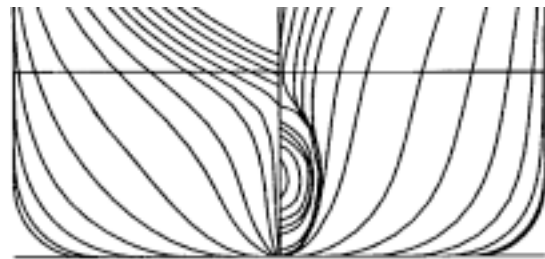


Figure A.1 AOJ-179 Body Plan.

Differences Between the Methods. 1. The single most significant difference between the ITTC-78 and DTMB extrapolation methods is the use, by ITTC-78, of the form factor (1+k). Figure A.2 is the Prohaska plot developed from the AOJ-179 low speed resistance data.

Form factor applied in the effective power (P_E) extrapolation results in a lower calculated value of the coefficient of residuary resistance (C_R) and therefore a lower value for the predicted ship scale coefficient of total resistance (C_{TS}) and P_E :

$$C_R = C_{TM} - C_{FM} (1+k) \quad (A.1)$$

$$C_{TS} = C_R + C_{FS} (1+k) + \Delta C_F \quad (A.2)$$

More importantly, form factor influences the determination of delivered power (P_D) because it affects the definition of the self-propulsion point. In the ITTC-78 method, form factor appears in the formula used to calculate the tow force (R_A) applied during the self-propulsion test:

$$R_A = 1/2 (\rho S V^2)_M [1+k (C_{FM} - C_{FS}) - \Delta C_F] \quad (A.3)$$

With form factor in the equation, the calculated value of tow force is greater. If a greater tow force is applied to the model, the measured values of model scale propeller shaft thrust, torque and RPM are less, and therefore, the predicted ship scale pd is less. The major

difference between the ITTC-78 and DTMB P_D extrapolations is, then, due to the fact that the two methods identify different self propulsion points for the same test condition.

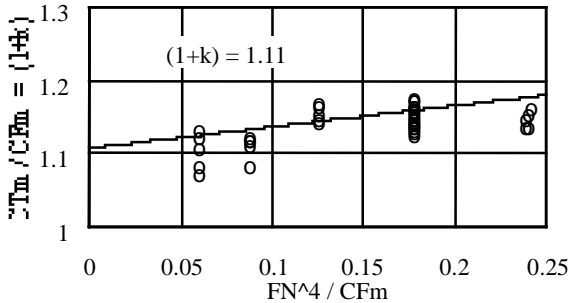


Figure A.2 Form Factor (1+k) for AOJ-179.

2. ITTC-78 and DTMB each use different empirically based roughness or correlation allowances (ΔC_F or C_A). Both formulations are very similar. The difference between $\Delta C_F = 0.312 \text{ E-}3$ and $C_A = 0.300 \text{ E-}3$ had very little effect on the results of this study.

3. ITTC-78 does not install bilge keels on ship models for either P_E or P_D tests. Rather, an estimated bilge keel drag, based on bilge keel wetted surface, is added as a correction to the final results. DTMB does install and test with bilge keels without additional corrections.

The raw data used as input to both the DTMB and ITTC-78 extrapolations shown here was from experiments with a model that included bilge keels. Therefore, the effect on the results due to the manner in which the two methods deal with bilge keels was not assessed here.

4. ITTC-78 corrects the model propeller open water characteristics for blade drag scale effects to obtain ship scale propeller open water characteristics. DTMB does not make this correction.

Correcting the model propeller open water characteristics reduces the value of the ship scale torque coefficient (K_{Qs}) with virtually no effect on the thrust coefficient (K_{Ts}). A lower K_{Qs} results in a lower predicted ship P_D . This has a relatively small effect. Approximately 2% of the difference between the ITTC-78 and DTMB P_D prediction is due to this correction.

5. ITTC-78 corrects the model scale wake (w_{TM}) to obtain ship scale wake (w_{TS}) to account for boundary layer scale effects. DTMB does not make this correction.

Correcting the model wake (w_{TM}) to obtain the ship wake (w_{TS}) affects the predicted ship RPM. A small part of the difference between the ITTC-78 and DTMB RPM prediction is due to this correction.

6. ITTC-78 makes final corrections to predicted delivered power (C_P) and rpm (C_N) to adjust the model results to current trial statistics. DTMB does not make this correction.

For these calculations C_P and C_N were assumed to be equal to 1.0 and therefore had no effect on the results.

Comparison of Results. ITTC-78 and DTMB extrapolated results are compared to the full scale standardization trial results in Figures A.3 and A.4. Approximately 98% of the difference between the ITTC and DTMB P_D prediction is due to the use of form factor. Details of the two prediction methods are further compared in Table A.1 by looking at the intermediate results for the 22 knot ship speed.

The ITTC-78 extrapolation underpredicts ship P_D relative to the DTMB prediction by approximately 6% to 8%. DTMB has had several occasions over the years to compare its results to those generated by the ITTC-78 method, and it has been noted that this difference is rather constant from case to case.

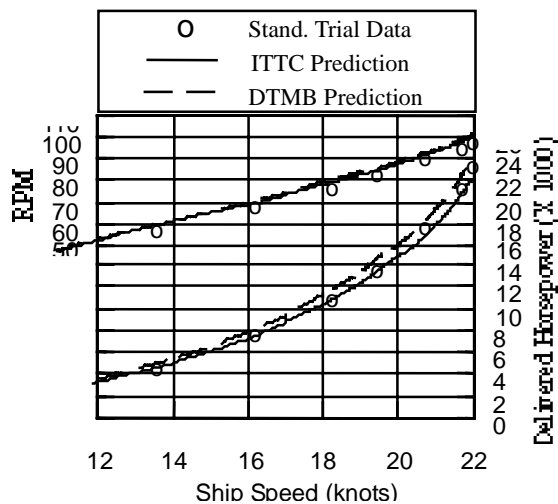


Figure A.3 Comparison of ITTC-78 and DTMB Prediction Results to Full Scale Standardization Trial Data (AO J 179).

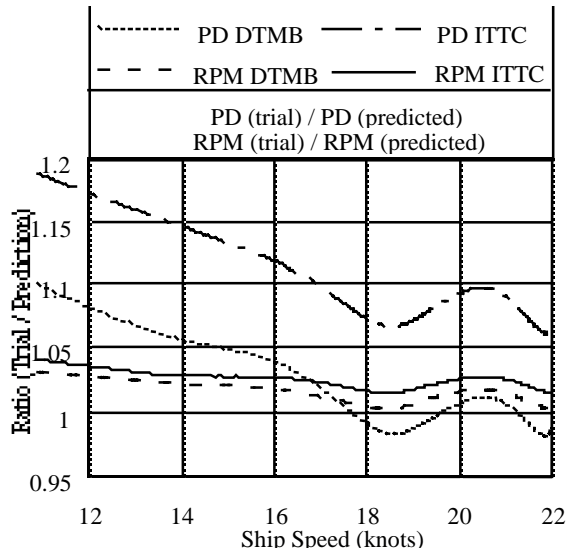


Figure A.4 Comparison of ITTC-78 and DTMB Prediction Results to Full Scale Standardization Trial Data (AOJ 179).

Table A.1 Comparison of Standard ITTC-78 and DTMB Extrapolations - Data Spot for $V_S=22$ kts, $F_n=0.255$. (Resistance Coefficients, x 1000)

	ITTC-78	DTMB
P_E Test:		
R _{TM} (lbf)	21.22	21.22
C _{TM}	3.497	3.497
C _{FM}	2.737	2.737
1+k	1.110	---
(1+k)*C _{FM}	3.038	---
C _{RM} =C _{RS}	0.459	0.760
C _{FS}	1.367	1.367
(1+k)*C _{FS}	1.518	---
ΔC _F or C _A	0.312	0.300
C _{TS}	2.288	2.427
P _E (Hp)	16269	17257
P_D Test:		
Model		
R _A (lbf)	7.33	6.49
T _M (lbf)	16.33	17.26
Q _M (lbf-in)	32.33	33.91
N _M (1/s)	8.41	8.53
K _{TM}	0.266	0.274
K _{QM}	0.054	0.055
J _a	1.065	1.050
1-w _{TM}	0.799	0.797
η _R	0.984	0.982
1-t	0.850	0.853
Ship quantities:		
1-w _{TS}	0.803	no correction
K _{TS}	0.266	"
K _{QS}	0.052	"
T _S (klbf)	283.4	299.7
Q _S (klbf-ft)	1181.5	1259.8
N _S (RPM)	99.7	101.0
P _D (Hp)	22438	24237
	0.725	0.712

5. PREPARE AN UP-TO-DATE BIBLIOGRAPHY OF RELEVANT TECHNICAL PAPERS AND REPORTS.

The Propulsion Committee continued the task to extend and compile an up-to-date bibliography of technical papers and reports. This task has been expanded to include the areas now covering Powering Performance, Propulsors, Cavitation and Waterjet Propulsion.

The bibliography now includes almost 8000 entries in the total area of ship propulsion, with emphasis on the hydrodynamic features. The bibliography compiled by the previous Propulsor Committees has been used as a basis. It was extended by adding older references in the other areas and by entering recent references. Many older references were taken from the past technical committees of the ITTC.

The bibliography contains the following fields:

- Author,
- year,
- title,
- publication,
- volume number,
- page indication,
- keywords,
- language indication,
- ITTC reference indication,
- with or without abstract,
- type of publication.

Care has been taken that names of authors, titles and keywords are spelled correctly since they will be used mainly for searching the bibliography. Still the bibliography contains several duplications, which are persistent due to spelling errors, the different use of abbreviations, capital letters, etc.

The keywords previously defined by the Propulsor Committee of the 18th through 21st ITTC have been preserved for consistency and are contained in Table 5.1 with associated abbreviations provided. These keywords were thought appropriate to cover the wider range of interest of the new Propulsion Committee.

The trends observed by the last Propulsor Committee have continued with the recent references. There is an abundance of articles on numerical hydrodynamics and cavitation. The number of papers dealing with design work and the more classical model experiments and full-

scale measurements in the field of powering performance is relatively small.

Table 5.1 Database key words

Design (DES)	Manufacture (MANUF)
Performance (PERF)	Automation(AUTOM)
Mathematical Model (MATHMOD)	Special Devices (SPEC)
Drag (DRAG)	Cavitation (CAV)
Testing (TEST)	Noise (NOISE)
Propeller Pressure Field (PRES)	Aircraft (AIRCRAFT)
Blade (BLADE)	Operation Conditions (OPERAT)
Testing (TEST)	

Though the compilation of the bibliography aims at presenting an exhausted survey of relevant papers, in practice there remain some papers which have not been referred to. In this respect it is useful to point at probably more exhaustive surveys, as e.g. "BMT Abstracts", which are compiled monthly and which permit a more thorough search to be made. In BMT Abstracts the subjects "Resistance and Propulsive Performance", "Aerodynamics", "General Hydrodynamics, Hydraulics and Oceanography" and "Corrosion and Fouling" are particularly of interest with emphasis on the first.

The bibliography has been converted from dBase to Microsoft Access format. The bibliography will be made available to the member organisations on the ITTC home page.

6. REVIEW THE DEVELOPMENT OF DESIGN AND ANALYSIS METHODS FOR PROPULSORS WITH SPECIAL EMPHASIS ON THE MODELLING OF VORTEX WAKE. THE COMMITTEE SHOULD CONSIDER REPEATING THE 18TH ITTC COMPARATIVE EXERCISE.

6.1 Introduction

The advances in numerical methods and computers continue, and therefore a review of the development of design and analysis methods is topical for ITTC. As a supplement to the customary review, the 22nd ITTC Propulsion Committee decided to organise a workshop on comparative calculations by

propeller RANS/Panel method codes (Gindroz et al., eds.,1998).

6.2 Developments in the Modelling of Vortex Wake

The Role of Vortex Wake. Depending on the case at hand the location and type of the vortex wake configuration may have a considerable effect on the calculated propulsor performance. In addition to the performance prediction of a single propeller, vortex wake models play a role in the calculation of interaction effects between the components of multi-component propulsors, between propulsors and neighbouring bodies such as rudders. Additional data on vortex wakes are found in Section 8.4 of this report.

Actuator Disk. Conway (1998) developed a method to solve the inviscid incompressible flow induced by a heavily loaded actuator disk with non-uniform loading. The method can treat both contra-rotating and normal propellers. The shape of the slipstream boundary through the propeller disk obtained in the sample calculations differs from those observed in cavitation tanks. This applies also to other non-linear actuator disk theories.

Lifting Line. Moulijn and Kuiper (1995) investigated the effect of wake alignment on the induced velocities and on the loading distribution of lifting lines. Moulijn and Kuiper compared three slipstream models: (1) fully linearised boundary condition and wake, (2) linearised wake condition where the bound vortices are located on the geometrical pitch plane and the trailing vortices are located on a helical surface of constant pitch as in the linearised wake condition, (3) aligned wake condition where the bound vortices are located on the geometrical pitch surface and the trailing vortices are aligned with the flow. The prediction differences in K_T between the linear wake and the aligned wake were about 3 % for both a non-skewed and a highly skewed propeller. The highly skewed propeller exhibited an additional difference of about 6 % between the fully linearised boundary conditions and the linear wake.

Achkinadze and Krasilnikov (1997) developed Generalised Linear Lifting Line Model (GLM) for use in propeller design. The GLM model assumes a fixed helical vortex sheet behind each blade. The pitch of the helicoidal

vortex sheet is determined on basis of statistical data on integral propeller characteristics such as thrust, torque, etc. Poustoshniy et al. (in Achkinadze et al., 1997) used the GLM design algorithm to design four model propellers, for which open water and cavitation tests were also made. The measured open water efficiencies agreed very well with predicted open water efficiencies. The predicted thrust coefficients differed by about 4.0...13.5 % from measured ones. The GLM design method is also applicable to multi-component propulsors such as contra-rotating propellers.

Lifting Surface. Liu (1995) developed a semi-empirical vortex wake model for vortex lattice method. Vortex sheets trailing from propeller blades roll up partially to form the tip and hub vortices. Vortex sheets exist between the tip and hub vortices. The contraction ratio is determined empirically as a function of the loading and the skew angle. The ultimate values of the pitch angles of the tip and hub vortices are calculated from the local induced velocities. The boundary layer development on the propeller blades is calculated using an integral method for the quasi-3-D boundary layer equations of a rotating helical surface. Comparisons between the predicted and measured performance were given for eight propellers. The correlation is either good or satisfactory.

Panel Methods. Pellone's (1991) vortex wake model in unsteady onset flow for the panel method code consists of a transition region and an ultimate wake region. The velocity field is induced by surface source and doublet distributions. The transition part of the wake is calculated by using either the Lagrangian procedure under steady conditions or by using the relaxation method. In the Lagrangian method the wake is lengthened by an additional row of panels at each subsequent time step. The relaxation procedure assumes that the whole initial wake geometry is known. The ultimate helical vortex filaments have pitch angles and radii equal to those obtained at the rear of the transition region. The K_T and K_Q correlation for the single sample propeller of simple geometry was very good, relative errors being in the range of 0.2...1.7 %.

Pyo et al. (1997a; 1997b; Kinnas & Pyo, 1997) continued the development of a potential based boundary element method. They developed an algorithm, called FLAG, to solve the convergence problem for typical grid arrange-

ments and for predicting the complete three-dimensional vortex wake sheet roll-up. The algorithm utilises a higher order panel method, which combines a hyperboloidal panel geometry with a bi-quadratic dipole distribution. The wake sheet roll-up is by a higher order panel method. Throughout the numerical calculation, rediscritization is applied as a smoothing scheme. In the flow adapted grid the position of the tip, "the computational tip", is determined by searching for the point for which the region of predicted singular pressures is minimised. The location of the computational tip depends on the loading (angle of attack). The code user needs to specify the detachment point of the tip vortex, i.e. in 1997 this process was applied manually. Conventional and new type grids are shown in Figures 6.1 for the sample propeller N4990. Table 6.1 compares the measured and predicted K_T and K_Q of the new method and a conventional code for the N4990 in spatially uniform flow. N4990 has five blades and skew angle extent of 34.49 deg. Pyo and Kinnas considered that for wide tip blades with high skew the new grid improves the prediction of pressures at the tip.

Belibakasis and Politis (1998) applied surface vorticity to the propeller flow analysis. They investigated several trailing vortex configurations. Takinaci (1996) improved the prediction accuracy of the surface panel method of Morino by adding estimates of the boundary layer at the trailing edge to the flow model.

Table 6.1 Predicted K_T and K_Q of propeller N4990 at $J=1.27$ in spatially uniform flow (Pyo & Kinnas, 1997).

GRID	K_T	Error	$10*K_Q$	Error
Convent	0.2242	8 %	0.6010	13 %
Adapted	0.2380	2 %	0.6872	0 %
Experim	0.243		0.691	

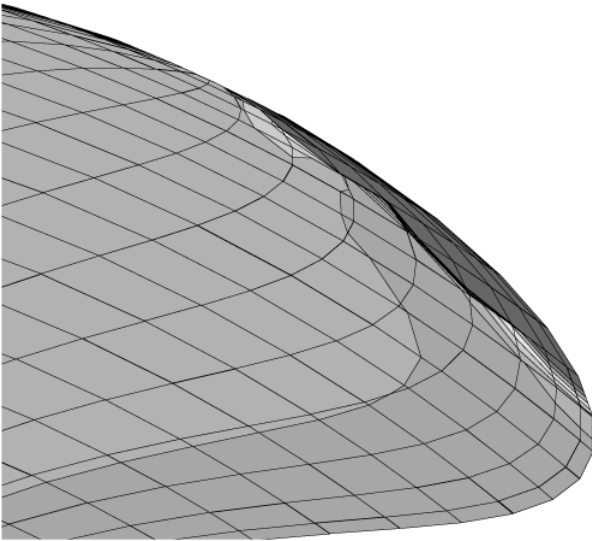


Figure 6.1a Conventional

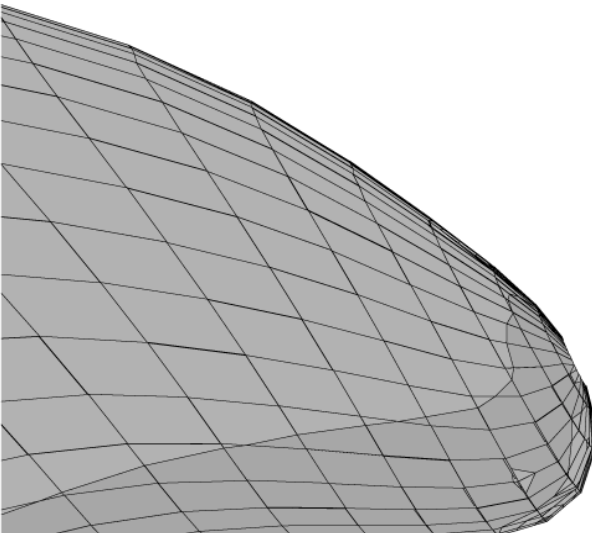


Figure 6.1b Flow-Adapted

Figure 6.1 Conventional and flow-adapted grid at the tip region of N4990 for $J=1.27$ (Pyo & Kinnas, 1997).

6.3 Developments in Panel Methods

Kinnas, Griffin, and Mueller (1997) applied a vortex-lattice method (THPUF-3A) and a panel method (PROPCAV) for the analysis of unsteady propeller cavitation to some propeller geometries in non-axisymmetric onset flows. Results are compared to those measured in experiments. Further, they have applied a recent optimisation technique for the design of cavitating blades to a case with given requirements and several constraints. The results from two

methods are found to be similar to each other in terms of cavity shapes but to differ from each other in terms of cavity volume velocities. They showed that the flow contraction at the blade tip increased the predicted tip cavity volume.

Caprino and Traverso (1997) applied a low order potential based panel method to calculate hydrodynamic performance of ship propellers operating in uniform flow. Flat panels with constant source and doublet distribution are used in the code. Computational results were compared with the experimental data of two DTMB propellers P4718 and P4282. As for the pressure distribution of the propeller P4718, the results are in very good agreement with experimental data.

Mishkevich (1997) developed a new non-linear theory based on vector potential to simulate the flow around a propeller. He used a continuously distributed vorticity over the blade and hub surfaces, and free vortex sheets representing the propeller wake. He showed that an additional component of induced velocity (“relative eddy” term) occurs due to the blade thickness effects in nonlinear hydrodynamics of rotary bladed machines. He derived the formulation of the new propeller theory but did not present calculation results or comparison with experimental data.

Chen and Dong (1997) developed an unsteady potential based panel method for the propeller subjected to a spatially non-uniform inflow. A non-linear pressure Kutta condition was implemented in the method by an iterative scheme at each time step of the propeller operating time domain. Calculation results of the pressure fluctuation over the propeller blade surface were compared with the experimental data and the calculations by Hoshino (1993). The results for a conventional propeller and a highly skewed propeller are in good agreement with the experiments and the previous 1993 calculations.

Pyo, Suh and Kim (1997) developed a low order potential based panel method to analyse propellers in steady flow. The propeller surface is discretised with hyperboloidal panels and a non-linear wake model is used in the method. An efficient numerical Kutta condition scheme has been applied to satisfy the zero pressure jump condition along the trailing edge of the blades. They showed that the resulting pressure distribution of DTMB propeller P4119 agreed

well with the experiment and other numerical method.

Yang, Wang and Yang (1997) developed a combined vortex lattice and surface panel method to predict the steady performance of ducted propellers operating in uniform flow. The propeller calculated with the vortex lattice method and the duct with the panel method, while the hydrodynamic interaction between them was treated in an iterative manner. Calculation results of the total thrust and torque for a ducted propeller series agree well with the experiments in a wide range of advance coefficients. The calculated thrust of the duct is lower than found in the experiments when the propeller loading is high.

Su, Ikehata and Kai (1997) presented a numerical method for designing a three-dimensional wing from a specified pressure distribution based on a surface panel method. Hydrodynamic characteristics of the original wing were calculated by potential based panel method employing the pressure Kutta condition. Then the geometry of the original wing was made to change by a small amount and the pressure increment due to this change was calculated by the method. From these data influence coefficient matrix of wing geometry on pressure distribution was constructed. The original wing geometry was modified with the influence matrix to form a new wing. By repeating this procedure, the wing geometry with the specified pressure distribution can be obtained. Several wings were designed as examples. The results showed that the method is effective in designing a three-dimensional wing having the specified pressure distribution. The designed wing shown in Figure 6.2 is obtained corresponding to the specified pressure distribution shown in Figure 6.3.

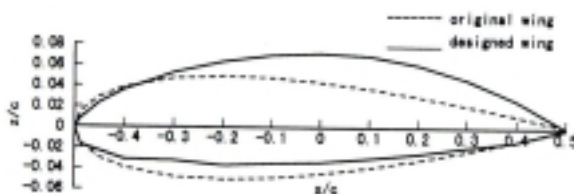


Figure 6.2 Designed wing for flattop pressure distribution, (Su, Ikehata and Kai, 1997).

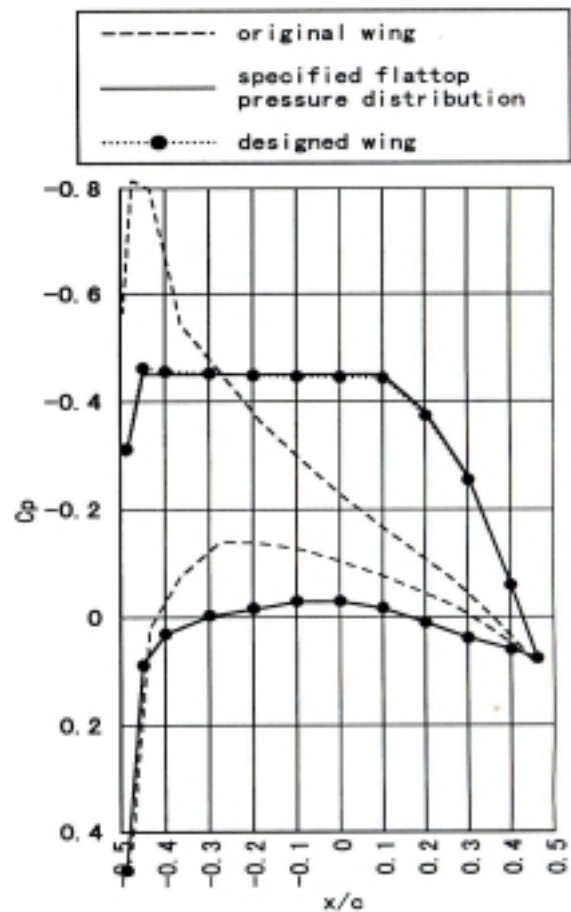


Figure 6.3 Comparison of specified flattop pressure distribution and pressure distribution of designed wing, (Su, Ikehata and Kai, 1997).

Maita, Ando and Nakatake (1997) have applied a simple surface panel method to the unsteady propeller problem by combining the source panels and unsteady Quasi-Continuous Method (QCM). They used source distribution of the Hess and Smith type on the wing surface and vortex distributions arranged on the camber surface according to QCM. Kutta condition at the trailing edge was satisfied by iterative calculations for equal pressure condition but the convergence of the iteration was found to be fast. Numerical results for two full-scale propellers (Seiun-Maru conventional and highly skewed propellers) in non-uniform flow were shown. Pressure distributions obtained by the method are in good agreement with experimental data.

Georgiev and Ikehata (1998a) computed the stress distribution and the deflection of blades of several screw propellers in steady flow by

the thick shell finite element (FE) method in combination with the surface panel method. They proposed a new general method to estimate the bicubic surface parameters of the deformed blade and to resolve the non-linear relation between the FE displacement distribution and the geometric parameters of blade profiles on cylindrical sections. They analysed the influence of the hydroelastic effects on the hydrodynamic performance of two full scale propellers, a conventional propeller (CP) and a highly skewed propeller (HSP) for “Seiun-Maru”. The pitch distribution of CP was increased due to the propeller loading but that of HSP was decreased.

Georgiev, Ikehata and Kai (1997) presented a new surface panel method using polyhedral decomposition of the boundary surfaces, minimisation of the computed perturbed velocities on the boundary surfaces, as well as subsequent repaneling adapted to the surface flow as shown in Figure 6.4. They concluded that the streamline-adapted repaneling of the boundary surface can precisely predict circulation, tip vortex position and pressure distribution on the tip regions of wings and propellers.

Georgiev and Ikehata (1998b) also extended their combined surface panel and thick shell finite element (FE) method to compute the performance of screw propellers in unsteady flow and the stress distribution and deflection of their blades. They proposed a new method to estimate the time derivatives of the perturbation potential on the basis of a minimisation of the change of its kinetic energy. The calculated pressure fluctuation and stress fluctuation during one revolution for two full-scale propellers, CP and HSP of “Seiun-Maru” are in good agreement with experimental data.

6.4 Review of RANS Methods

Turbulence Models. There is often strong physical interaction between the surface layers and the rotational inviscid regions, but the turbulence itself may be important only in very limited regions such as the surface layers and may not need be modeled very accurately in much of the flow (Arabshahi et al., 1998). If detached flow structures are present in which the turbulent shear stresses are not negligible, then they would require adequate modeling. The importance and difficulty of modeling turbulence depends on the particular domain. It can be dangerous to generalise about the

validity of turbulence models. The lack of a generally valid universal turbulence model may not prevent substantial progress in particular applications.

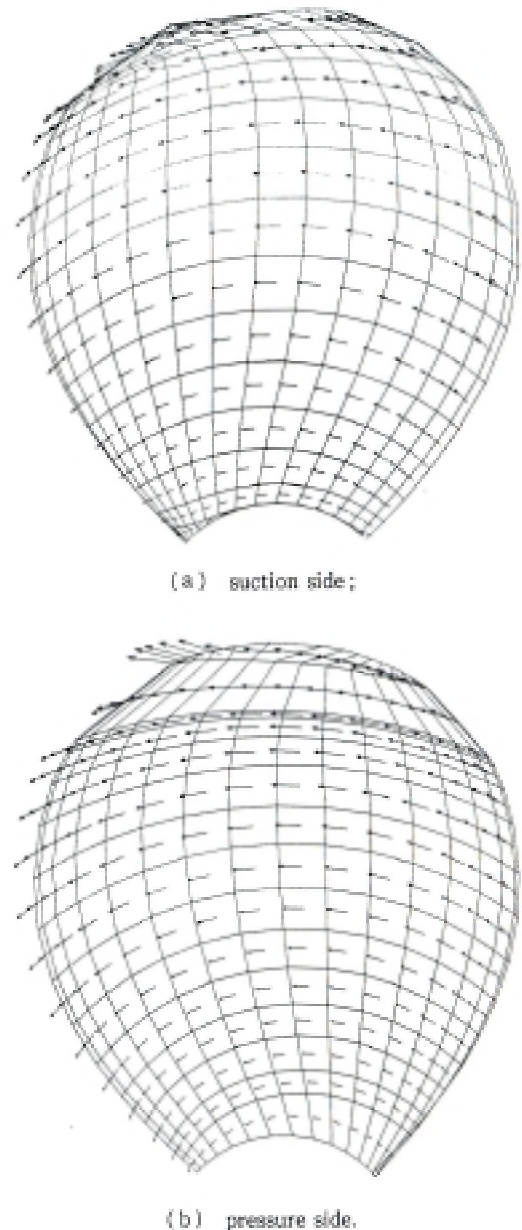


Figure 6.4 SAR mesh model of propeller 4119 with relevant tangential velocities in panels control points, $J=0.833$, (Georgiev, Ikehata and Kai, 1997).

Open Water Flow. Abdel-Maksoud, Menter and Scheuerer (1996) applied the incompressible RANS equation code TASCflow to marine screw propeller analysis. The finite volume equations are solved in a rotating coordinate system. The $k-\epsilon$ turbulence model is used. Abdel-Maksoud et al. presented the results for

two propellers, SVA4020 and SVA4021, at their design advance number of $J=0.6788$. Two grid sizes were investigated for each propeller. Table 6.2 gives a comparison of the measured and predicted performance. The prediction accuracy of K_T and K_Q for the skewed propeller was 3.6 % and 4.4 %, respectively. In the main the agreement between the measured and predicted velocities was good. The largest differences were found in the tip region. Abdel-Maksoud, Menter and Wuttke (1998b) carried out additional open water calculations for a wide advance number range with the CFX-TASC flow code. They refined the grid development process. Templates that are independent of the geometry, were written. In this way grids for different geometries can be generated automatically. The flow field was not fully resolved with grids of 260000 knots, but this grid size captured major flow features correctly. The agreement between the calculations and measurements for conventional or moderately skewed propeller is good or very good.

Sánchez-Caja (1996) applied the compressible flow RANS code FINFLO to flow pattern and performance prediction. The propeller geometry and the inflow velocities were scaled for constant Reynolds number and for a low Mach number. The Navier-Stokes equations with the $k-\epsilon$ turbulence model are solved in a rotating frame using the finite volume method. The predictions of thrust and torque for propellers of simple geometry are accurate for the design advance number when more than 700000 cells are used. Differences lower than 1.5 percent are found. The corresponding efficiency is calculated with an error lower than 3 percent. At advance numbers about half of the design advance number, the differences from the experimental values are greater for the thrust and torque coefficients, however the efficiency is reasonably predicted. Later calculations with an artificial compressibility version of FINFLO showed insignificant differences from the earlier performance predictions for P4119 (in Gindroz et al., eds., 1998). Sánchez-Caja and Pylkkänen (1998) used an old icebreaker propeller with very thick blade sections as their second validation propeller.

Table 6.2. Comparison of calculated and measured performance of SVA4021 and SVA4020 propellers (Abdel-Maksoud et al., 1996).

$J=0.6788$	SVA4021	SVA4020
Skew angle extent	46.0 deg	16.0 deg
$K_T:155000$ knots	0.1978	0.1932
$K_T:315000$ knots	0.1911	0.1896
K_T (experimental)	0.1890	0.1830
$K_Q:155000$ knots	0.03375	0.03334
$K_Q:315000$ knots	0.03267	0.03274
K_Q (experimental)	0.03470	0.03420

Stanier (1998a) investigated the effect of skew on propeller flow patterns using a RANS equation code. The finite volume RANS code of Stanier has a mixing length, 3-D version of the Baldwin-Lomax turbulence model. Two propeller models of 0.3048 m diameter were investigated. Propeller C624 had straight blades with a conventional blade sections consisting of an elliptic/parabolic thickness form and a NACA $a=0.8$ camber line. C637 was a skewed propeller based on the same design requirement as C624, the same design thrust coefficient, radial and chordwise loading. Because of the skew, C637 has slightly different pitch and camber. In the calculations 458297 nodes were used. For C624 at the design advance number $J=0.771$ the RANS predictions for thrust and torque were within 1 % of the open water experimental results. For C637 at $J=0.771$ the RANS prediction for thrust was less than 2 % higher than the open water experimental result and the prediction for torque less than 4 % lower than the open water experimental result. Stanier hypothesised that the difference in the predicted torque between the straight and skewed propeller may be due to shortcomings in the turbulence model. Figure 6.5 depicts the predicted static pressure coefficients at $r/R=0.793$ for the two propellers at the design advance number. At $J=0.76$ C624 had a nearly constant pressure over the first 80 % of the section. C637 does not have this characteristic and the predicted pressure indicates better back sheet cavitation performance.

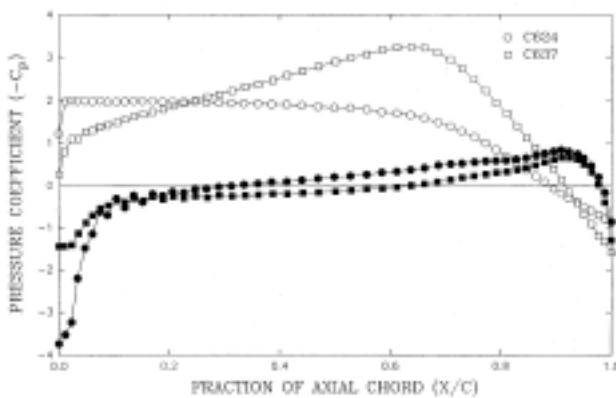


Figure 6.5. Blade surface static pressure distribution at $r/R=0.793$ for $J=0.76$ (Stanier, 1998a).

Stanier (1998b, 1998c) also investigated propeller scale effects by making calculations for five propellers with the model diameter of 0.3048 m and the assumed ship scale diameter of 6.096 m. For the ship scale turbulent flow developed from the leading edge. For the model scale transition was specified at a fixed percentage of the chord. The two straight bladed propellers exhibited small scale effects at the design operation point. Two skewed propellers showed significant scale effect having the thrust coefficients reduced from their model scale values. Boundary layer separation near the trailing edge was predicted. The separation was reflected in the suction side static pressure and velocity diagrams. The third skewed propeller showed scale effect having the thrust and torque coefficients increased by 1.4 % and 3.1 % from their respective model scale predictions.

Hsiao and Pauley (1998) applied the RANS solver INS3D-UP to calculate the rotating propeller flow. The INS3D-UP code is based on Chorin's artificial compressibility approach. The INS3D-UP code is accompanied by the Baldwin-Barth one-equation turbulence model which is derived from a simplified form of the standard $k-\epsilon$ equations. This model is simpler than the two-equation model and also eliminates the need to define the turbulent mixing length which is required in Baldwin-Lomax algebraic model. The spatial differencing of the convective terms uses a fifth-order accurate flux-difference splitting. A second-order central differencing is used for the viscous terms.

Hsiao and Pauley (1998) conducted calculations for the DTMB Propeller P5168 of the

diameter 0.4 m for three advance numbers. The grid had 2.4 million points. Table 6.3 compares the predicted and measured performance. The calculations for P5168 under-predicted the tip vortex strength with about 10 % difference. Figure 7.3 compares the computed and measured tip vortex structures. Since the grids used had at least 16×20 grid points within the tip vortex core, Hsiao and Pauley considered that the discrepancy between the numerical and experimental results was likely to have been caused by the one-equation turbulence model used. The pressure coefficient along the tip vortex core indicated that the minimum pressure coefficient occurred very close to the tip trailing edge. This implied that tip vortex cavitation also occurred near the trailing edge.

Table 6.3. Comparison of K_T and K_Q for P5168 at three advance numbers (Hsiao & Pauley, 1998).

J	$K_T(\text{cal})$	$K_T(\text{ex})$	$K_Q(\text{cal})$	$K_Q(\text{ex})$
0.98	0.404	0.371	0.0901	0.0888
1.10	0.333	0.313	0.0781	0.0783
1.27	0.238	0.229	0.0606	0.0618

After the validation calculations for P5168, a propeller with a modified tip geometry was designed. The modification was made by increasing the thickness of the blade tip gradually from zero at $0.8R$ to 50 % at the tip. The modified tip has a larger low pressure region near the tip trailing edge which indicated the tip vortex roll-up position moved further upstream for the modified tip case. In this way the roll-up entrains more low momentum boundary layer flow into the tip vortex and attenuates the tip vortex strength.

Viot et al. (1998) investigated the ability of two commercial RANS codes to predict the tip vortex flow very near the tip of an elliptical wing. The model parameters varied in the investigation were spatial resolution along the path of the tip vortex, turbulence models, convection schemes, and exit boundary conditions. The total number of cells of the mesh was 350000. The conclusions of Viot et al. were as follows. (1) The agreement between the numerically predicted and experimentally obtained non-dimensional vortex intensities along the vortex path is very good for all RANS codes and turbulence models tried. (2) The local vortex core radii are systematically over-estimated and, in consequence, the pressure on the vortex axis is under-predicted. (3) Grid refinement has a relatively low influence

on the local vortex intensity and slightly decreased the local vortex core radius. (4) The use of a $k-\epsilon$ RNG or a non-linear $k-\epsilon$ model decreased the local core radius compared with the $k-\epsilon$ model and thus improved correlation. The higher order discretisation scheme strongly decreased the local core radius as compared to the first order scheme.

Chen (1996) applied incompressible RANS equation code to calculate the unsteady four-quadrant marine screw propeller flow. The computational method is similar to that used by Stern et al. (1994).

The flow of crashahead and crashback condition is unsteady (see also Section 8.5). Time-accurate simulations were not attempted as this would have involved the simulation of all the blades with free surface or cavitation effects. Mean solutions were obtained by averaging the unsteady results and assuming that the periodic symmetry plane acts as a splitter plane, i.e., the flow in one blade passage was studied. The prediction of large negative pressures resulted in large over-predictions of K_T and K_Q . The over-predicted pressure is caused by disregarding free surface, ventilation and cavitation effects, and possibly by the inadequacies of the Baldwin-Lomax turbulence model. A cavitation correction based on two-dimensional flow model was introduced. In the cavitation correction vapour pressure coefficient replaces the coefficient of surface pressure where the surface pressure coefficient is lower. The effect of the cavitation correction on performance is clearly shown in Table 6.4.

Table 6.4. Comparison of the calculated and measured performance of DTMB P4381 (Chen, 1996).

J	0.5	0.8
Operation	Crashback	Crashback
K_T (calc.)	0.651	0.710
K_T (calc.+cavit.c.)	0.255	0.603
K_T (exp.)	0.331	0.618
K_Q (calc.)	0.1370	0.1380
K_Q (calc.+cavit.c.)	0.0561	0.1184
K_Q (exp.)	0.0671	0.1110

Chen (1996) also provided an uncertainty analysis that follows the standards and guidelines of ASME. The solutions have an overall uncertainty of about 3.5 % for the integral

quantities, i.e., for K_T and K_Q , at the design condition. Uncertainty in the predicted flow is due to both modelling and numerical errors. In a later paper Stern et al. (Kim, Kim, and Stern, 1998) improved grid generation especially near the leading edge.

Propeller-Hull Interaction. Several researchers performed viscous interaction calculations for ship hull and the propeller, in which the propeller effects are replaced by body forces that are obtained propeller lifting surface or panel method programs. Hally and Laurens (1998) developed a procedure to simulate hull-propeller interaction using force fields within the Navier-Stokes equation code. The propeller is modelled by a panel code, and time dependence is ensured by the Lagrangian method. The pressure coefficient distribution on the blade surface by the potential code is transformed into a force field within the Navier-Stokes mesh. The procedure implies a time average. Chung and Min (1998) investigated the interaction flow of an axisymmetric body and propeller. Korpus et al. (1998) investigated the interaction flow of a tanker and an azimuthing thruster.

McDonald and Whitfield (1996) reported on a computational method for predicting the trajectory of a fully appended self-propelled underwater vehicle that has a rotating propeller. The numerical solution of the three-dimensional unsteady incompressible turbulent Navier-Stokes equations is supplemented by a six-degree of freedom computational method. The artificial compressibility method is applied. The thin-layer approximations of an algebraic turbulence model is implemented. The Navier-Stokes equations are solved using a multiblock multigrid scheme with relative motion structured sub-blocks for handling the rotating propeller. The approach to model the actual propeller is to use relative motion blocks that include the rotating blades moving relative to adjacent blocks with a region of blocks near the relative interface being treated using a localised grid distortion technique. This method of handling the relative motion blocks insures the continuity of grid lines. The relative motion blocks change partners periodically. This approach also eliminates the need to interpolate the solution vector from one grid to another. The cell volumes do change in time and hence the geometric conservation law must be satisfied. The grid of the particular sample case consisted of 11.6 million points and 51 blocks. It turned out that the effect of the rotation of the

propeller was such that the vehicle initially had more drag than thrust and consequently the rotation rate of the propeller was increased to compensate for this imbalance of the axial force.

Abdel-Maksoud, Menter and Wuttke (1998a) addressed the ship-propeller interaction problem with the RANS equation code CFX-TASCflow. In the grid of the ship a cylinder is left behind the ship for the grid of the propeller. The diameter of and the length of cylinder are equal to the outside dimensions of the propeller grid. CFX-TASCflow features a generalised grid interface which allows to combine grids with non-matching points. Most of the computations were based on a so-called "frozen rotor" assumption. The unsteady computations were started from a converged frozen rotor calculation. In the ship-propeller interaction calculations 65000 nodes per propeller were used. The calculated axial wake field without the propeller was in good agreement with the measurements in the region below the propeller shaft. Some differences were seen in the region above it. The comparison between measured and calculated results of propeller slipstream showed that the resolution of the numerical grid was not sufficient for the prediction of the high velocity gradient at the outside boundary of the slipstream where the interaction between the rotating and non-rotating flow takes place. The calculated velocity diagrams for the frozen rotor assumption clearly showed the suction effect of the propeller. The comparison of predicted suction side pressures between quasi-steady and unsteady calculations in the region above propeller shaft level, showed differences. Otherwise the predicted pressure distribution by the two methods agreed. The mean quasi-steady predicted $(1-t_R)$ was 0.804 which is 8.6 % lower than the measured $(1-t)$.

6.5 Conclusions

RANS equation codes are capable of predicting accurately propeller open water performance and pressure distributions on the blade at the design advance number. The accuracy of performance prediction for off-design advance numbers that are about half of the design advance number is good or acceptable. The main features of the flow field are generally well predicted. With an adequately dense grid and a suitable turbulence model RANS codes are capable predicting the tip vortex flow accurately. In the 1990's time-accurate solu-

tions of unsteady propulsor flow are very time consuming. As an alternative quicker method mean solutions are obtained by the quasi-steady method or averaging procedures. Since the mid 1990's more attention has been paid to the creation of grids (meshing). The prediction accuracy can be increased by optimizing the cell distribution in areas of particular interest or importance. By using templates meshes can be generated automatically and quickly.

Potential based panel methods are most widely used. In the 1990's the development emphasis of vortex wake models has been in more accurate modeling of the tip region flow and in the inclusion of simple viscous considerations in the model. Panel methods have been extended to problems of the unsteady performance and cavitation prediction of propellers. The recent improvements in panel method codes have resulted in good agreement between the measured propeller and predicted performance and pressure distributions on the blade for most types of propellers. Panel method predictions of the details of slipstream velocity field are not accurate. Viscous corrections and modeling of the trailing vortex sheet would be important for further improvement of the accuracy of the panel methods.

Additional experimental data of blade surface pressures and slipstream velocities are needed for the validation of RANS equation and panel method codes. Very little flow field data for off-design operation conditions and ship scale propellers have been published.

7 REVIEW OF TASK 5 RANS/PANEL METHOD WORKSHOP

7.1 Introduction

The 22nd ITTC Propulsion Committee decided to organise a workshop of comparative exercise of propeller performance by RANS and/or panel method code and unsteady fluctuating pressure on propeller blades by panel method code. The aims of the workshop were to clarify the accuracy of the calculations of RANS and the panel method for the analysis of marine propellers and to investigate the applicability of such methods.

Table 7.1 lists three propellers selected as the test propellers. The DTMB P4119 propeller has been used in the 20th ITTC (1993) com-



parative calculations of surface panel methods (Koyama, 1993). At the present workshop the comparative calculations of flow fields around this propeller were added (Jessup, 1998a). Two more propellers, DTMB P4679 (Jessup, 1998b) and Seiun-Marun HSP (Hoshino, 1998), with their experimental data of the pressure distributions on the blades of the propeller operating in non-uniform flow, eg. behind a ship, were made available for the workshop.

Table 7.1 Test Propellers

	Propeller	Method
Steady Calculation	DTMB P4119	RANS and Panel Method
Unsteady Calculation	DTMB P4679	Panel Method
Unsteady Calculation	Seiun-Marun HSP	Panel Method

Twenty-nine organisations expressed an interest in conducting the comparative calculation by RANS and/or the panel method. The Committee furnished them with the calculation documents on December 8, 1997. A total of twenty organisations have sent the results of calculations by RANS and/or the panel method to the Committee. The workshop was held in Grenoble on 5-6 April 1998. The original manuscript of the workshop proceedings is kept at Bassin d'Essais des Carènes in Val de Reuil (Gindroz et al., eds., 1998)

7.2 Comparison of RANS Method Calculations in Uniform Flow

Propeller P4119. The data set selected for the comparison of propeller RANS computations are measurements obtained on Propeller DTMB P4119 (Jessup, 1989, 1994). Extensive LDV measurements were performed of field velocities about the propeller operating in uniform inflow in the DTMB 24" Water Tunnel. Blade boundary layers were also measured with LDV and blade pressure distributions were derived from boundary layer edge velocity measurements. Open water tests were performed earlier in the DTMB tow tank.

The propeller DTMB P4119 is a three bladed, 12" (D=304.8mm), propeller designed in the 1960's to validate lifting surface design methods. The propeller has no skew or rake, and is spanwise optimally loaded. The

propeller geometry is given in the reference (Jessup, 1998a).

The test conditions are given in Table 7.2. During LDV tests, distributed roughness was applied to the leading edge of two blades, the third blade was untripped without roughness. The data provided is for the untripped blade without leading edge roughness applied.

Table 7.2 Test Conditions for P4119

$J = V/nD$	0.833
V, advance velocity	8.33 f/s (2.540 m/s)
n, rotation speed	10 rps

Calculations. The following eight organisations have conducted RANS calculations on the DTMB P4119 propeller. HMRI conducted two calculations based on different RANS method codes but one result set is compared in the present report. Seven organisations excluding CSSRC presented the results at the workshop.

- 1) Dr. J. M. Laurens, Bassin d'Essais des Carènes (BEC), FRANCE
- 2) Dr. H. Streckwall, Hamburg Ship Model Basin (HSVA), GERMANY
- 3) Dr. K.-N. Chung and Dr. B.-J. Chang, Hyundai Maritime Research Institute, HMRI, KOREA
- 4) Dr. S. Uto, Ship Research Institute (SRI), JAPAN
- 5) Mr. M. Stanier, Defense Evaluation Research Agency (DERA), UNITED KINGDOM
- 6) Dr. A. Sánchez-Caja, Technical Research Center of Finland (VTT), FINLAND
- 7) Dr. B. Chen and Prof. F. Stern, University of Iowa (UI), USA
- 8) Dr. D.-H. Tang, Dr. J.-D. Chen, China Ship Scientific Research Center (CSSRC), CHINA

HSVA used commercial RANS code STAR-CD. VTT used RANS code FINFLO developed at the Technical University of Helsinki. Other organisations used their own developed RANS codes.

Comparisons for P4119. The calculation results of thrust and torque coefficients K_T , K_Q are compared with the experiments as shown in Figure 7.1. The scatter of the calculation results among the organisations is very small especially for the thrust coefficients. The

agreement between the calculations and the experiments is very good over the wide range of advance ratio J . In particular, the calculation results of K_T agree surprisingly well with the experiments over the wide range.

The calculation results of pressure coefficients C_p at 0.3 (not shown, see workshop report) and 0.7 radii are compared with the experiments as shown in Figure 7.2. The definition of C_p is as follows:

$$C_p = (p - p_0) / (1/2\rho V_R^2) = 1 - (V_t/V_R)^2 \quad (7)$$

$$V_R^2 = V_x^2 + (2\pi nr)^2 \quad (8)$$

where,

- p = pressure on the blade
 p_0 = static pressure in infinity
 V_t = total boundary layer edge velocity.

The scatter of the calculation results at 0.3 radius is relatively large but the scatter of the calculation results at 0.7 radius is small. The calculation results of SRI show different tendencies for the chordwise pressure distribution. HMRI and UI had used the same RANS method code and therefore both results coincided very well with each other. The agreement between the calculations and the experiments is generally good. VTT and DERA calculated the pressure coefficient in two different ways: using the calculated static pressures on the blade surface $C_p(P)$ and using the calculated velocities at the edge of the blade boundary layer $C_p(V)$. The calculation results of VTT are shown as VTT(P) and VTT(V) in Figure 7.2. The pressures using the edge velocities VTT(V) are closer to the experiments than those using the blade surface pressures VTT(P), because the experimental pressures had been determined from the velocities at the edge of the blade boundary layer measured by LDV.

The calculation results of the field point velocities at the $x/R=0.3281$ plane behind the propeller are compared with the experiments as shown in Figures 7.3-7.5. The circumferential averaged axial velocities are compared in Figure 7.3. The agreement with the measurements is good except for the calculation results of SRI. The phase averaged velocities at 0.7 and 0.924 radii are compared in Figures 7.4 and 7.5. The agreement with the measurements is good in the inner radius (0.7R) but not so good in the radius of the tip vortex (0.924R). The velocity changes due to the wake of the blade at 0.7 radius are simulated well in the calculations. However, the calculation results of the velocity

changes at the tip vortex position differ from the experiments.

7.3 Comparison of Panel Method Calculations in Uniform Flow

Calculations. The following fourteen organisations have conducted panel method calculations on the DTMB P4119 propeller operating in uniform flow and have sent the calculation results. Eleven organisations excluding MIT, CSSRC and SSMB presented the results at the workshop.

- 1) Dr. J. M. Laurens, Bassin d'Essais des Carènes (BEC), FRANCE
- 2) Dr. T. Hoshino, Mitsubishi Heavy Industries, Ltd. (MHI), JAPAN
- 3) Dr. H. Streckwall, Hamburg Ship Model Basin (HSVA), GERMANY
- 4) Dr. K. Koyama, Ship Research Institute (SRI), JAPAN
- 5) Dr. C. L. Narayana, National Aerospace Laboratories (NAL), INDIA
- 6) Mr. B. Ganea, Research and Design Institute for Shipbuilding (ICEPRONAVSA), ROMANIA
- 7) Prof. G. Politis, National Tech. University of Athens (NTUA), GREECE
- 8) Prof. J. Ando, Kyushu University (KU), JAPAN
- 9) Dr. J.-T. Lee, Korean Research Institute of Ships (KRISO), KOREA
- 10) Dr. M. Hughes, Analytical Method, Inc. (AMI), USA
- 11) Dr. Ju Timoshin and Ms. I. Frolova, Krylov Shipbuilding Research Institute (KSRI), RUSSIA
- 12) Prof. J. E. Kerwin, Massachusetts Institute of Technology (MIT), USA
- 13) Dr. D.-H. Tang, Dr. J.-D. Chen, China Ship Scientific Research Center (CSSRC), CHINA
- 14) Dr. Y. G. Kim, Samsung Ship Model Basin (SSMB), KOREA

Most of the organisations used a potential based panel method. Some organisations used a velocity based panel method.

Comparisons for P4119. The calculation results of thrust and torque coefficients K_T , K_Q are compared with the experiments as shown in Figures 7.6 and 7.7. The scatter of the calculation results among the organisations is small but larger than the RANS calculations. The agreement between the calculations and the



experiments is very good over a wide range of advance ratio.

The calculation results of pressure coefficients C_p at 0.7 radii are compared with the experiments in Figures 7.8. The scatter of the calculation results is smaller than the RANS calculations except the calculation results of MIT. The agreement between the calculations and the experiments is good and better than the RANS calculations. In the panel method the blade pressures are calculated by using the surface velocities on the blade that are similar to the experimental pressures determined from the velocities at the edge of the blade boundary layer measured by LDV.

The calculation results of the circumferential averaged field point velocities at the $x/R=0.3281$ plane behind the propeller are compared with the experiments as shown in Figures 7.9. The agreement with the measurements is generally good but worse than the RANS calculations.

7.4 Comparison of Panel Method Calculations in Non-Uniform Flow

Propeller P4679. The data set selected for comparison of unsteady panel method computations are measurements obtained on DTMB P4679 (Jessup, 1982). In the tests conducted in the DTMB High Speed Basin, the propeller was driven from downstream with a strut/pod open-water drive system, whose shaft was inclined 7.5 degrees from the horizontal axis. Unsteady blade surface pressure measurements were obtained at approximate 40 locations on the suction side and 40 locations on the pressure side of the blade at the 0.5, 0.7, and 0.9 radius.

These data are considered a good initial test case for unsteady panel methods because of the simplicity of the wake and measured unsteady response. The pressure is presented as the mean and first harmonic amplitude and phase at each gage location. The intent of the workshop was not to evaluate steady panel methods, but it may be useful to compare the mean pressure distributions with the steady panel method predictions prior to performing the unsteady panel calculation.

The propeller DTMB P4679 is a three bladed 24''(607mm) diameter right handed propeller designed to incorporate the features

of a modern Controllable Pitch Propeller (CPP). The wide chords were a result of maintaining the same blade area and loading as a typical five bladed propeller. The propeller geometry is given in the references (Jessup, 1982, 1998b).

The propeller was tested in uniform inflow, driven from downstream at a shaft inclination of 7.5 degrees to the horizontal. Test conditions for comparative studies are shown in Tables 7.3 and 7.4.

Table 7.3 Test Conditions for P4679

$J = V/nD$	1.078	0.719
V , advance velocity	17.67 f/s (5.39m/s)	11.80 f/s (3.60 m/s)
n , rotation speed	8.20 rps	8.21 rps

The 7.5 degree shaft inclination produced a first harmonic variation in the two of the three components of propeller inflow. No wake surveys were conducted, so that the geometric flow variation, described below, should be assumed. The effect of the flow around the hub is known to augment the tangential velocity variation near the hub, but no attempt has been made to predict the near hub flows. Since the inner most pressure measurements were made at 0.5 radius, it is not expected that flows near the hub significantly effected the measured result.

Table 7.4 Onset Flows for P4679

Velocity	first harmonic amplitude, V_1	$V(\theta)$
axial	0	$V_x(\theta) = V \cos(7.5^\circ) = 0.991 V$
tangential	V_T	$V_t(\theta) = V_T \sin \theta = 0.1305 V \sin \theta$
radial	V_T	$V_r(\theta) = -V_T \cos \theta = -0.1305 V \cos \theta$

The symbols are as follows.

- θ = Position angle about propeller axis, measured from top position, positive counterclockwise looking downstream
- V_T = Inclination crossflow, $V_T = V \sin(7.5^\circ) = 0.1305 V$
- $V_t(\theta)$ = Tangential velocity at propeller plane, positive in propeller rotation direction
- $V_r(\theta)$ = Radial velocity at propeller plane, positive outward
- $V_x(\theta)$ = Axial velocity at propeller plane
- V = Carriage velocity, speed in horizontal direction.

The blade pressure data are provided as the mean, first harmonic amplitude and phase of the blade surface pressure coefficient, C_P , at the two specified advance coefficients. The definitions are listed below.

$$C_P = (p - p_0) / (1/2\rho V_R^2) \quad (9)$$

$$C_P(\theta) = C_{P,M} + C_{P,1} \cos(\theta - \phi_1) \quad (10)$$

where,

$C_{P,M}$ = Mean value of pressure coefficient
 $C_{P,1}$ = First shaft rate harmonic amplitude of pressure coefficient
 ϕ_1 = Cosine phase angle, corresponding to the angle of maximum pressure.

Phase data are contained in the Workshop Proceedings.

Seiun-Maru HSP. The second data set selected for comparison of Unsteady Panel Method Computations is the full scale measurements obtained on a Seiun-Maru propeller. Very few experimental data of unsteady pressure distributions on propeller blades are available for comparison, because of the difficulty in mounting pressure transducers of high response on the propeller blade. Available full scale data sets are those obtained on the blade of a conventional propeller (CP) and a highly skewed propeller (HSP) of the training ship "Seiun-Maru", which were conducted by Ukon et al. (1991a, 1991b).

Unsteady blade surface pressure measurements were performed at 15 locations on the suction side and 9 locations on the pressure side of the blade at the 0.5, 0.7, 0.9 and 0.95 radius for the two propellers, CP and HSP. The Seiun-Maru HSP was selected for the present comparative study because some discrepancies between the measurements and theory had been observed for the HSP. This second data were considered a more applicable test case to evaluate unsteady panel methods because of the propeller data operating in a merchant ship type wake field.

The Seiun-Maru HSP is a five bladed skewed type propeller designed to reduce propeller induced hull pressure fluctuations. The propeller geometry is given in the reference (Hoshino, 1998).

The unsteady pressure measurements on the propeller blade of the HSP were performed at

several working conditions of propeller rotational speed 70, 90, 110 and 149 rpm. The pressure data measured at the rotational speed of 90 rpm were selected because of the accuracy in the measurements and the small area of sheet cavitation on the propeller blade. Operating conditions of the HSP during the pressure measurements are shown in Table 7.5.

Table 7.5 Test Conditions for "S-M" HSP

V, ship speed	9.0 knots
n, rotation speed	90.7 rpm
$J = V/nD$	0.851
$K_T = T/\rho n^2 D^4$	0.172
$K_Q = Q/\rho n^2 D^5$	0.0268

Wake distribution used in the present comparative calculation is the ship wake estimated by Sasajima and Tanaka's method from the wake measurements in model scale performed in a towing tank. Estimated wake distribution in full scale is shown in the reference (Hoshino, 1998). Not only the axial component but also the tangential and radial components were to be taken into consideration in calculation.

The unsteady blade pressures are expressed as the pressure coefficient C_P defined by

$$C_P(\theta) = (p(\theta) - p_0) / (1/2\rho n^2 D^2) \quad (11)$$

where

$p(\theta)$ = unsteady blade pressure
 p_0 = static pressure in the undisturbed inflow.

Note that the definition of the pressure coefficient is different from that used for DTMB P4118 and P4679.

Calculations. The following thirteen organisations have conducted panel method calculations on the DTMB P4679 and/or the Seiun-Maru highly skewed propeller. Ten organisations excluding MIT, CSSRC and SSMB presented the results at the workshop.

- 1) Dr. J. M. Laurens, Bassin d'Essais des Carènes (BEC), FRANCE
- 2) Dr. T. Hoshino, Mitsubishi Heavy Industries, Ltd. (MHI), JAPAN
- 3) Dr. H. Streckwall, Hamburg Ship Model Basin (HSVA), GERMANY
- 4) Dr. S. Jessup, Naval Surface Warfare Center, Carderock Div. (DTMB), USA
- 5) Mr. B. Ganea, Research and Design Institute for Shipbuilding (ICEPRONAVSA), ROMANIA



- 6) Prof. G. Politis, National Tech. University of Athens (NTUA), GREECE
- 7) Prof. J. Ando, Kyushu University (KU), JAPAN
- 8) Dr. J.-T. Lee, Korean Research Institute of Ships (KRISO), KOREA
- 9) Dr. M. Hughes, Analytical Method, Inc. (AMI), USA
- 10) Dr. P. Liu, MMC Engineering & Research (MMC), CANADA
- 11) Prof. J. E. Kerwin, Massachusetts Institute of Technology (MIT), USA
- 12) Dr. D.-H. Tang, Dr. J.-D. Chen, China Ship Scientific Research Center (CSSRC), CHINA
- 13) Dr. Y. G. Kim, Samsung Ship Model Basin (SSMB), KOREA

Most of the organisations used a potential based panel method. Some organisations used a velocity based panel method.

Comparisons for P4679. The calculation results on the blade section at 0.7 radius of the propeller operating at $J=1.078$ are shown in the following, because the same tendency was observed for the results at other radii.

The calculation results of the mean pressure distributions C_p on the blade section at 0.7 radius are compared with the experiments as shown in Figure 7.10. The agreement between the calculations and the experiments is reasonably good.

The calculation results of the first harmonic amplitude $C_{p,1}$ distributions of the blade pressure are compared with the experimental results in Figures 7.11. The scatter of the calculated amplitudes of the first harmonic pressure fluctuation is relatively large and the agreement with the experiments is not so good. The scatter of the calculated phase angles (not shown here) is small for several calculation results but some results differ from the experiments.

Comparisons for Seiun-Maru HSP. The calculation results of the blade thrust fluctuations of the Seiun-Maru HSP are compared in Figure 7.12 as a function of the blade angular position θ .

The thrust at $\theta=90$ deg is larger than those at $\theta=270$ deg, which may be caused by the tangential inflow component. This tendency is shown in most of the calculation results except the results of BEC and MMC.

The calculation results of the pressure fluctuations on the back (suction) side and the face (pressure) side of the blade section at 0.7 radii during one revolution are compared with the experiments in Figures 7.13 and 7.14 as a function of the blade angular position θ .

The scatter of the pressure fluctuations among the organisations is relatively small except the results of BEC and SSMB. The agreement with the experiments is reasonably good at the chordwise position $x/c=0.25$ near the leading edge but the agreement with the experiments becomes worse at the chordwise position $x/c=0.8$ near the trailing edge.

7.5 Conclusions

Conclusions of the comparative calculations and workshop are as follows,

- (1) RANS and the panel method can predict the open water performance of a propeller very accurately and therefore can be used in the design stage of marine propellers.
- (2) RANS and the panel method can predict precisely the pressure distributions on the blade of a propeller operating in uniform flow. In the RANS there are two different ways to calculate the pressure on the blade: using the calculated static pressures on the blade and using the calculated velocities at the edge of the blade boundary layer. The pressures using the edge velocities were closer to the experiments because the experimental pressures had been determined from the velocities at the edge of the blade boundary layer measured by LDV.
- (3) RANS codes can predict the velocity distributions of propeller slipstream with reasonable accuracy but the accuracy of the velocity predictions by the panel method is not enough because of the lack of the viscous effect in the theory.
- (4) The panel method can predict the pressure fluctuations on the blade surfaces of a propeller operating in non-uniform flow behind a ship with reasonable accuracy and thus would be able to predict the occurrence of cavitation on the blade.
- (5) All of the panel methods overpredicted the pressures on the back side near the trailing edge of the blade section at 0.9 radius of Seiun-Maru HSP. This could be due to viscous effects. Further calculations by RANS codes would be awaited.

7.6 RANS/Panel Method Workshop Figures

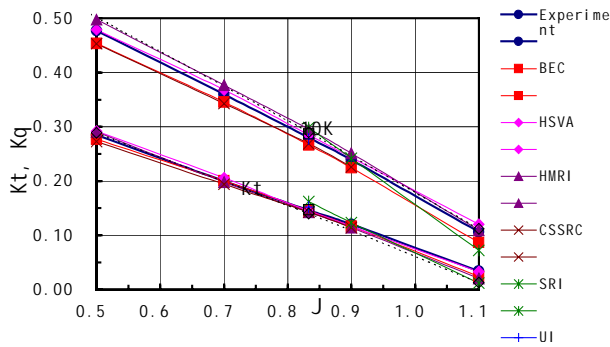


Figure 7.1 Comparison of open water characteristics of DTMB P4119 (RANS)

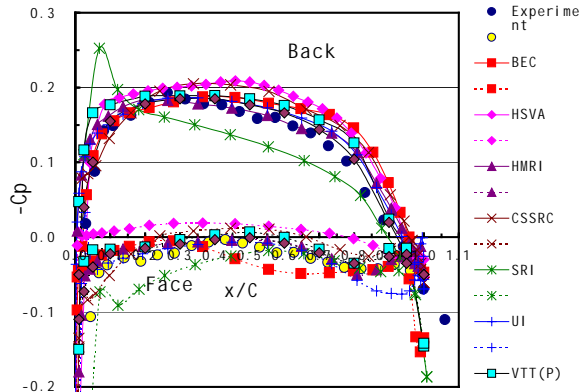


Figure 7.2 Comparison of chordwise pressure distributions at 0.7R for P4119 (RANS, J=0.833)

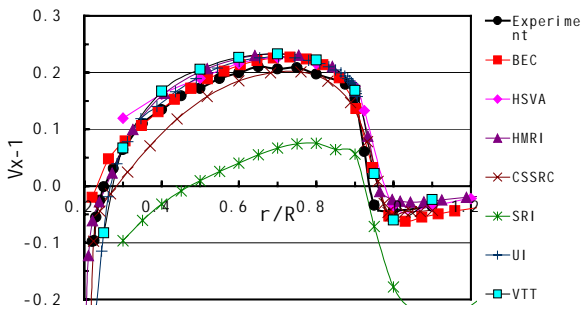


Figure 7.3 Comparison of circumferential average axial velocities at $x/R=0.3281$ for P4119, (RANS, $J=0.833$)

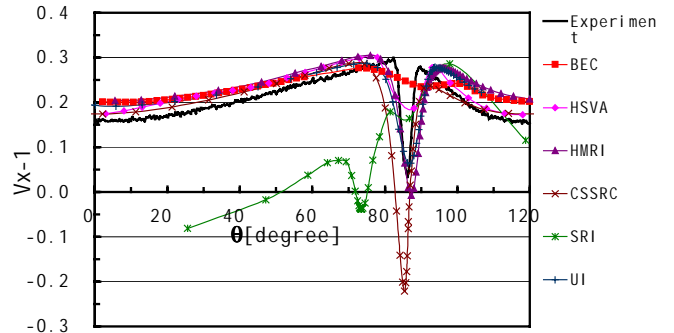


Figure 7.4 Comparison of phase average axial velocities at $x/R=0.3281$, $r/r=0.7$ for P4119 (RANS, $J=0.833$)

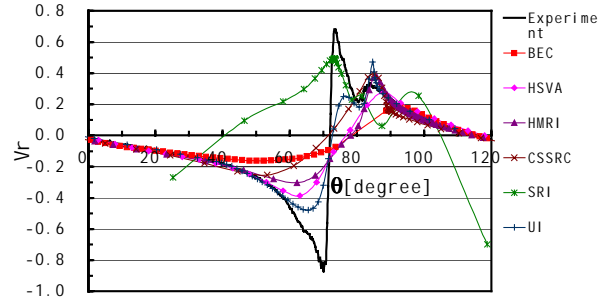


Figure 7.5 Comparison of phase average radial velocities at $x/R=0.3281$, $r/R=0.924$ for P4119 (RANS, $J=0.833$)

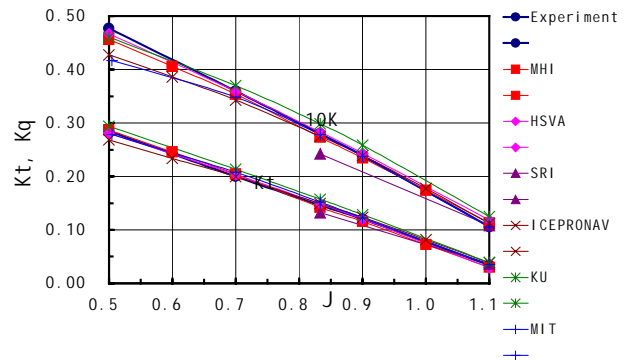


Figure 7.6 Comparison of open water characteristics of DTMB P4119 (Panel)

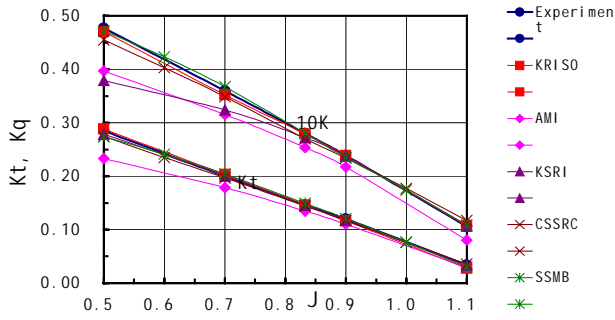


Figure 7.7 Comparison of open water characteristics of DTMB P4119 (Panel)

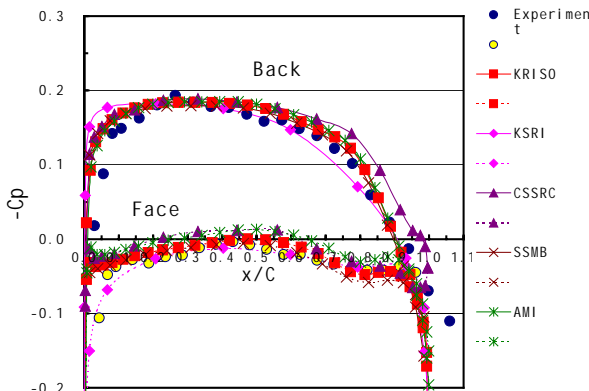
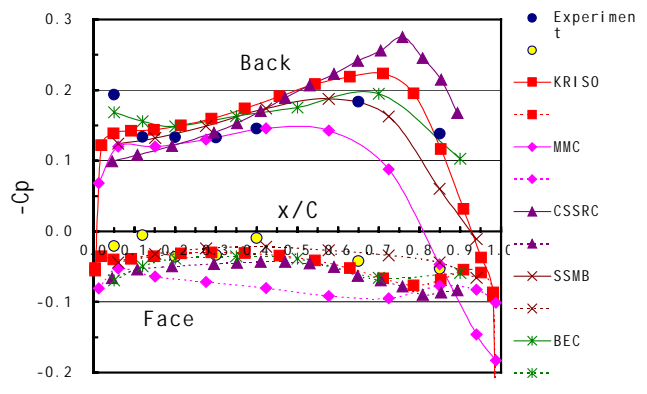
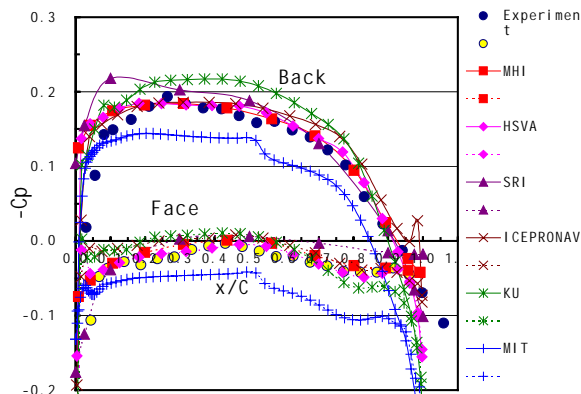
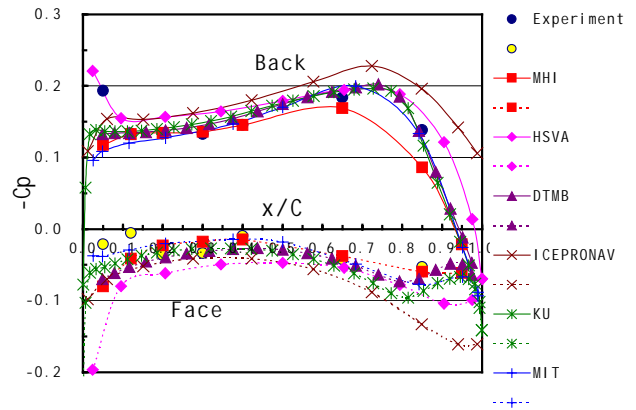


Figure 7.8 Comparison of chordwise pressure distributions at 0.7R for P4119 (Panel, J=0.833)

Figure 7.10 Comparison of chordwise mean pressure distributions at 0.7R for P4679 (Panel, J=1.078)

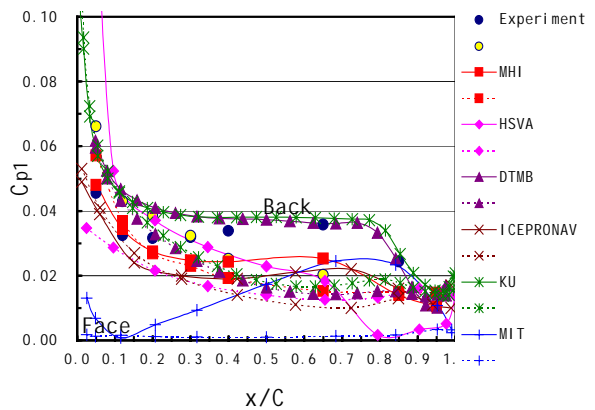


Figure 7.11 Comparison of first harmonic amplitude of pressure at 0.7R for P4679 (Panel, J=1.078)

Figure 7.9 Comparison of circumferential average axial velocities at $x/R=0.3281$ for P4119 (Panel, $J=0.833$)

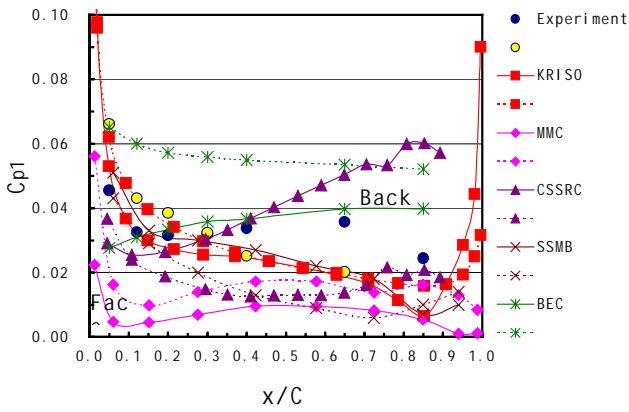


Figure 7.11 Comparison of first harmonic amplitude of pressure at 0.7R for P4679 (Panel, $J=1.078$)

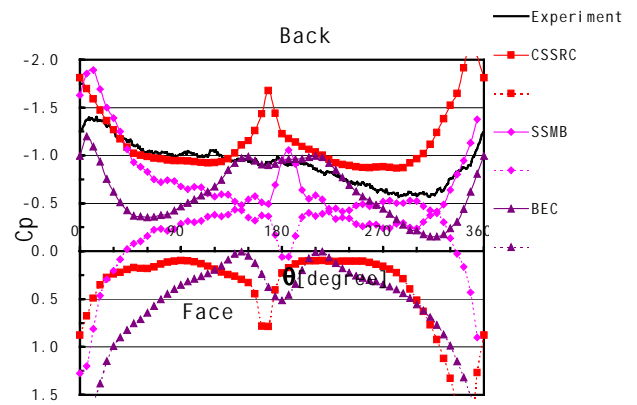


Figure 7.13 Comparison of pressure fluctuation of Seiu-Marui HSP at 0.7R (Panel, $x/c=0.25$)

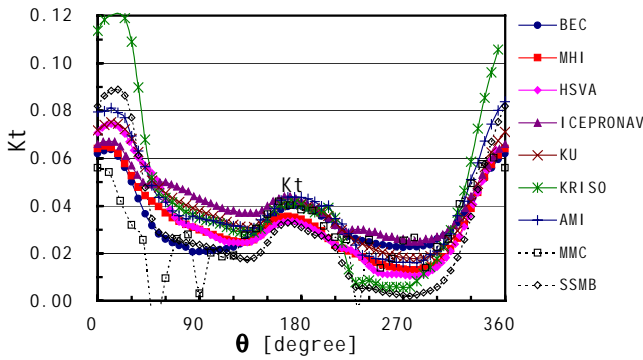


Figure 7.12 Comparison of thrust fluctuation of one blade of Seiu-Marui HSP (Panel)

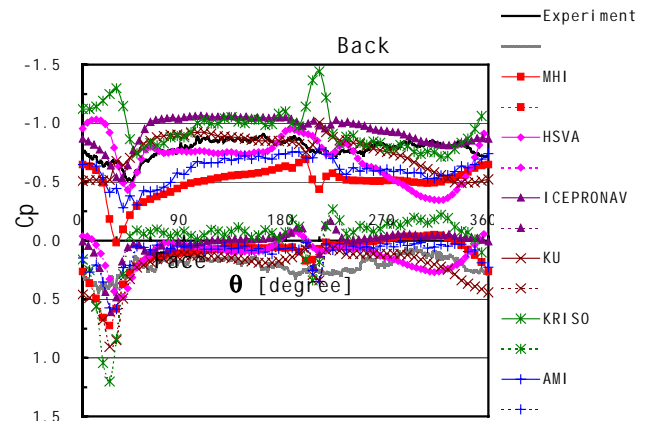


Figure 7.13 Comparison of pressure fluctuation of Seiu-Marui HSP at 0.7R (Panel, $x/c=0.25$)

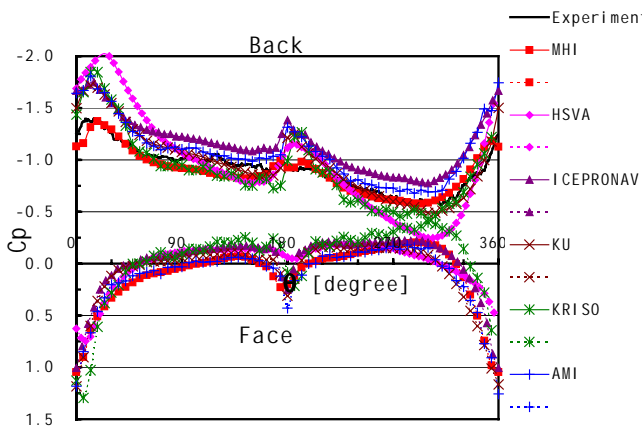


Figure 7.13 Comparison of pressure fluctuation of Seiu-Marui HSP at 0.7R (Panel, $x/c=0.25$)

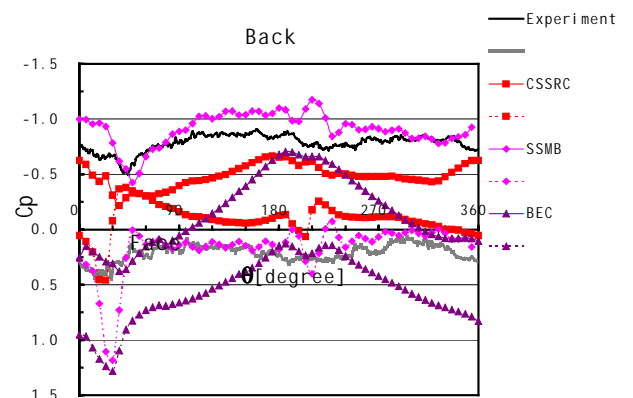


Figure 7.14 Comparison of pressure fluctuation of Seiu-Marui HSP at 0.7R (Panel, $x/c=0.8$)

8. REVIEW RESEARCH ON THE PERFORMANCE OF PROPELLERS IN VARIOUS CONDITIONS SUCH AS FOR SHIPS WHEN TURNING, ACCELERATING, DECELERATING, BACKING, OR OPERATING IN WAVES

8.1 Introduction

When a propeller operates in unsteady working conditions, such as for ships when turning, accelerating, decelerating, backing, or in waves, the inflow field into propeller disc is very different from steady ahead operation in calm seas. Severe problems, for example propeller strength and speed loss, occur due to the unsteady inflow field, due to waves and ship motions. Ship manoeuvres and operation in seaway affect cavitation behavior of the propellers and therefore also propeller induced pressure pulses and noise. Thus it is necessary for the propeller designer to take these effects into consideration.

8.2 Performance of the Propeller Operating in Waves

For ships operating in a rough sea, the propeller designer should consider the unsteady contributions to the wake field caused by the waves and wave induced ship motions. The combined effect of these two contributions has been investigated in the past by means of measuring load fluctuations on the propeller of ship models traveling in waves. Measurements were carried out by van Sluis (1972) on the shaft thrust fluctuations of an O.B.O. carrier type vessel in regular and irregular waves. It was concluded that the surge motion was an important influence. Jessup et al. (1982) tested a captive model in waves and carried out forced pitching tests in calm water and waves. They concluded that the wake field contributions due to wave particle velocity and pitch motion may be linearly superimposed.

Lipis (1975) developed a method for the calculation of hydrodynamic characteristics of the propeller which fluctuated harmonically in heave type motion. The unsteady lifting surface method was applied with allowance of the change of oblique angle in propeller disk and of vortex deformation due to motion.

Aalbers et al. (1985) carried out regular wave tests for a frigate type ship model. Tests

in calm water and regular waves were conducted with a captive model and a free (towed) model respectively. The motion of a ship in waves was calculated by means of a computer program based on three-dimensional diffraction theory. The amplitude of the oscillating local fluid velocity at a location in the propeller disc was obtained. It was proved from the comparison of average advance speed in waves with the calm water results that the potentials for the calm water wake field and the potentials due to wave action and motions may be linearly superimposed. An application in propeller design taking into consideration of the contributions of waves and ship motion showed that a complete picture of the influence of waves and ship motions on wake velocity and local pressure was necessary before a statement about changes in cavitation condition for the propeller could be made.

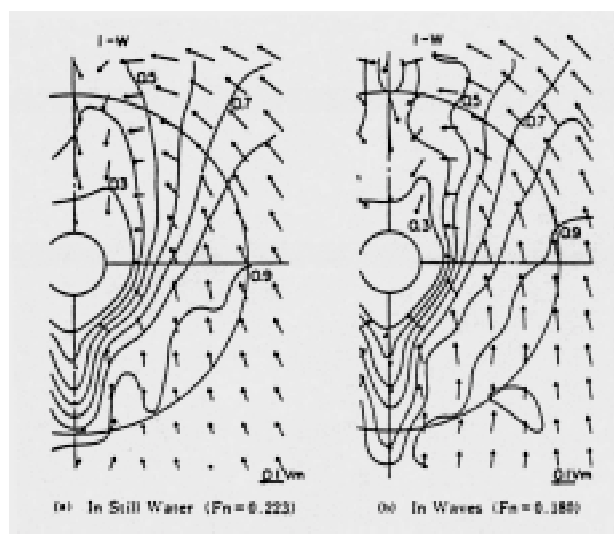


Figure 8.1 Velocity distribution at propeller disk (Takei et al., 1987).

Takei et al. (1987) carried out some experiments to study a car carrier model ship wake in regular head waves. Experimental results of circumferential average value of the wake fraction in the waves were compared with those in calm water. It is clear from the comparison that $(1-w)_w / (1-w)_s$ is nearly equal to 1.0 in the outer part of the radius and larger than 1.0 in the inner part of the radius, even up to 1.4 near the shaft of the propeller. That means the income flow to the propeller disk is accelerated, especially near the shaft of the propeller. Figure 8.1 shows the distribution of $(1-w)$ and velocity vector in the propeller disk in the calm water and waves. Variations of $(1-w)$ and velocity vector with time were also given in the paper. It can be seen from those

results that $(1-w)$ is larger than 1.0 appears in the lower part of the propeller disk due to the effect of waves. An extremely large change of wake pattern is found in the region of $(1-w) \geq 0.6$.

Chevalier et al. (1995) developed a numerical procedure to predict the unsteady onset flow into a propeller due to the waves and the wave-induced ship motions. The relative importance of the different components, incident wave, diffracted wave, and ship motions were studied. Data of MARIN experiments for a frigate type ship with a transom stern were applied for the validation of computation code SWAN (Ship Wave Analysis), which handles the complete 3-D potentials. It was confirmed that the flow can be linearised and the total flow can be obtained by linearly superposing the basic flow, steady wave flow, and unsteady wave flow. Extensive experiments were conducted at DTMB between 1979 and 1982 to study the effect of hull pitching motion and waves on propeller performance. The experiment confirmed the theoretical assumption that the individual influence of the wave and the induced velocities due to pitching in calm water can be linearly superimposed. Computer code PUF3 was used for predicting the unsteady loading and sheet cavitation extent on a propeller working in a non-uniform flow field. Further, PSF10 (Propeller Steady Flow Analysis Program) was used for the quasi-steady (instantaneous wakes at each time step in a wave period) computation. Unsteady forces on one blade computed in a quasi-steady approach are in good agreement with the experiments. The most significant contribution comes from the vertical motion of the propeller section, i.e., transverse flow from ship motion. Heave and pitch motions are responsible for the highest first harmonic variations. The biggest variations are encountered when wave length is close to the ship length and the vertical motions of the hull section above the propeller are the most important. The performance analysis of the DD963 propeller in regular waves representing sea state 3 to 4 showed that the surface cavitation inception speed would drop from 23 to 15 knots.

Jessup et al. (1996) developed a computational procedure to predict the influence of ship motions in waves on propeller cavitation inception. With SWAN code for predicting the ship motion in regular waves, it was appropriate to develop a numerical procedure to calcu-

late the time varying flow field into the propeller disk due to a ship operating in regular waves and calculate the effect of the unsteady flow field on propeller performance. The propeller performance was calculated in a quasi-steady fashion using a potential based panel code. Calculations were performed for a transom stern, frigate type combatant hull form operating in regular, ahead seas. The following conclusions were reached from calculations. (1) Of the flow variations calculated at propeller disk, the axial velocity variations were somewhat larger than the tangential velocities, and resulted in a larger effect on cavitation inception speed. (2) Of the three forms of cavitation predicted, the loss in inception speed due to seaway was larger for tip vortex, then blade surface, and least for root cavitation. (3) Propeller modifications to improve seaway cavitation performance must be traded off against adverse effects of cavitation at high speeds, such as thrust breakdown.

8.3 Performance of Propellers for Ships when Turning

Meyne (1974) developed a computer program to calculate the propeller blade stresses for various maneuvering conditions. It was assumed for all calculations that the axial wake field appropriate to a straight course and an upward flow of 10% in way of the propeller was maintained for all maneuvering conditions. For calculating the conditions obtaining during the turning circle a horizontal inflow angle of $0^\circ, 5^\circ, 15^\circ, 25^\circ, 35^\circ$ (for turns to port) and $-5^\circ, -15^\circ, -25^\circ, -35^\circ$ (for turns to starboard) was assumed. Results of the calculations show that the horizontal components of the thrust eccentricity remain vertically constant for the various helm angles to port and starboard, while there are considerable variations in vertical components. As a result the bearing loads are considerably increased and a large helm angle, in the case of a turn to port, would cause a well-defined increase in the stresses for the right-handed propeller, assuming full power and speed. A turn to starboard, on the other hand, would cause a slight reduction in the stresses. It was also found that there can be considerable increase in the stress levels in the propeller blades when the ship turns on a circular course.

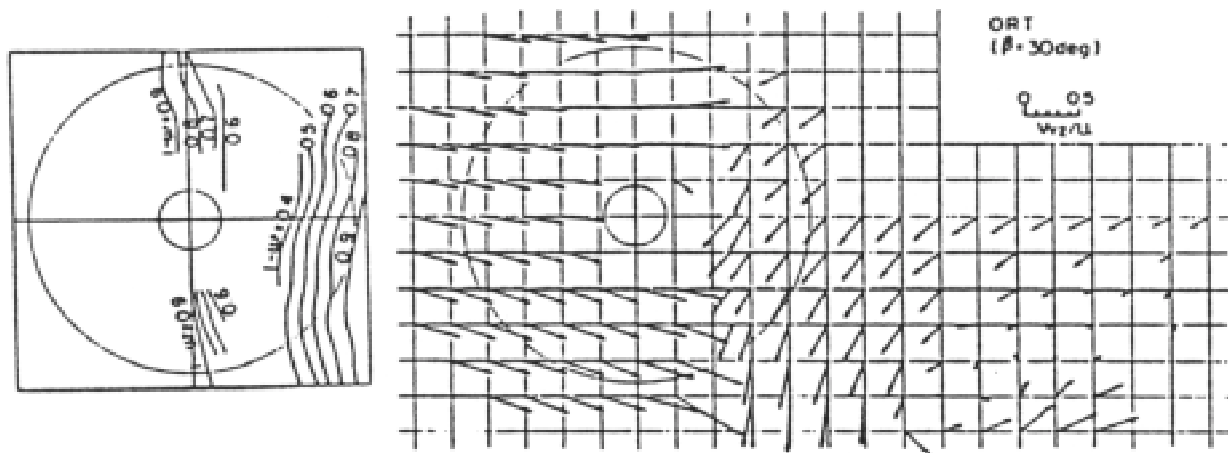


Figure 8.2 Wake distribution at propeller position under oblique motion (Matsumoto et al., 1986).

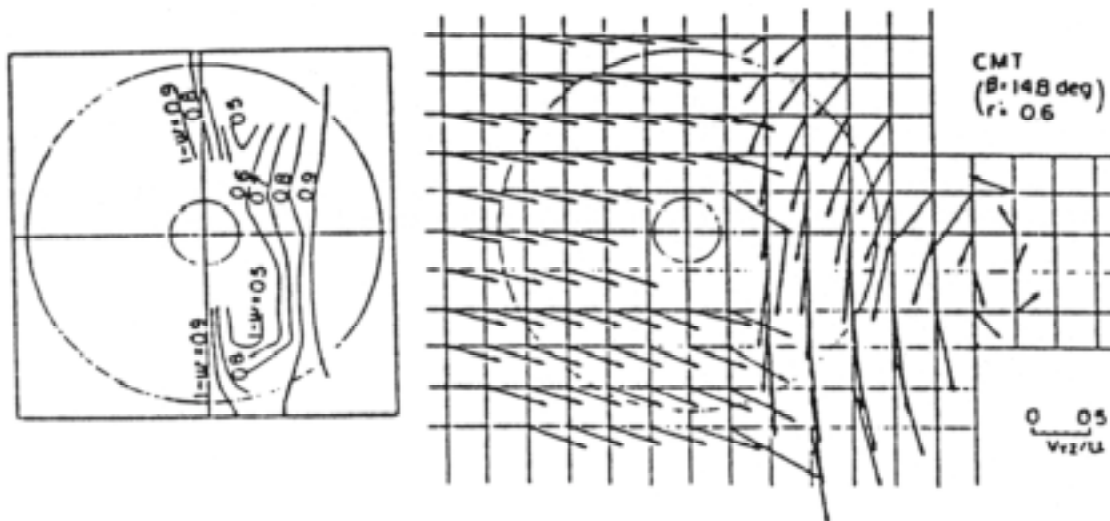


Figure 8.3 Wake distribution at propeller position under circular turning motion (Matsumoto et al., 1986)

Matsumoto et al. (1986) carried out systematic experiments to study the mathematical modeling of inflow velocity to a ship propeller undergoing maneuvers. The wake distribution at the propeller disc under ship maneuvering motion was measured. Significant difference in the wake distribution patterns under oblique or circular turning motion occurs in the location of the longitudinal vortex center, as shown in Figs. 8.2 and 8.3. The distance of the location of longitudinal vortex center from propeller plane is larger and the strength of the vortex is stronger when ship motion turns on a circular course. Hirano et al. (1992) proposed a simple prediction method for the maneuvering motion of SWATH ships.

8.4 Performance of Propellers when Ships Accelerating or Decelerating

Kim et al. (1991) analysed the transient response of propellers to changes in rotation rate and forward speed using a general unsteady vortex-lattice method. The thrust coefficient versus time step for the transient/maneuvering process was given; the initial steady-state solution was first obtained for $J=1.0$, then the ship speed was decreased for each time step until J reached 0.85 while propeller RPM was held constant. When J reached 0.85 during this transient process, the ship speed was assumed constant.

Wang et al. (1992, 1997) developed a unsteady nonlinear vortex lattice method (UNVLM) for calculations of propeller hydrodynamic performances, including steady and unsteady characteristics, the influence of the blade tip vortex separation on the propeller performance and calculations of the transient response of propellers to changes in advance coefficient J . In this approach the shape and roll-up of the wake vortex sheet were not known a priori, but was determined as part of solution by the time-dependent vortex shedding procedure. The transient analysis of the P4118 was conducted to calculate the variations of K_T and K_Q with J . It was proved that the method could be a promising tool in propeller performance prediction, especially under start or stop conditions, and for the study of the geometric shape of free vortex wake.

8.5 Performance of Propellers for Ships when Backing

Peak loads in backing often are the most extreme loading conditions, often determining the strength of the propeller. This can be especially true for electrically driven propellers, highly skewed propellers or CP propellers. Knowledge of the fluctuating forces is most important in assessing the peak loads.

Basin et al. (1963) proposed a theory for propellers in reverse mode. The complicated character of the theoretical solution was shown. As an alternative, the open water test diagrams of two series of propellers with three and four blades in four quadrants were published. K_T and K_Q were presented as a function of the advance ratio and the inverse of the advance ratio, providing one of the best material for practical calculations of crash-stop and astern propulsion. Similar work for three bladed CPP's was published by Zhu et al. (1979). Roussetsky (1968) developed an approximate vortex theory of CPP at crash-stop mode. Both the performance and spindle torque could be evaluated.

Jiang et al. (1991) developed an analysis approach to assess skewed propeller loading, blade stresses, and deflections during steady backing and crashback operations. Predictions of backing and crashback pressure distributions on blade surfaces were estimated from a modified propeller steady force computer program, PSF3. A finite element computer program, NASTRAN, was used to predict blade stresses

and elastic deflections. Iteration procedures between hydrodynamic loading and blade pitch changes at each radius of a skewed propeller during backing operations were employed. Calculations were made using a blade section drag coefficient, $C_D=0.02$. Very good agreement with the experimental data over a wide range of advance coefficients for P4381 and P4383 was obtained. Crashback is an unsteady operation. Only open water steady crashback ($+V_S, -n$) was considered in this paper. A simplified approach was adopted to consider flow separation due to a relatively large angle of attack at the reversal of the propeller rpm. The lift coefficient for a 2-D flat plate, when the flow separates from the leading edge under large angle of attack, becomes

$$C_L = 2\pi \sin \alpha / (4 + \pi \sin \alpha). \quad (12)$$

The lift ratio between separated flow and non-separated flow is thus $C = 1 / (4 + \pi \sin \alpha)$. This factor applied only to the 2-D flat plate case. For the propeller case, the modification was simplified by considering the camber correction factor at $r/R=0.7$,

$$C' = 1 / (4 / k_c + k_c \pi \sin \alpha), \quad (13)$$

where k_c was the camber correction factor and the values were taken or interpolated from Morgan et al. (1968) for different propellers and advance coefficients. An empirical linear transition curve was applied to calculate this factor for the reattached flow. A linear transition region was chosen between $C' = 1 / (4 / k_c + k_c \pi \sin 8^\circ)$ at $\alpha = 8$ degrees and $C' = 1$ at $\alpha = 3$ degrees for P4381. For P4383 the transition region was chosen in the range of $C' = 1 / (4 / k_c + k_c \pi \sin 5.2^\circ)$ at $\alpha = 5.2$ degrees and $C' = 1$ at $\alpha = 1$ degree. K_T correlated better with experimental data than K_Q .

Biskoup (1992) and Xiong et al. (1997) proposed a strength analysis approach for skewed propellers operating in the emergency stopping maneuver, which was assumed to be most dangerous from the point of view of ultimate hydrodynamic load. A simple blade element theory was applied for calculation of the propeller forces, in which $C_L=C_D=0.7$ was assumed by Biskoup, and $C_L=0.7, C_D=0.6$ (for $r/R \leq 0.7$) and $C_D=1.3-r/R$ (for $r/R > 0.7$) under separated flow conditions by Xiong, respectively.

Chen (1996) made comprehensive investigations into the four-quadrant marine propulsor flow by CFD. The unsteady incompressible RANS equations were solved. CFD results of P4381 were presented for the forward, backing, crashahead and crashback conditions. The computational results of performance, surface pressure, and streamline distributions, velocity distribution in front of and behind the propeller, development of the boundary layer and wake, and tip vortex were given. It should be mentioned that extremely large angle of attack near the root can be expected under crashback and crashahead conditions. Thus, the predicted performance with comparison to the experimental data showed a large difference, especially in the higher loading condition. After the cavitation correction, the vapor pressure was used in place of blade pressure lower than the vapor pressure, the predicted performance was improved (see Table 6.4).

Jiang et al. (1996) conducted experimental investigations on the vortex flow field near a propeller tip during crashback in 24-inch water tunnel by Particle Displacement Velocimetry (PDV). An unsteady ring vortex is formed during crashback operation of the propeller. Often the vortex ring seems to start from the tips and to move initially downstream and then return. This ring vortex is highly unsteady, and yet possesses a dominant frequency of movement and dispersion. The periodicity and motion of the ring vortex are governed by the reversal of mass flow through propeller disk. The transverse force of the propeller, which has the same frequency of the ring vortex, was measured during the crashback test. The force is unsteady with an unsteady peak to peak value of approximately one quarter of the steady thrust for the Propeller 4381. Attempts were made towards the modeling of the unsteady flow field. In that approach, a two dimensional quasi-steady approach was investigated by the authors. A two-dimensional RANS code was exercised and the propeller was replaced by a specified time-dependent body force obtained from propeller lifting surface code. Although, those results show the observed features of a moving vortex field, they can not model the origin of unsteadiness. The 24-inch water tunnel experiment demonstrated that the dynamic behavior of the ring vortex is directly related to the unsteady forces that the propeller experiences. The flow field analysis from PDV images can provide quantitative measurements of the velocity and vorticity fields. The results contribute not only

a data base, but also provide some physical insights for future numerical simulation of this complex flow problem.

8.6 Conclusions

The propeller designer should consider the unsteady contributions to the wake field caused by waves and the wave induced ship motions, which can adversely effect propeller cavitation, propeller induced hull pressures and noise. From experiments and comparisons with calculations it is confirmed that the potentials for the calm water wake field, the potentials due to wave action and motions may be linearly superimposed and calculated by means of three-dimensional diffraction theory. The performance of propeller operating in waves can be reasonably estimated by a propeller theory based on the obtained wake field.

There can be considerable increase in the stress levels in propeller blades when the ship turns on a circular course. The calculation accuracy of propeller load and blade stress for ships when turning depends mainly on the wake field prediction, which is usually obtained by experiments. An appropriate theoretical method needs to be developed.

Unsteady nonlinear vortex lattice method may be promising tool for the estimation of propeller performance for ships when accelerating or decelerating.

The emergency stop, or crashback transient maneuver often results in the most extreme hydrodynamic propeller loads, especially for highly skewed propellers. Though the problem has been attempted using potential theory with some success, the unsteady RANS code will be the most appropriate approach to describe the complicated flow under such conditions. Calculation of the loading on propellers in crash stop conditions requires validation with experimental results. It is essential that the fluctuating part of the loading, which results from instabilities in the flow, is properly reproduced and that the instability is correctly reflected.

9. REVIEW AVAILABLE LDV and PIV DATA FOR PROPULSORS

9.1 Introduction

Contained within the 21st ITTC Propulsor Committee report (1996) was a guide for the use of LDV for the collection of propulsor data suitable for the validation of numerical calculations. Since then a number of new efforts using LDV have been reported. Although a limited number of direct LDV applications to propellers were reported since the last Committee report, LDV has been demonstrated to be a useful tool for flow measurements in areas related to propellers. Also, the measurement of turbulence quantities has become more routine.

9.2 Derivation of Pressure From Velocity Measurements

Dong et al. (1997) presented an experiment to demonstrate an improvement in the derivation of field and surface pressure from velocity measurements using LDV. Equations were derived including contributions of vorticity, viscous and Reynolds stress. LDV velocity measurements were made near the upper surface of a hydrofoil at an 8 degree angle of attack. Two component measurements were performed in coincident mode so that Reynolds stress could be derived. Measurements were made about a central node to determine velocity gradients for the derivation of vorticity. Results showed that over the after-half of the chord, where the boundary layer was thick, the calculation of pressure from Bernoulli's equation was not as accurate as the calculated pressures including the terms of vorticity and Reynolds stress.

9.3 Tip Vortex Measurements

Chesnakas and Jessup (1998) performed detailed three component LDV measurements of the tip vortex of a typical controllable pitch Propeller P5168, operating in uniform flow. Measurements were made at a number of planes downstream of the propeller at four advance coefficients. Information was also obtained about the general wake structure and Reynolds stress quantities. The data were obtained primarily to validate RANS calculations of the tip vortex structure and the prediction of tip vortex cavitation inception. The data also

included tip vortex cavitation inception over a range of J .

The LDV measurements were performed in a similar fashion as Jessup (1989), but with much improved LDV signal processing, data handling, and graphical representation of the data. Correlator processors were used to obtain improved signal to noise and increase data collection rate. The PC based, commercial LDV data collection software was coupled with in-house C programs to sort the velocity measurements at 1024 angular positions per revolution, and a spreadsheet to provide on-line data plotting. Three-dimensional graphical representations were performed using Tecplot, a commercial graphics package, to show crossplane vector and contour plots of velocity and derived vorticity.

Initially, the Laser system utilised a combined two component lens system measuring axial and tangential velocity from the side, and a one component fiber optic probe measuring the radial velocity from below. Later, the lens system was replaced with a second fiber optic probe with both probes mounted on a single traverse system inside the water tunnel. This permitted precise six beam crossing, and coincident measurements of three component velocity. The two systems are shown in Figures 9.1a and 9.1b.

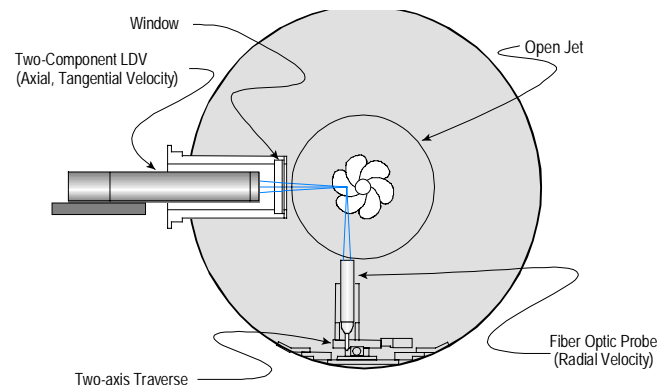


Figure 9.1a LDV systems used in 36" water tunnel: hybrid lens and probe system (Chesnakas et al., 1998).

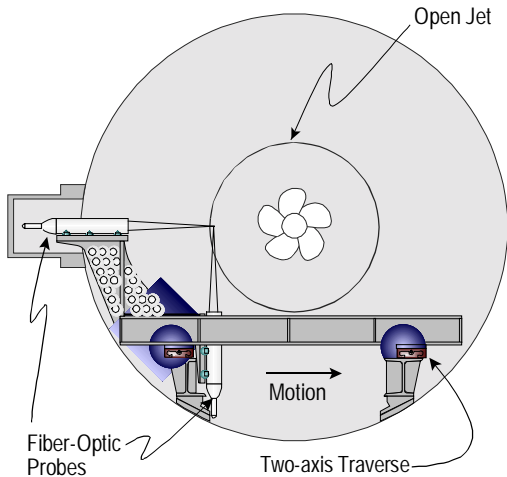


Figure 9.1b LDV systems used in 36" water tunnel: two probe system for coincident measurements (Chesnakas et al., 1998).

Results showed the structure of the vortex including the blade wake roll-up. A sample is shown in Figure 9.2 at an advance coefficient of 1.1, at $x/R=0.239$. The axial measurement plane is projected into a direction perpendicular to the vortex core axis in the rotating frame. Cross plane vectors and the streamwise velocity contours are shown.

Hsiao and Pauley (1998) performed RANS calculations of the flow field about Propeller 5168. Iterative grid refinement was utilised to produce refined calculations of the tip vortex. Reasonable prediction of cavitation inception was obtained, but there was a lack of general validation with global quantities of thrust, torque, and blade pressure distribution. The calculated tip vortex structure is shown in Figure 9.3.

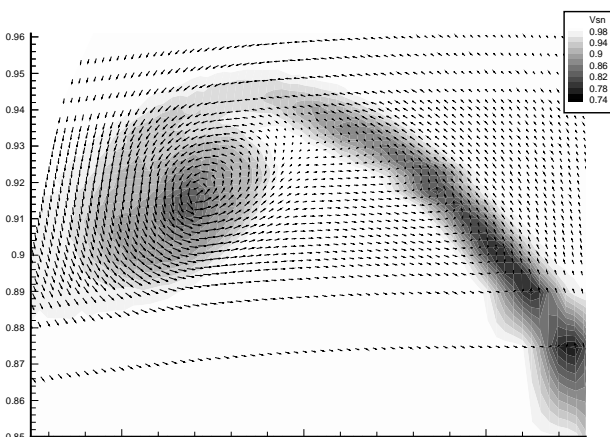


Figure 9.2 Measured tip vortex structure downstream of P5168, $J=1.1$, $x/R=0.239$ (Chesnakas et al., 1998).

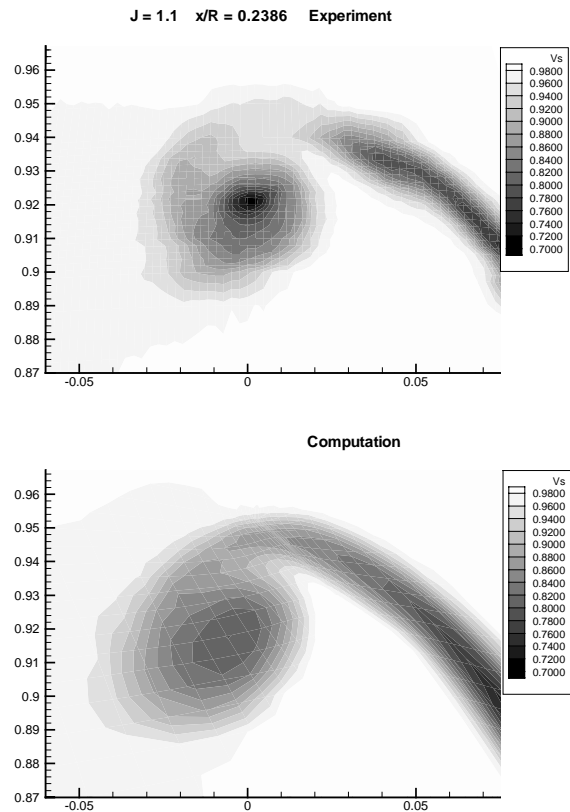


Figure 9.3 Prediction of tip vortex of P5168 with RANS compared to measured result (Hsiao and Pauley, 1998).

Stella et al. (1998) presented LDV measurements of propeller tip vortex flow in a water tunnel. Phase averaging was used to map the blade wake structure. Measurements were performed, relatively far downstream, showing the occurrence of vortex instabilities at axial positions greater than 2 diameters downstream. This study showed the obvious need for PIV measurements at locations far downstream of the blades, where vortex wandering dominates.

9.4 Propeller Related Studies

Cordier et al. (1997) used LDV to measure the shaft and strut wake of a typical open shaft combatant configuration. The motivation was to ultimately validate RANS calculations of appendage flow. Measurements were made in the water tunnel on an appended and unappended model tested at high Reynolds number. The unappended model showed expected trends with Reynolds number. Results showed primarily axial velocity contours with complex flows associated with the shaft and

struts. CFD calculations of the unappended hull showed good correlation with measurements, while the calculation of the appended case showed significant discrepancies attributed to inaccuracies in the body force approximation of the shaft.

An idealised inclined shaft configuration was examined, simulated with an eight degree inclined shaft emanating from a wall, imbedded within various wall boundary layer thickness'. Velocity data showed the boundary layer-shaft wake interaction causing low velocity fluid from the boundary layer convected into the shaft wake, with thicker boundary layers producing a more pronounced effect. CFD calculations with the shaft fully gridded showed good qualitative comparison with measure results. An attempt was also made to grid the shaft and brackets for the model hull case using hybrid grids, which showed some promise, but requires more sophisticated gridding procedures.

Min et al. (1997) presented measurements of a nominal wake survey using a three component LDV system. Measurements were performed on a ship model in the towing tank. Coincident measurements were performed permitting the measurement of Reynolds stress.

Cox et al. (1997) presented an experimental study of two dimensional foil sections with thick trailing edges. LDV was used to measure the lift and drag characteristics of the hydrofoils tested in the water tunnel. A method similar to Lurie (1993) was used involving integrations of velocity. The drag was computed from the wake deficit relative to a quadratic curve fit between the upper and lower potential flow regions in a downstream plane. The lift was calculated from the contour integral on a rectangular path (box) around the foil. Second order effects due to momentum flux through the sides of the box were also considered, but perceived effects of tunnel wall boundary layer were concluded to reduce the accuracy of the approach.

Pauchet (1996) presented an analysis of LDV velocity fluctuations within the tip vortex core of a three dimensional elliptic wing. Measurement of two component axial and tangential velocities of the vortex core showed large differences in the velocity fluctuations determined from the RMS of the measurement sets at a given traverse location. Analysis showed that the tangential velocity measure-

ment was greatly effected by the length of the measurement volume spanning the vortex core. Both the positive and negative extremals of tangential velocity about the core were contained in a single traverse position measurement, thus artificially increasing the fluctuating RMS velocity. Corrections were performed by analyzing the histograms of the velocity separately at the two velocity extremals at each traverse location. This paper demonstrates the importance of consideration of the LDV measurement volume geometry relative to the velocity gradients in the flow field.

9.5 Applications of Particle Image Velocimetry (PIV)

Particle Image (or displacement) Velocimetry (PIV or PDV) is a measurement technique that has been developed for more than a decade and implemented for quantitative flow visualisation, and velocity field measurement in ship hydrodynamic research. PIV is the technique for measuring an instantaneous two dimensional velocity of a flow field. For example, using PIV, one can measure the global instantaneous velocity in a vortex core including the true maximum tangential and axial velocities. PIV has been used for the measurement of complex, turbulent flows where knowledge of instantaneous velocity is important.

PIV is a two dimensional quantitative flow visualisation and measurement technique. This technique involves illuminating a section of the flow field with a pulsed laser sheet, while seeding the water with microscopic particles and recording a multiple exposures of the particle traces. Film or digital camera recording mediums are used on a single dual exposure of particle traces. Silver coated spherical particles or neutrally buoyant particles imbedded in fluorescent dye are used to seed the flow. An auto-correlation or cross-correlation is applied to calculate the displacement of particles within a small interrogation area (64x64 pixels typical) on the image. Each vector on the velocity map represents a spatial average velocity in the interrogation site.

Shekarriz et al. (1992,1993) studied junction and tip vortices trailing behind a submarine model sail. The experiment was performed in the CDNSWC 43m tow tank on a 0.3m diameter model. PIV visualised the juncture vortex embedded within the boundary layer.



The vortex meandered primarily in a direction parallel to the body and less in the direction normal to the surface. The junction vortex detaches from the surface with increasing x/c with circulation decreasing with downstream distance. Profiles of the tip vortex flow convected along the body showed the predicted r^2 and $\log r$ forms within the inner and outer sections of the core, respectively. The vortex is observed to expand in the afterbody region, without a change in its total strength. Later Liu et al. (1994) used PIV to measure flow structures around a submarine model in the CDNSWC rotating arm facility. Liu et al. (1994) demonstrated implementing PIV measurement to larger scale test facility, the CDNSWC high speed towing basin, providing images (1.22m \times 1.22m) of a tip vortex from a submerged large model sail.

Jiang et al. (1996) implemented PIV measurement in a 0.61m diameter open jet water tunnel to investigate flow structure during propeller crashback. The results demonstrate vortex structures and velocity distributions in the vicinity of a propeller tip at different test conditions. It also provides quantitative and qualitative flow visualisation of these flow structures. They found out that the dynamic behavior of the ring vortex is directly related to the unsteady force that the propeller experiences. Typically, a low frequency of about 0.5Hz is observed in the images of flow field and it matches the unsteady frequency of the propeller side forces at the corresponding advanced coefficient.

Some PIV work has been conducted to study body-free surface interaction. Dong et al. (1996, 1997) measured flow structures of bow waves on a ship model by using PIV. The experiments were performed in the CDNSWC 43m tow tank. They demonstrated the characteristic structure of mid and steep bow waves, including velocity and vorticity distributions. They documented the thin liquid sheet attached at the bow. Pogozelski et al. (1996) investigated the shoulder wave and separation generated by a surface-piercing strut model with long draft.

In order to resolve the three dimensional velocity field, a Stereoscopic Particle Image Velocimetry (SPIV) technique is under development. This technique requires two cameras mounted at the same distance from the laser sheet at some separation distance. A Holo-

graphic Particle Image Velocimetry (HPIV) is also under development. This measurement technique requires a coherent ruby laser and a holographic system. neither system has been implemented for hydrodynamic research yet.

9.6 Conclusions

Application of LDV to propeller flows has continued since the last committee report. Numerous measurements of propeller and hydrofoil tip vortex has been performed. Turbulence has been measured in a number of studies utilizing multicomponent coincidence. LDV has and will continue to be used to validate CFD.

PIV has the advantage of capturing highly unsteady or transient flows. Measurements have been made primarily on small hull models, with only limited measurements performed on propellers.

10. REVIEW THE CORRELATION OF LIQUID QUALITY (LIQUID TENSION AND NUCLEI DISTRIBUTION) WITH CAVITATION INCEPTION AND THE STABILITY OF CAVITATION PATTERNS. OF CAVITATION EXPERIMENTAL TECHNIQUES SHOULD BE REVIEWED TO PREDICT CAVITATION BEHAVIOR MORE ACCURATELY. THE EFFECTS OF TURBULENCE AND PROPELLER BLADE ROUGHNESS SHOULD BE TAKEN INTO ACCOUNT.

10.1 Introduction

The results of several studies jointly conducted by Bassin d'Essais des Carènes and the ITTC Cavitation Committee, can be summarised by stating that it is not possible to conduct cavitation tests without determining the complete nuclei distributions, thus allowing the determination of both water tension and nuclei content as a function of the critical pressure (21st ITTC Cavitation Committee Report, 1996). The influence of water quality is taken into account more widely in cavitation testing. However, during the period 1995-1998 not much has been published on the influence of water quality, turbulence, and blade roughness on cavitation.

10.2 Status of Water Quality Control

Minimizing the liquid tension and maximizing the number of nuclei is one method to reduce scale effects; however, in many facilities, this is not practical. Also, in some cases, this can alter the bubble dynamics and appearance of the cavitation, especially when the increase of nuclei number distribution is obtained by strongly increasing the dissolved air content in the facility.

The “natural” nuclei spectrum of any cavitation facility depends on the history of the fluid through the different parts that constitute the facility. This means that this spectrum will depend on conditions, such as dissolved air content, pressure level, velocity, and the transit time through any part of the circuit, such as the main pump, vanes, resorber, etc. As a consequence, the “natural” spectra is different in each cavitation facility (21st ITTC Cavitation Committee Report, 1996, Gindroz et al., 1996)

In order to evaluate the cavitation tests procedures in use, the 22nd ITTC Propulsion Committee sent a questionnaire to all ITTC members. They were asked to answer the questions given in Tables 10.1 and 10.2. Twenty five completed questionnaires were sent back. The main conclusions are summarised in Table 10.2.

To minimise the scale effects, the experiments should be run at high R_n and high flow velocity with high nuclei content, which is often reached by increasing the dissolved air content.

Table 10.1 Questions on cavitation test conditions in the questionnaire.

Test condition:
<ul style="list-style-type: none"> • Range of dissolved gas content • Range of flow velocities • Range of R_n (based on propeller diameter) • Range of temperature • Number of water changes per year • Type of colorant • Inception criteria for: bubble, sheet, tip vortex, hub vortex cavitation

The injection of nuclei and nuclei measurements are still rarely conducted and only in a

very few facilities. Electrolysis is used for the same purpose. A recent series of systematic tests conducted by Bassin d’Essais des Carènes at MARIN DTT, has shown the excellent efficiency and accuracy of this device as a nuclei generator (Figure 10.1). However, the use of electrolysis for the generation of adequate nuclei distribution, requires experience on the location of the wires, their size and the electrical current.

The injection of colorant is sometimes performed for flow visualisation or LDV seeding. However, even at low concentrations, the majority of colorants used can decrease the water surface tension by 30% or more. A typical cavitation development can be affected by a change in surface tension and thus must be taken into account. In most cases, tunnel water is frequently changed, which reduces the risk of shifting the water surface tension characteristics. Even under these conditions, the measurement of the surface tension is necessary as it interacts directly with cavitation patterns. This measurement is also a good indicator of the water cleanliness.

In 90% of the facilities, detection of the cavitation inception is made visually, either directly, using stroboscopic light or indirectly, using video cameras. However, the analysis of the questionnaire shows a large range of inception criteria used as summarised in Table 10.3. The criteria cover a typical range between the first appearance and a continuous appearance of events. This wide range will make it difficult to compare cavitation inception data between different facilities.

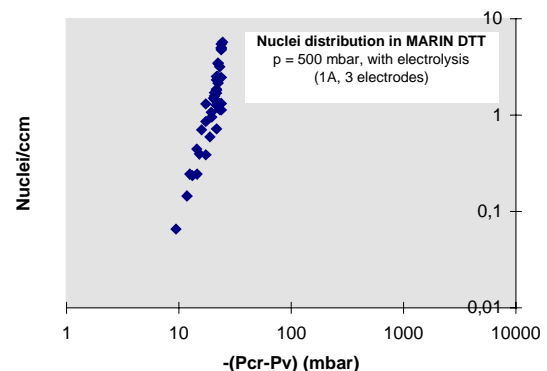


Figure 10.1. Steep nuclei spectrum obtained by electrolysis; to be compared with Figure 10.2 (courtesy MARIN).

Table 10.2 Analysis of cavitation test procedures from the questionnaire.

Water quality in cavitation tank	Used by
Type of contents measured:	
• O ₂	60 %
• Total gas	44 %
• Nuclei	12 %
Typical dissolved gas content:	
• High	16 %
• Medium	40 %
• Low	36 %
Injection:	
• Air	0 %
• Nuclei	20 %
• Colorant injection	32 %
Surface tension	8 %
Detection of cavitation inception:	
• Visual	96 %
• Video	36 %
• Acoustic	40 %
Meas. of cavitation development:	
• Visual	92 %
• Video	56 %
• Acoustic	16 %

Table 10.3 Cavitation inception criteria from the questionnaire.

Cavitation inception criteria:	Used by
Continuous appearance	16 %
50 % of time	12 %
10 % of time	4 %
First appearance	28 %
One per few sec.	4 %
One per 5 sec.	4 %
One per 5-10 sec.	4 %
One per 10 sec.	4 %
Aggregate of small events	4 %
More than two events	12 %
Noise at $f > 10$ kHz	4 %

Cavitation development is nowadays frequently analysed through numerical imaging from video records. Weitendorf and Tanger (1992) reported on a video recording system

coupled with efficient postprocessing software that permitted the representation of cavity fluctuation. Johannsen (1998) further developed video techniques by simultaneously recording hull pressure pulses and high speed video, and displaying pressure pulse levels superimposed on the video image to show temporal effects of cavity and hull pressure variations.

The natural generation of free nuclei in a facility is different in each facility and changes with the operating conditions set during the tests. This explains also the large difference that can be observed when comparing results obtained in different facilities using the same equipment. The precise measurement of dissolved air content and water surface tension, as well as the free nuclei spectrum, will generally lead to a better understanding and interpretation of these measured differences. A way to minimise the effect of the free nuclei content on cavitation inception data obtained in different tests facilities, is to ensure a water tension as low as possible, with a very steep nuclei spectrum (a narrow nuclei size histogram) as shown in Figure 10.2. Thus, even for large difference of inception criteria (Table 10.3), the values of cavitation index will be similar. These parameters as well as the wake field should be carefully measured and controlled during a test.

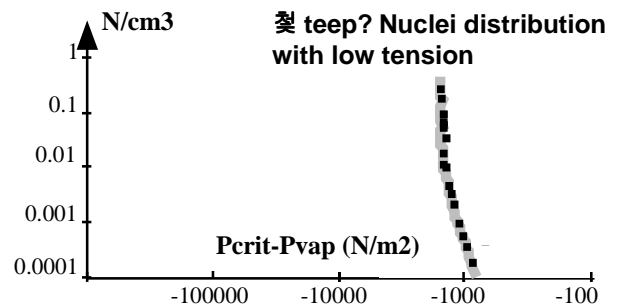


Figure 10.2 : A steep nuclei spectrum will minimise the effect of different criteria on the determination of the cavitation inception characteristics.

10.3. The influence of nuclei on cavitation inception

Since 1995, Liu and Brennen (1995, 1996), Rood (1997) and Ceccio (1997) have investigated the influence of the water quality on the cavitation characteristics. Moreover, following the studies from Gindroz and Billet (1993, 1994), Liu et al. (1996) confirm the necessity to

take into account both water tension, nuclei size, or critical pressure distributions. In order to allow precise determination of the free nuclei distribution, a few facilities have recently been equipped with a centerbody venturi device.

A set of propellers (Kuiper, 1981) could be used as standard cavitators, one per type of cavitation. Prior to a propeller cavitation test, it would be necessary to mount one or several of these standard propellers and check their cavitation characteristics, in order to determine the nuclei content or water quality in the test facility. This could significantly increase test duration. An additional limitation would be the possible restrictions on the range of tunnel flow conditions; velocity, pressure, specific to the standard propeller's characteristics. The same applies to other kinds of standard cavitators, i.e., headforms, profiles, etc.

Progress has been made recently in the measurement of nuclei size distribution by Phase Doppler Technique (Bultynck, et. al., 1998, Gouesbet, 1996, Gréhan, et. al., 1993). The joint 20th ITTC Cavitation Committee - GTH (Bassin d'Essais des Carènes) test found the practical limitation of that technique. It was impossible to measure precisely small nuclei and directly separate the results corresponding to solid particle and nuclei. Thus, the spectra obtained were not consistent. Blondel (1998, 1999) developed a miniature waterproof phase doppler device with signal processing that allows a precise and direct discrimination between nuclei and solid particles. Velocity and size distributions can be measured in real time for both nuclei and solid particles. Validation was carried out confirming the efficiency and precision of the newly developed device.

10.4 Influence of turbulence and blade roughness

For tests conducted at low R_n numbers, surface roughness can influence boundary layer transition and thus, cavitation inception. This is especially true for the stability of blade surface cavitation and sometimes for bubble cavitation. Moreover, roughness could also create nuclei to feed the tip vortex. Thus, in such cases, it could be important to control the blade roughness.

10.5 Conclusions

The results from the questionnaire sent to the ITTC members show a large range of criteria for the determination of the cavitation inception data. For that reason, comparing cavitation inception results conducted in different facilities, with their own water quality characteristics, their own criteria for quantifying the inception point, is very difficult. Setting a "steep" nuclei distribution with low water tension in the facility, will minimise the differences measured between facilities. Further work is required to include these effects in the cavitation tests procedure, in order to try to specify recommendations on water quality characteristics for cavitation experiments.

It is not yet possible to quantify the influence of turbulence and blade roughness on cavitation characteristics. Research in this area is needed.

11. GENERAL TECHNICAL CONCLUSIONS

Applications of the new blade section propeller design method have included both the extending of cavitation inception speed, and the improvement of propeller performance with cavitation. The method of Eppler along with various optimisations procedures have been used.

Optimisation techniques have been applied to relatively simple, multiple design trade-offs, and for specific, detailed design procedures. Studies have shown the capability to arrive at an optimum with little design expertise. Further advances will be expected utilizing more advanced calculations and consideration of more design parameters.

Performance prediction methods for azimuthing thrusters as main propulsors are not well established. Turbulence stimulators on the housings of model podded propulsors with pushing propellers are necessary.

In the area of powering performance extrapolation the situation has developed that the diversity of the procedures has widened instead of converging to one or two standard methods.



RANS equation codes are capable of predicting accurately the propeller open water performance and pressure distributions on the blade at the design advance number. The accuracy of performance prediction for off-design advance numbers that are about half of the design advance number is good or acceptable. The main features and the main variables of the flow field, streamlines and boundary layer are generally well predicted. With an adequately dense grid and a suitable turbulence model RANS codes are capable of predicting the tip vortex flow accurately. Time-accurate solutions of unsteady propulsor flow are very time consuming. Approximate unsteady solutions are obtained more quickly by the quasi-steady method or averaging procedures.

Potential based panel methods are most widely used. In the 1990's the development emphasis of vortex wake models has been in more accurate modeling of the tip region flow and in the inclusion of simple viscous considerations in the model. Panel methods have been extended to problems of the unsteady performance and cavitation prediction of propellers. The recent improvements in panel method codes have resulted in good agreement between the measured propeller and predicted performance and pressure distributions on the blade for most types of propellers. Panel method predictions of the details of slipstream velocity field are not accurate.

Additional experimental data of blade surface pressures and slipstream velocities are needed for the validation of RANS equation and panel method codes. Very little flow field data for off-design operation conditions have been published.

Propeller modifications to improve seaway cavitation performance must be traded off against adverse effects of cavitation at high speeds. From experiments and comparisons with calculations it has been confirmed that the potentials for the calm water and the potentials due to wave action and motions may be linearly superimposed and calculated by 3-D diffraction theory. This forms a reasonable wake field for propeller analysis.

The stress levels on propeller blades of ships turning on a circular course can increase substantially. The calculation accuracy of propeller performance and propeller stresses depends mainly on the prediction accuracy of the wake

field. The wake field is usually obtained experimentally.

Unsteady vortex lattice method seems to be a promising propeller analysis tool for accelerating or decelerating ships.

RANS method is the appropriate analysis tool for the complicated flow under backing.

Numerous LDV measurements of propeller and hydrofoil tip vortex has been performed since the last committee report. Turbulence has been measured in a number of studies utilizing multi-component coincidence. PIV (particle image velocimetry) has the advantage of capturing highly unsteady or transient flows. PIV measurements have been made primarily on small hull models, with only limited measurements performed on propellers.

The results from the questionnaire sent to ITTC members show a large range of criteria for the determination of cavitation inception data. For that reason, comparing cavitation inception results conducted in different facilities with their own water quality characteristics, is difficult. Setting a "steep" nuclei distribution with low water tension in the facility, will minimise the differences measured between facilities.

It is not yet possible to quantify the effect of turbulence and blade roughness on cavitation characteristics.

12. RECOMMENDATIONS TO THE CONFERENCE

Salt water data with salinity of 3.5 per cent are to be derived from Hardy's formula (ITTC, Procedure 4.9-03-01-03). For intermediate values of salinity the viscosity is to be found by linear interpolation between fresh water and the (standard 3.5 per cent) salt water viscosity data. (The recommendation is given as APPENDIX 1: INTERPOLATION OF VISCOSITY at the end of this report.)

13. RECOMMENDATIONS FOR FUTURE WORK

Review the state-of-the-art, comment on the potential impact of new developments on ITTC, identify the need for research and development in the areas of propulsors, cavitation and

powering performance. Monitor and follow the development of new experimental techniques and extrapolation methods.

Update propulsion literature database.

Scaling procedures should be improved component-wise. Select the components for improvement from the list: (1) Improve and validate scaling procedures for appendage drag; (2) Develop scaling procedures for the passive components of multi-component propulsors; (3) Develop a method for propeller scale effects with emphasis on the occurrence of laminar flow in model scale. Also consider turbulence tripping on propellers; (4) Validate new formulations for flat plate friction line; (5) Compile a guide for the assessment of experimental form factors and their use; (6) Develop guidelines for testing separation prone hull forms.

Review the development of numerical design and analysis methods for propulsors. Follow the developments in the modeling of unconventional and multi-component propulsors.

Evaluate performance prediction procedures for ships with azimuthing thrusters as the main propulsor.

Review developments in experimental techniques and analytic methods for modeling the propulsive effects of propeller-rudder interaction including cavitation and cavitation effects.

Review developments in analytic and experimental methods for hydroelastic phenomena on propulsors. Recommend procedures for accounting for hydroelastic effects in predicting and evaluating propulsor performance.

Review the development and suggest guidelines for water quality measurements and conditions to minimise the scale effects in cavitation.

Review the techniques and procedures for controlling and adjusting water quality characteristics in cavitation test facilities.

Review the development of new extrapolation methods for cavitation inception data with regards to water quality parameters.

Review and evaluate the techniques for cavitation pattern measurement and cavitation inception determination.

Make some additions to the Procedure for Model Manufacture: Ship Models (ITTC Procedure 4.9-02-01-01), particularly for the manufacture of multi-component propulsors and openings in the hull.

Rewrite the Procedure for Propulsion: Propulsion Tests (ITTC Procedure 4.9-03-03-01.1)

Rewrite the Procedure for Open Water Model Tests (ITTC Procedure 4.9-03-03-02.1).

Include in the Section "Extrapolation" of Propulsion Tests (ITTC Procedure 4.9-03-03-01.1) guidelines to account the influence of cavitation on performance prediction.

Redraft the Section for "Parameters" of the Procedure Guide for Model Scale Cavitation Pattern Test (ITTC Procedure 4.9-03-03-03.1) and check the other sections of the procedure after the redrafting.

Check the Procedure for Description of Cavitation Appearances (ITTC Procedure 4.9-03-03-03.2) after the redrafting of ITTC Procedure 4.9-03-03-03.1 to ensure the consistency of the two Procedures.

Make additions to the Guide for Speed/Powering Trials (ITTC Procedure 4.9-03-03-01.3) with regards parameters, preliminary controls, trial measurements, and operation of the ship.

14. REFERENCES

- Aalbers, A.B., Gent, W. van, 1985, "Unsteady wake Velocities Due to Waves and Motions Measured on a Ship Model in Head Waves", 15th SNH, Hamburg.
- Abdel-Maksoud, M., Menter, F., Scheurerer, G., 1996, "Numerische and experimentelle Untersuchung der viskosen Strömung um einen Skew-Propeller." Jahrbuch der STG, Vol. 90.
- Abdel-Maksoud, M., Menter, F., Wuttke, H., 1998a, "Numerical Computation of the Viscous Flow Around the Series 60 CB=0.6 Ship with Rotating Propeller", Third Osaka Colloquium on Advanced



- CFD Applications to Ship Flow and Hull Form Design, Osaka.
- Abdel-Maksoud, M., Menter, F., Wuttke, H., 1998b, "Viscous Flow Simulations for Conventional and High-Skew Marine Propellers", Ship Technology Research, Vol. 45, No. 2.
- Achkinadze, A.A., Krasilnikov, V.I., 1997, "A Generalized Optimum Condition of Wake Adapted Propellers", Propellers/Shafting '97 Symposium, Virginia Beach.
- Aleksandrov, K., Semionicheva, E., 1994, "Improvement of Cavitating and Vibroacoustic Characteristics of Blade Hydraulic Apparatus by Optimisation of the Blade Cylindrical Section", Proc. of International Shipbuilding Conference (ISC), St.-Petersburg. (in Russian)
- Alexandrov, K., 1981, "Designing of Cavitating Profiles, Working in Predetermined Range of Angles of Attack", Theses of XXX Krylov's Conference, Sudostroenie, Leningrad. (in Russian)
- Ando, J., Maita, S., Nakatake, K., 1998, "A New Surface Panel Method to Predict Steady and Unsteady Characteristics of Marine Propeller", 22nd SNH, Washington, D.C.
- Arabshahi, A., et al., 1998, "A Perspective on Naval Hydrodynamic Flow Simulations", 22nd SNH, Washington, D.C.
- Basin, A., Miniovitch, I., 1963, "Theory and Calculation of the Screw Propellers", Sudpromgiz, Leningrad. (in Russian)
- Belibasakis, K.A., Politis, G.K., 1998, "A Nonlinear Velocity Based Boundary Element Method for the Analysis of Marine Propellers in Unsteady Flow", Int. Shipbuilding Progress, Vol. 45, No. 442.
- Biskoup, B., Ivanov, A., Semionicheva, E., Eller A., 1998, "Influence of Local Separation on Hydrodynamic Characteristics of Multi-point Wing's Profiles", Transactions KRSI, Vol. 8, No. 292. (in Russian)
- Biskoup, B.A., 1992, "Estimation of the Highly Skewed Propeller Blades Strength in a Stopping Manoeuvre", ISPC'92, Hangzhou.
- Black, S., 1995, "The Use of Numerical Optimisation in Advanced Blade Section Design", 24th ATTC, College Station, Texas.
- Blondel, D., 1999, "Conception et réalisation d'une sonde de métrologie optique pour l'étude de milieux industriels complexes", Ph.D. Thesis, Université de Rouen.
- Blondel, D., Gréhan, G., Gouesbet, G., 1998, "In Situ Phase Doppler in Three Phase Flows", Third International Conference on Multiphase Flow ICMF'98, Lyon.
- Bruzzzone, D., Cassella, P., Miranda, S., Pensa, C., Zotti, I., 1997, "The Form Factor by Means of Multiple Geosim Model Tests", NAV & HSMV International Conference, Sorrento.
- Bultynck, H., Gouesbet, G., Gréhan, G., 1998, "A Miniature Monoblock Backward Phase-Doppler Unit", Measurement Science Technology, Vol. 9.
- Bussemaker, O., 1987, "Performance Comparison of Thruster Units", Marine Propulsion, September/October.
- Caprino, G., Traverso, A., 1997, "Improvements in Propeller Design Using Surface Panel Methods", NAV & HSMV International Conference, Sorrento.
- Ceccio, S., Gowing, S., Shen, Y.T., 1997, "The Effects of Salt Water on Bubble Cavitation", J. Fluids Engineering, Vol. 119, No. 2.
- Chalov, A.V., Ilyin, V.P., Levkovsky, Yu.L., 1998, "The Influence of Nuclei Content on the Inception of Bubble and Vortex Cavitation", 3rd International Symposium on Cavitation, Grenoble.
- Chen, B., 1996, "Computational Fluid Dynamics of Four-Quadrant Marine Propeller Flow", Ms.Sc. Thesis, The University of Iowa.

- Chen, J.D., Dong, S.T., 1997, "Calculation of Unsteady Pressure over Propeller Surface with a Potential-Based Panel Method", China-Korea Marine Hydrodynamics Meeting, Shanghai.
- Chesnakas, C., Jessup, S.D., 1998, "3-D LDV Measurements of the Flow Around Propeller 5168", 22nd SNH, Washington, D.C.
- Chevalier, Y., Kim, Y.-H., 1995, "Propeller Operating in a Seaway", PRADS'95, Seoul.
- Chung, K.N., Min, K.S., 1998, "A Study of Viscous Flow around an Axisymmetric Body with Propeller", Third Osaka Colloquium on Advanced CFD Applications to Ship Flow and Hull Form Design, Osaka.
- Conway, J.T., 1998, "Exact Actuator Disk Solutions for Non-uniform Heavy Loading and Slipstream Contraction", Journal of Fluid Mechanics, Vol. 365.
- Cordier, S., Legrand, F., Pinard, J.C., 1997, "Hull and Shaft Wake Interaction", Propellers/Shafting '97, Virginia Beach.
- Cox, B., Kimball, R., Scherer, O., 1997, "Hydrofoil Sections with Thick Trailing Edges", Propellers/Shafting'97, Virginia Beach.
- Dai, C., Hambric, S., Mulvihill L., Tong, S.T., Powell, D., 1994, "A Prototype Marine Propulsor Design Tool Using Artificial Intelligence and Numerical Optimization Techniques", SNAME Trans., Vol. 102.
- Denisov, V., Sadovnikov, D., Semionicheva, E., Tumashik, A., 1996, "Design of Propulsion Devices of Multi-Mode Ships on Example of Arctic Nuclear-Power Lighter Carrier Sevmorput", Proc. Polar Tech'96, Workshop B, St.Petersburg.
- Dong, R.R., Katz, J., Huang, T.T., 1995, "PIV Measurements of the Flow Structure around a Ship Model", Laser Anemometry Conference and Exhibition, ASME/JSME Fluids Engineering, FED-Vol. 229.
- Dong, R.R., Katz, J., Huang, T.T., 1997, "On the Structure of Bow Wave on a Ship Model", Journal of Fluid Mech., Vol. 346.
- Dong, S.-T., Ji, Z.-Y., Zhou, W.-X., 1997, "Pressure Distribution Determined by Using Measured Velocity Field Data and RANS Equations." Proceedings of China-Korea Marine Hydrodynamics Meeting, Shanghai.
- Drela, M., 1989, "An Analysis and Design System for Low Reynolds Number Airfoils", Conference on Low Reynolds Number Airfoil Aerodynamics, University of Notre Dame.
- Eppler, R., Sommers, D., 1980, "A Computer Program for the Design And Analysis of Low Speed Airfoils", NASA Technical Memorandum 80210.
- Forgach, K., 1999, "Comparison of ITTC-78 and DTMB Standard Ship Performance Prediction Methods", CDNSWC Report 50-TR—1999/027.
- Georgiev, D.J., Ikehata, M., 1998a, "Hydrodynamic Effects on Propeller Blades in Steady Flow", J. SNAJ, Vol. 184.
- Georgiev, D.J., Ikehata, M., 1998b, "Analysis of Pressure and Stress Distribution on Propeller Blades in Unsteady Flow", J. KSNA, No.230.
- Georgiev, D.J., Ikehata, M., Kai, H., 1997, "Application of Dirichlet's Principle in a New Panel Method for Surface and Tip Flows of Lifting Bodies", J. SNAJ, Vol. 182.
- Ghassemi, H., Ikehata, M., Yamasaki, H., 1995, "An Investigation of Wake Model and Its Effect on the Hydrodynamic Performance of Propellers by Using a Surface Panel Method", J. SNAJ, Vol. 178.
- Gindroz, B., 1997, "Cavitation Inception of Marine Propellers : Why and How Cavitation Nuclei Must be Taken into Account", Joint Korea-China Workshop on Marine Research, Shanghai.
- Gindroz, B., Bailo, G.M., Matera, F., Elefante, M., 1996, "Influence of the Cavitation Nuclei on the Cavitation Bucket, When Predicting the Full-scale Behavior of a Marine Propeller", 21st SNH, Trondheim.



- Gindroz, B., Billet, M.L., 1993, "Influence of the Nuclei on the Cavitation Inception for Different Types of Cavitation on Ship Propellers", ASME FED-WM, New Orleans.
- Gindroz, B., Billet, M.L., 1994, "Nuclei and Acoustic Cavitation Inception of Ship Propellers", Second International Symposium on Cavitation, Tokyo.
- Gindroz, B., Geistdoerfer, P., Billard, J.-Y., 1995, "Cavitation Nuclei Measurements at Sea", ASME FED-WM, San Francisco.
- Gindroz, B., Hoshino, T., Pylkkänen, J.V., eds., 1998, "22nd ITTC Propulsion Committee Propeller RANS/Panel Method Workshop Proceedings", Grenoble, France, 5-6 April, Privately printed, Val de Reuil.
- Gouesbet, G., 1996, "Exact Description of Arbitrary Shaped Beams for Use in Light Scattering Theories", J.O.S.A.A., Vol. 13.
- Gréhan, G., Gouesbet, A., Naqwi, A., Dürst, F., 1993, "Particle Trajectory Effects in Phase Doppler Systems: Computations and Experiments", Part. Syst. Charact., Vol. 10.
- Grigson, C.W.B., 1993, "An Accurate Smooth Friction Line for Use in Performance Prediction", Trans. RINA, Vol. 135.
- Grigson, C.W.B., 1994, "An Improved Method for the Predicting the Performance of Merchant Ships from Models", Trans. RINA, Vol. 136.
- Grigson, C.W.B., 1995, "A Reanalysis of the Lucy Ashton and Victory Experiments", Trans. RINA, Vol. 137.
- Hally, D., Laurens, J.-M., 1998, "Numerical Simulation of Hull-Propeller Interaction Using Force Fields Within Navier-Stokes Computations", Ship Technology Research, Vol. 45, No. 1.
- Heinke, H.-J., 1998, "Azimuthing Propulsion - Experiences of SVA", 6. SVA-Forum, Potsdam.
- Heller, W., 1997, "Zum Einfluss der Turbulenz der Anströmung auf die Druckwirkungen in Grenzschichten und den Kavitationsbeginn", TU Dresden.
- Hirano, M., Takashima, J., Fukushima, M., 1992, "A Study on Maneuvering Motion Prediction of SWATH Ships", in Hydrodynamics: Computations, Model Tests and Reality, Elsevier, Amsterdam.
- Holtrop, J., 1989, "Scale Effect on Appendage Drag", Marin Report No. 50902-1-SP.
- Hoshino, T., 1993, "Hydrodynamic Analysis of Propeller in Unsteady Flow Using a Surface Panel Method", J. SNAJ, Vol. 174.
- Hoshino, T., 1998, "Experimental Data for Unsteady Panel Calculations and Comparisons (SEIUN-MARU HSP)", In 22nd ITTC Propulsion Committee Propeller RANS/Panel Method Workshop Proceedings, Gindroz, B., et al., eds.
- Hsiao, C.-T., Pauley, L.L., 1998, "Numerical Computation of the Tip Vortex Flow Generated by a Marine Propeller", ASME FED-SM, Washington D.C.
- Iannone, L., 1997, "Power Performance Analysis and Full-Scale Prediction without Towing Tests", NAV & HSMV International Conference, Sorrento.
- Ilyin, V.P., Roussetsky, A.A., Chalov, A.V., 1998, "Prediction of Screw Cavitation Characteristics on the Basis of Model Tests Results", 3rd International Symposium on Cavitation, Grenoble.
- ITTC, 1984, "Report of Propulsion Committee", 17th ITTC, Vol. 1, Kobe.
- ITTC, 1993, "Report of Propulsor Committee", 20th ITTC, San Francisco.
- ITTC, 1996, "Report of Cavitation Committee", 21st ITTC, Trondheim.
- ITTC, 1996, "Report of Propulsor Committee", 21st ITTC, Trondheim.
- Ivanov, A., 1980, "Hydrodynamics of Advanced Cavitating Flow", Sudostroenie, Leningrad. (in Russian)
- Jessup, S., Berberich, W., Remmers, K., 1994, "Cavitation Performance Analysis of

- Naval Surface Ship Propellers with Standard and New Blade Sections”, 20th SNH, Santa Barbara.
- Jessup, S., Wang, H.-C., 1997, “ Propeller Design and Evaluation for a High Speed Patrol Boat Incorporating Iterative Analysis with Panel Methods”, Propellers/Shafting’97, Virginia Beach.
- Jessup, S.D., 1982, “Measurements of the Pressure Distribution on Two Model Propellers”, DTMB Report DTNSRDC-82/035.
- Jessup, S.D., 1989, “An Experimental Investigation of Viscous Aspects of Propeller Blade Flow”, Ph.D. Thesis, School of Engineering and Architecture, The Catholic University of America.
- Jessup, S.D., 1994, “Propeller Blade Flow Measurements Using LDV”, ASME FED-SM, Lake Tahoe.
- Jessup, S.D., 1998a, “Experimental Data for RANS Calculations and Comparisons (DTMB P4119)”, In 22nd ITTC Propulsion Committee Propeller RANS/Panel Method Workshop Proceedings, Gindroz, B., et al., eds.
- Jessup, S.D., 1998b, “Experimental Data for Panel Calculations and Comparisons (DTMB P4679)”, In 22nd ITTC Propulsion Committee Propeller RANS/Panel Method Workshop Proceedings, Gindroz, B., et al., eds.
- Jessup, S.D., Boswell, R.J., 1982, “The Effect of Hull Pitching Motions and Waves on Periodic Propeller Blade Loads”, 14th SNH, Ann Arbor.
- Jessup, S.J., Wang, H.-C. 1996, “Propeller Cavitation Prediction for a Ship in a Seaway”, DTMB Report CRDKNSWC/HD-1282-01.
- Jiang, C.-W., Dong, R., Liu, H.-L., Chang, M.-S., 1996, “24-Inch Water Tunnel Flow Field Measurements During Propeller Crashback”, 21st SNH, Trondheim.
- Jiang, C.-W., Huang, T.T., Ng, R., Shin, Y.S., 1991, “Propeller Hydrodynamic Loads and Blade Stresses and Deflections During Backing and Crashback Operations”, Propellers/Shafting’91, Virginia Beach.
- Johannsen, C., 1998, “Investigation of Propeller Induced Pressure Pulses by Means of High-Speed Video Recording in the Three-Dimensional Wake of a Complete Ship Model”, 22nd SNH, Washington, D.C.
- Karafath, G., 1997, “U.S. Navy Ship-Model Powering Correlation and Propeller RPM Prediction”, Propellers/Shafting’97, Virginia Beach.
- Karafath, G., 1998, “Hydrodynamic Performance with Pod Propulsion – US Navy Experience”, 25th ATTC, Iowa City.
- Kawakita, C., Hoshino, T., 1998, “ Design System of Marine Propellers with New Blade Sections”, 22nd SNH, Washington, D.C.
- Kim, H.T., Kim, J.J., Stern, F., 1998, “Numerical Simulation of Turbulent Flow around a Marine Propeller”, Third Osaka Colloquium on Advanced CFD Applications to Ship Flow and Hull Form Design, Osaka.
- Kim, M.H., Glover, L.B., Mook, D.T., 1991, “Transient Analysis of Propellers”, Propellers/Shafting’91, Virginia Beach.
- Kinnas, S., Lee, H., Mueller, A., 1998, “Prediction of Propeller Blade Sheet and Developed Tip Vortex Cavitation”, 22nd SNH, Washington, D.C.
- Kinnas, S.A., Griffin, P.E., Mueller, A.C., 1997, “Computational Tools for the Analysis and Design on High-Speed Propulsors”, The International CFD Conference, Ulsteinvik.
- Kinnas, S.A., Pyo, S., 1997, “Propeller Wake Alignment Models”, Propellers/Shafting’97, Virginia Beach.
- Kodama, Y., 1998, “Scope of CFD for Computing Ship Flows”, Third Osaka Colloquium on Advanced CFD Applications to Ship Flow and Hull Form Design, Osaka.
- Korpus, R., Hubbard, B., Jones, P., Stromgren, C., Bennett, J., 1998, “Hydrodynamic Design of Integrated Propulsor/Stern

- Concepts by Reynolds-Averaged Navier-Stokes Techniques”, PRADS'98, The Hague.
- Koyama, K., 1993, “Comparative Calculations of Propellers by Surface Panel Method – Workshop Organized by 20th ITTC Propulsor Committee”, Papers of Ship Research Institute, Supplement No. 5.
- Kristensen, H.O.H., 1998, “Aspects of Propulsion and Manoeuvring Characteristics of Double Ended Ferries”, SVA-Forum, Potsdam.
- Krüger, S., 1998, “A Panel Method for Predicting Ship - Propeller Interaction in Potential Flow”, Ship Technology Research, Vol. 45, No. 3.
- Kuiper, G., “Cavitation Inception on Ship Propellers Models”, Ph.D. Thesis, Delft TU.
- Kurimo, R., Poustoshniy, V.A., Syrkin, E.N., 1997, “Azipod Propulsion for Passenger Cruisers”, NAV & HSMV International Conference, Sorrento.
- Lipis, V., 1975, “The Allowance of the Change of Averaged Propellers Characteristics at the Ship Motions in the Problem of Rough Sea Propulsion”, in Problems of Applied Hydrodynamics Sudostroenie, Leningrad.
- Liu, H.L. M.S., Chang, 1994, “PDV Measurement of Vortical Structures from a Large Model Sail/Sailplane Configuration”, Laser Anemometry Symposium: Advances and Applications, ASME Fluid Engineering Division Summer Meeting, Lake Tahoe.
- Liu, H.L, Fu, T., 1994, “PDV Measurement of Vortical Structures in the DTMB Rotating Arm Facility”, DTMB Report CRDKNSWC/HD-1416-02.
- Liu, Y.-H., 1995, “Prediction of Steady Propeller Performance with a Nonlinear Slipstream and Boundary-Layer Effect”, J. Ship Research, Vol. 39, No. 4.
- Liu, Z., Brennen, C.E., 1995, “Models of Cavitation Event Rates”, CAV'95, Deauville.
- Liu, Z., Brennen, C.E., 1996, “Cavitation Nuclei Population and Event Rates”, Paper prepared for the 21st ITTC Cavitation Committee.
- Lurie, E.H., 1993, “Unsteady Response of a Two Dimensional Hydrofoil Subject to High Reduced Frequency Gust Loading”, MIT Report 93-5.
- Maita, S., Ando, J., Nakatake, K., 1997, “A Simple Surface Panel Method to Predict Unsteady Marine Propeller Performance”, J. SNAJ, Vol. 182. (in Japanese)
- Maitre, T.A., Rowe, A.R., 1991, “Modeling of Flow around a Marine Screw Propeller using Potential Based Methods”, J. Ship Research, Vol. 35, No. 2.
- Matsumoto, N., Suemitsu, K., Kusakawa, Y., 1986, “Characteristics of Flow Field in Stern’s Neighborhood under Manoeuvring Motion”, J. KSNA, Vol. 201.
- McDonald, H., Whitfield, D., 1996, “Self-Propelled Manoeuvring Underwater Vehicles”. 21st SNH, Trondheim.
- Mewis, F., 1998, “Podded Drives im Vormarsch – hydrodynamische Aspekte”, Schiff & Hafen, Vol. 50, No. 11.
- Meyne, K.J., 1974, “The Effect of Steering Maneuvers on the Propeller Blade Stresses”, Int. Shipbuilding Progress, Vol. 21, No. 237.
- Min, K.S., Choi, J.E., Seo, H.W., 1997, “Flow Measurements on the Propeller Plane at Towing Tank Using Fiber Optics LDV”, Proceedings of China-Korea Marine Hydrodynamics Meeting, Shanghai.
- Mishima, S., 1996, “Design of Cavitating Propeller Blades in Non-Uniform Flow by Numerical Optimization”, Ph.D. Thesis, MIT.
- Mishkevich, V., 1997, “Flow Around Marine Propeller : Nonlinear Theory Based on Vector Potential”, Propellers/Shafting'97, Virginia Beach.
- Morgan, W.B., Silovic, V., Denny, S.B., 1968, “Propeller Lifting-Surface Corrections”, Trans. SNAME, Vol. 76.
- Moulijn, J.C., Kuiper, G., 1995, “The Influence of the Wake Model on Induced Velocities

- in the Propeller Plane”, PROPCAV’95, Newcastle upon Tyne.
- Pauchet, A., 1996, “Velocity and Turbulence in the Near Field Region of Tip Vortices from Elliptical Wings. Its Impact on Cavitation”, 21st SNH, Trondheim.
- Pellone, C., 1991, “Calculation of the Vortex Sheets Downstream of Propeller Blades Using Non-Linear Theory”, European Journal of Mechanics, B/Fluids, Vol. 10, No. 4.
- Pogozelski, E., Katz, J., Huang, T.T., 1996, “The Shoulder Wave Separation Generated by a Surface-Piercing Strut”, 21st SNH, Trondheim.
- Poustoshniy, A., Semionicheva, E., 1996, “Minerhunter: Choice of Propulsor with Improved Cavitation Characteristics at Positioning Mode”, Proc. of Conf. Navy & Shipbuilding Nowadays, Sec.A, Vol.2, St.Petersburg.
- Poustoshniy, V.A., Haberzettel, F.I., 1998, “Investigation of Flow Around Pushing Thrusters”, Proceeding of ISC’98, Section B, St. Petersburg.
- Pozharsky, A., 1986, “Computation and Decision the Optimal Configuration of Supercavitating Profiles”, In Improving Run, Seaworthy Qualities and Maneuverability of Ships, The Collection NTO, Sudostroenie, Leningrad. (in Russian)
- Praefke, E., 1997, “Reduction of Propeller-Induced Hull Pulses by Means of Unconventional Propeller Profile Sections”, Propellers/Shafting’97, Virginia Beach.
- Pylkkänen, J.V., 1998, “Incremental Resistance Coefficient of Fast and Large Vessels for Model Ship Correlation”, Int. Shipbuilding Progress, Vol. 45, No. 442.
- Pyo, S., 1997a, “Numerical Modelling of Tip Vortex Flow of Marine Propellers”, Journal of Ship and Ocean Technology, Vol. 1, No. 2.
- Pyo, S., Kinnas, S.A., 1997b, “Propeller Wake Sheet Roll-up Modeling in Three Dimensions”, J. Ship Research, Vol. 41, No. 2.
- Pyo, S.W., Suh, J.C., Kim, K., 1997, “Improvements on a Steady Panel Method for Propellers”, China-Korea Marine Hydrodynamics Meeting, Shanghai.
- Rood, E.P., 1997, “Critical Pressure Scaling of Schiebe Headform Travelling Bubble Cavitation Inception”, ASME FED-SM, Vancouver.
- Roussetsky, A., 1968, “Hydrodynamics of Controllable Pitch Propellers”, Sudostroenie, Leningrad.
- Sánchez-Caja, A., 1996, “Numerical Calculation of Viscous Flow Around DTRC Propeller 4119 for Advance Number Range 0.3-1.1 Using the FINFLO Navier-Stokes Solver”, Espoo, VTT Technical Report VALB141A.
- Sánchez-Caja, A., Pylkkänen, J.V., 1998, “Numerical Calculation of Viscous Flow Around an Old Icebreaker Propeller for a Wide Advance Number Range Using the FINFLO Navier-Stokes Solver”, Espoo, VTT Technical Report VALB306.
- Scherer, O., Stairs, R., 1994, “Propeller Blade Sections with Improved Cavitation Performance”, Propellers/Shafting’94, Virginia Beach.
- Schweighofer, J., 1997, “Evaluation of the Fully Turbulent Flow over a Flat Plate for a Large Range of Reynolds Numbers”, Ms.Sc. Thesis, Helsinki TU.
- Semionicheva, E., 1986, “Designing the Cascades of Profiles with Improved Cavitating Characteristics on the Required Range of Changing the Angles of Attack”, In Improving Run, Seaworthy Qualities and Manoeuverability of Ships, The Collection NTO, Sudostroenie, Leningrad. (in Russian)
- Shekarriz, R., Fu, T., Katz, J., Huang, T.T., 1993, “Near-Field Behavior of Tip Vortex”, AIAA Journal, Vol. 31, No. 1.
- Shekarriz, R., Fu, T., Katz, J., Liu, H.L., Huang, T.T., 1992, “Study of Junction and Tip Vortices Using Particle Displacement



- Velocimetry”, AIAA Journal, Vol. 30, No. 1.
- Shen, Y., Eppler, R., 1981, “Wing Sections for Hydrofoils - Part II: Nonsymmetrical Profiles”, J. Ship Research, Vol. 25, No. 3.
- Sluijs, M.F. van, 1972, “Performance and Propeller Load Fluctuations of a Ship in Waves”, Publication No. 1635 of the Netherlands Ship Research Center TNO.
- Stanier, M., 1998a, “Investigation into Propeller Skew Using a RANS Code, Part 1: Model Scale”, Int. Shipbuilding Progress, Vol. 45, No. 443.
- Stanier, M., 1998b, “Investigation into Propeller Skew Using a RANS Code, Part 2: Scale Effects”, Int. Shipbuilding Progress, Vol. 45, No. 443.
- Stanier, M., 1998c, “The Application of RANS Code to Investigate Propeller Scale Effects”, 22nd SNH, Washington, D.C.
- Stella, A, Guj, G., Felice, F.D., Elefante, M, 1998, “Propeller Wake Evolution Analysis by LDV”, 22nd SNH, Washington D.C.
- Stern, F., Zhang, D.H., Chen, B., Kim, H.T., Jessup. S.D., 1994, “Computation of Viscous Marine-Propulsor Blade and Wake Flow”, 20th SNH, Santa Barbara.
- Su, Y., Ikehata, M., Kai, H., 1997, “A Numerical Method for Designing Three-Dimensional Wing Based on Surface Panel Method”, J. SNAJ, Vol. 182.
- Takei, Y., Kadoi, H., Okamoto, M., Hoti, Y., Makino, M., 1987, “Experimental Study on the Ship Stern Wake in Waves”, Papers of Ship Research Institute, Vol. 24, No. 5.
- Takinaci, G.D., 1996, “A Wake Rollup Model for Heavily Loaded Marine Propellers”, Int. Shipbuilding Progress, Vol. 43, No. 435.
- Thomas, M., 1998, “A Pareto Frontier for Full Stern Submarines via Genetic Algorithm”, Student Paper, SNAME, Boston.
- Ukon, Y., et al., 1991a, “Measurement of Pressure Distribution on a Full Scale Propeller -Measurement on a Highly Skewed Propeller”, J. SNAJ, Vol. 170.
- Ukon, Y., Kudo, T., Yuasa, H., Kamiirisa, H., 1991b, “Measurement of Pressure Distribution on Full Scale Propellers”, Propellers/Shafting’91, Virginia Beach.
- Viot., X., Fruman, D., Deniset, F., Billard, J., 1998, “Numerical Simulation of Tip Vortices Roll-Up”, 22nd SNH, Washington, D.C.
- Wang, G.-Q., Xu, L.-X., Yang, C.-J., Tamashima, M., Ogura, M., 1992, “Unsteady Nonlinear Vortex Lattice Method for Prediction of Propeller Performances”, 19th SNH, Seoul.
- Wang, G.-Q., Yang, C.-J., 1997, “Propeller Performances under Transient Working Conditions”, Journal of Shanghai Jiao Tong University.
- Weitendorf, E.-A, Tanger, H., 1992, “Cavitation Correlation and Nuclei Investigations in Two Water Tunnels – Comparisons in the HYKAT and the Medium Size Tunnel”, Cavitation, IMechE International Conference, Cambridge.
- Xiong, Y, Qu, S.H., 1997, “A Method for Checking the Propeller Strength under Backing Condition”, Sixth Symposium on Propulsion and Cavitation (CSNAME).
- Yan, K., 1996, “A Summary of Study on Methods of Measuring Nuclei by Venturi”, Sixth CSNAME, Shanghai.
- Yang, C.J., Wang, G.-Q., Yang, J.M., 1997, “Numerical Prediction of the Steady Performance of Ducted Propellers”, China-Korea Marine Hydrodynamics Meeting, Shanghai.
- Zhu, C., Chen, Z. L., 1979, “The 3-Bladed JD CPP Series”, 4th Lips Propeller Symposium, Drunen.

APPENDIX 1: INTERPOLATION OF VISCOSITY (Supplement to 4.9-03-01-03)

The formula by Hardy for viscosity of salt water is

$$\mu_S = \mu_0 (K / (1 + 0.03338 T + 0.00018325 T^2)),$$

where



$K = 1.052$

$\mu_s =$ viscosity of salt water at $T^\circ \text{C}$

$\mu_0 = 0.01787$ poise, viscosity of fresh water at 0°C .

For intermediate values of salinity the viscosity is to be found by linear interpolation between fresh water and the (standard 3.5 per cent) salt water viscosity data.

The Propulsion Committee

Committee Chair: Dr. Jaakko V. Pylkkanen (VTT)

Session Chair: Dr. Hans Broberg (SSPA)

I Discussions

Contribution to the Discussion of the Report of the 22nd ITTC Propulsion Committee on a New Flat-Plate Friction Formula

by C.W.B. Grigson

The Committee cites new formulae, eqns. (3) and (4) for the planar drag coefficients C_F . Among future tasks they mention “*Validate new formulae for the flat plate friction line*”. By implication, eqns. (3) and (4) and the ITTC line itself are not satisfactorily validated. Experimentally and theoretically it has been shown that the form factor of streamlined bodies should scale with C_F , but unless a trustworthy expression for C_F is available for the analysis of model tests, neither the form factor nor the wave-making drag can be correctly determined.

At Madrid in 1957 DTMB asked that any new formula for drag coefficients should agree with the Schoenherr Line at the Reynolds numbers of the 6 m models and higher. The explicit equation of R.N. Newton does. So, the validity of the ITTC Correlation Line is really that of Schoenherr’s law.

A study of Schoenherr’s paper (1932) reveals that the form of his equation is that of von Karman’s law for c_f skin friction. Schoenherr’s line is purely empirical, its constants chosen so that it is placed satisfactorily amid a collection of scattered observations of C_F , all of which contain unknown edge effects. Above $R_n = 10^8$ there are 9 data which reach only to 4.5×10^8 . At R_n above 5×10^7 ,

the trend of the data is clearly above the Schoenherr Line. Unfortunately the form of von Karman’s equation is not right, because the correct equation was truncated and it can be shown today that the part excised is not negligible compared with the part retained. Thus the Schoenherr and ITTC equations are wholly empirical, based on measurements which trend above the line as R_n increases, and which extend only to modest Reynolds numbers. Use of the equations at ship scale is pure extrapolation not justified theoretically or experimentally.

In introducing eqns (3) and (4) Grigson (1993) discussed the problems of verification in some detail. It is argued that the only method is to compare a theoretical algorithm with measurements of skin friction. Towing of plates always involves edge effects which can not be accounted for. Skin friction experiments requires flows which accurately fulfill the assumptions of the theory. The flows must be time-mean two-dimensional at constant pressure from the trip to the measuring station. Trips should have very low drag. Satisfactory experiments are available from Gaudet (Figs. 1 & 2). C_F itself may be determined by moving-element balance or by Cole’s computer-based fits to the velocity profiles. Does the Committee not accept this?

The equations for c_f must be theoretical. The momentum lost across the thickness δ of the boundary layer at each station is calculated, using modern expressions for the velocity distribution extending from the surface to the time-mean edge at which $u(y) \rightarrow U$, the velocity of the free stream. This was the method used for the first valid estimates of C_F at ship scale, when Prandtl (1935)

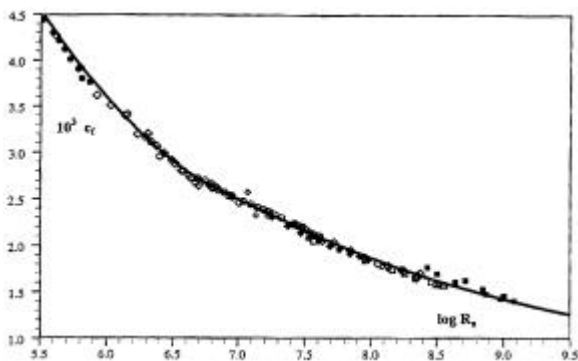
devised separate equations for $R_n(\delta)$ and for $C_F(\delta)$, although his profile did not include a wake term.

Do the Committee not accept calculations of c_f from momentum loss? Please would the Committee discuss their doubts of the foundations of equations (3) and (4), which are of course just representations of the results of a theoretical calculation based on momentum loss. What alternative methods would the committee advise? It should be borne in mind that numerical solutions of the Navier Stokes equations do not reach even ship-model scales. And that the RANS equations are approximate: they require mathematical models of the turbulence and empirical closure relations; the models are always very simplified; and the accuracy of the closure relations is seldom high. In reality, it is observation which is required to support the computations.

In work continuing Grigson (1993), analyses of c_f from momentum loss are now based on more accurate representations of the velocity profiles, which fit observations closely from the surface to the outer edge. As always, the wake component and its changes with R_n must be taken into account. The accompanying figures compare calculations with observation up to the scale of medium-sized ships. Agreement is within the accuracy of measurement, and leads to slightly modified versions of the equations (3) and (4).

References

- Grigson, 1993, Trans RINA.
 Prandtl, 1935, in Durand, ed., "Aerodynamic Theory", Vol. 3, pp. 145-150.
 Schoenherr, 1932, Trans SNAME.



$10^3 c_f$ versus $\log R_n$

Figure 1. Balance measurements: Dhawan, Gaudet, Moore and Harkness, Winter and Gaudet, c_f by Coles's method: Smith and Walker, Winter and Gaudet at Ma 0.2,

Wieghardt. The predicted changes in slope are closely observed.

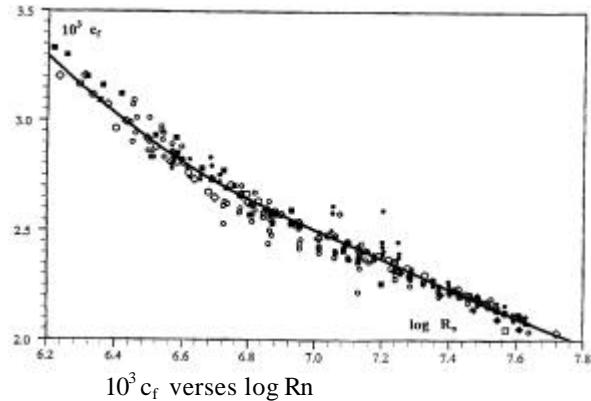


Figure 2. 17 measurements of Schulz-Grunow, and 221 measurements of Smith and Walkerall by balance added.

The ITTC 1978 Performance Method

by B.S. Bowden, Secretary of the 22nd ITTC Advisory Council

The 1978 ITTC Performance Method is based on using the 1957 ITTC Ship-Model Correlation Line with form factors. I was a member of the Performance Committee when the 1978 Method was developed but I now believe that it is scientifically unsound to attempt to derive form factors using the 1957 ITTC Line.

The 1957 Line was derived empirically, by adjusting the slope of the Schoenherr line, to improve the predictions of full-scale power and it is certainly not a two-dimensional skin friction line. There are a number of problems associated with the use of form factors but they will never be resolved satisfactorily until a two-dimensional skin friction line is used instead of the 1957 ITTC Ship-Model Correlation Line. In recent years Dr. Grigson has carried out extensive studies on the use of two-dimensional skin friction extrapolation lines and his work deserves to be carefully considered and evaluated.

US Navy Database of Speed Powering Trials

by G. Jensen, HSVA

The Committee reviewed that the US Navy database of speed powering trials indicates that for newer ships smaller C_A values would improve correlation. The conclusion was also that the improvements in surface quality cannot fully explain this change over time, so that there must be a hydrodynamic reason. Does the Committee have any idea as to which hydrodynamic effect that could be? Is it in the resistance scaling, the

interaction effects, or the scaling of the propeller open water curves?

Hardy's Formula for Viscosity

by G. Strasser, Vienna Model Basin, Chairman Quality Systems Group

My contribution concerns the determination of the viscosity. The Propulsion Committee has recommended to use Hardy's formula for salt water together with the tables for fresh water as accepted in by the ITTC in 1963. This involves a problem because the ITTC 1978 method uses a different formulation. In fact, the determination within the ITTC 1978 method should have been adjusted accordingly. If we adjust the method what difference in results might we expect?

Addition of Abstracts to Propulsion Database and the RANS/Panel Method Workshop

by Pengfei Liu, Institute for Marine Dynamics

It is obvious that the Committee has done a huge amount of work, over the wide scope of topics previously covered by three earlier committees. The report is informative and instructive.

The establishment of a comprehensive bibliography as a database covering publications over an extended period of time, not just the current ITTC period, is a very good initiative which other committees should follow. It is not clear from the format outlined on page 14 of the report if the database includes the abstract where one is available. The inclusion of abstracts would make the bibliographic database even more valuable. Perhaps with modern techniques for extracting information from other published databases, it may be practical for the Committee to do this.

The workshop on RANS/PANEL methods was very useful and such activities should become a regular feature of the work of ITTC technical committees. The comparisons, such as presented in Section 7.6 of the Committee report, represent snapshots in time. I am sure that partly as a result of the workshop, many participants will have revised and updated their calculations. A mechanism is needed to coordinate and present such revised data and information on the nature of revisions made. Perhaps this could be a job for the next committee?

This workshop demonstrated a practical application of the use benchmark experiment data as the basis for the comparisons. As a participant in the workshop it was evident that more work needs to be done on the format and supporting material associated with such benchmark data. The benchmark document should be standalone and include all the details of the experiment procedures and measurements and definitions of any technical terms not defined in the ITTC list of symbols. In this way it will be possible for all participants to be sure they are carrying out calculations for the appropriate conditions and remove the need to contact members of the committee or authors of earlier publications for clarification.

Finally, on a technical point, the first conclusion drawn from the comparative calculations (Section 7.5 #1) is not quite true. While it is well known that panel method predictions for K_T and K_Q are usually good for conventional propellers in the normal operating range of advance ratios (at service speed) such close agreement would not be expected if the propeller was working under very heavy loading conditions such as ice breaking or towing or operating in a duct. RANS and panel methods are very accurate only for lightly loaded propellers and for open propeller geometry. Under other operating conditions there may be a need to model boundary layer separation in RANS methods. In addition both RANS and panel methods may have some problems with complicated geometry such as the propeller-duct-rudder assembly, especially for the hydrodynamic prediction for the duct itself.

To support robust code development the Committee is encouraged to continue the comparative calculations to include more propeller geometry's and non-uniform flow conditions.

Contribution to Development in Panel Methods

by J. Bosschers, MARIN

The results of the 1998 RANS/Panel Method Workshop were very interesting and I would like to make some comments. It is concluded that the panel method can predict the pressure distribution on the propeller blade precisely for a propeller operating in uniform flow. However, no sections in the tip region have been investigated, although it is well known that most panel methods fail in the tip region. This has been the motivation for the flow aligned grid methods of Pyo et al (1997) and Georgiev et al (1997) which claim to calculate more accurately the circulation and pressure distribution in the tip region. It would have been interesting to also present in the workshop the pressure distributions in the tip region of propeller blades to get an idea about the accuracy of the different methods, even though no experimental data is available. In order to avoid grid problems, a suitable grid for blade and wake should then be provided. Comparing calculations on fully identical grids is generally very useful for comparing computational methods and avoids misinterpretations in the propeller blade geometry.

Panel Methods and Propeller Onset Velocity of Random Fluctuations

by U. Bulgarelli, I.N.S.E.A.N.

In the CFD analysis of propeller performance the onset flow field plays a role of prime importance. However, it is a fact that the onset velocity field that is determined in towing tank tests or by numerical simulations is not deterministic, but is affected by random fluctuations. It should not be impossible to develop a stochastic boundary element analysis method to properly account for this randomness (Song, 1973; Schuss, 1975). The result of a stochastic perturbation analysis should provide the average efficiency, thrust and torque, and their standard deviations in the case the statistical data of the wake can be provided. Is the Committee aware of any such work?

References

- Song, 1973, "Random Differential Equations in Science and Engineering", Academic Press, New York.
Schuss, 1975, "Theory and Applications of Stochastic Differential Equations", Wiley, New York.

Contribution to the Review of Research on the Performance of Propellers in Various Conditions such as for Ships when Turning, Accelerating, Decelerating, Backing or Operating in Waves

by T. van Terwisga, MARIN

It is concluded that the unsteady nonlinear vortex lattice method may be a promising tool for the estimation of propeller performance for ships when accelerating or decelerating.

This conclusion is somewhat surprising if one thinks of realistic acceleration times for (larger) ships in relation to accelerations in a seaway and if one keeps in mind the conclusion drawn on page 33 of the report where it is stated that the "unsteady forces on one blade computed in a quasi steady approach are in good agreement with the experiments".

It would be beneficial for those people involved in unsteady analysis, if the Committee could derive generic guidelines as to when an unsteady analysis is desired in favor of a quasi steady approach.

The Term "Cavitation Performance" and the Use of Steep Density Distribution

by G. Kuiper, MARIN

My question is if the term "cavitation performance" or "cavity performance" of a foil can be better defined. When an increase of inception speed or decrease of the inception index of a foil is meant there is no confusion. When an optimum lift/drag ratio of a section is meant, the problems begin when the foil cavitates. The calculation of the foil drag in cavitating conditions is still very difficult. In other cases the cavity performance is used for a wide bucket, suggesting that this mean less pressure fluctuations, which is not necessarily true. In yet another cases the thickness or another property is meant. How should the term "cavitation performance" be specified?

The recommendation of the Committee is that the whole nuclei spectrum should be measured at all times and that a "steep" density distribution should be generated at low tensile strength. My question is if this ensures absence of scale effects? In my opinion this may be true for sheet cavitation inception, but certainly not for bubble cavitation. (For sheet cavitation the density distribution is probably irrelevant.) I therefore doubt if it is useful to aim at a steep density distribution, the more since the Committee does not indicate how to obtain such a distribution.

A Criteria for Cavitation Pattern on Propeller Models

by Y. Kawanami, Y. Ukon and T. Kudo,
Ship Research Institute, Japan

Not only the inception but also sheet cavitation at shock free operation are strongly affected by water quality and Reynolds number. Observing the cavitation on propeller blade, it is clear that the cavitation pattern after inception is also significantly affected by propeller revolution rate or Reynolds number. The variation of cavitation pattern with Reynolds number has not been fully understood. Cavitation pattern is directly connected with propeller performance such as thrust, torque and efficiency, especially in the fully cavitating condition, that is, "transcavitating condition". Thus, the variation of cavitation pattern with Reynolds number should be focused on as the cavitation inception is intense. We made a series of experiments to verify the effect of Reynolds number on the variation of propeller performance and cavitation appearance using a conventional model propeller in a cavitation tunnel.

Experiments were made in the circular test section ($d = 750$ mm) of the Large Cavitation Tunnel at SRI. The blade profile of a model propeller was NACA profile and the boss ratio was 0.3. Propeller performances of thrust, torque and efficiency were measured identifying the advance coefficient at various propeller revolution rates. The tested cavitation number was kept to 1.021 throughout the test. The experimental conditions are shown in Table 1.

Table 1: Experimental conditions

J [-]	σ_v [-]	n_p [rps]	α/α_s [-] by D.O.meter
0.850	1.021	28 – 45	0.35
0.916		28 – 45	0.33
0.950		30 – 45	0.33

The measurement started from the lowest propeller revolution rate of 28 rps, increasing to 45 rps and then decreasing again. The measured results K_T , K_Q and η_O are shown in Figure 1. In the region of low Reynolds number, difference among the data for increasing rate and for decreasing rate was visible, which was due to cavitation hysteresis, while the difference in high Reynolds number regime was relatively small. Cavitation patterns at various Reynolds number

are shown in Figure 2. In Figure 2(a), a streak type of sheet cavitation was observed (indicated by the arrow) at 0.95R. This streak cavitation appeared and disappeared intermittently at the low Reynolds number. As the propeller

revolution rate increased, the period of the appearance of streak cavitation became long and in the high Reynolds number regime, the streak cavitation continuously attached to the blade leading edge. The cavitation which appeared at the blade root position was significantly affected by the revolution rate. When the revolution rate was 30 rps, traveling (bubble) cavitation appeared at the root (Figure 2(b)). The bubble cavitation evolved into transparent sheet cavity as the revolution rate increased to 40 rps (Figure 2(c)). This variation of cavitation pattern may be due to the transition of boundary layer on the blade surface.

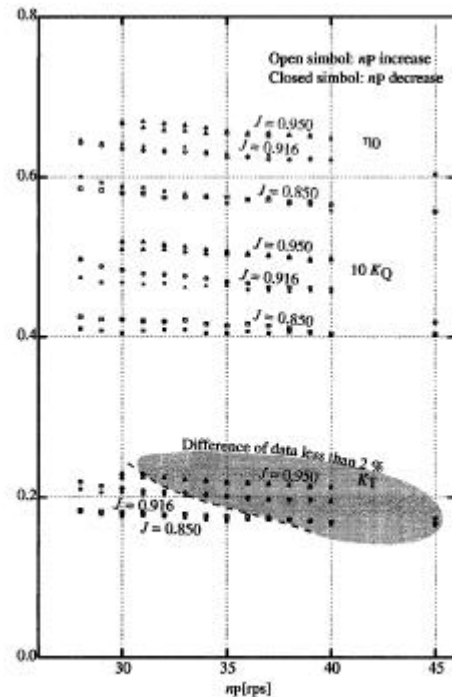


Fig.1: Variations of propeller performance with respect to propeller revolution and advance coefficient; M.P.No.411; $\sigma_v = 1.021$; $\delta = 0^\circ$

As discussed above, cavitation appearance varied with the Reynolds number at various radial positions. The cavitation hysteresis caused the differences of performance as mentioned above. In our research, we defined the propeller revolution rate at which the difference of performance became less than 2 % as the critical revolution rate. The critical propeller revolution rate for the case $J = 0.850, 0.916$ and 0.950 are 37, 33 and 31 rps, respectively. Figure 3 shows the variation of corresponding Reynolds number (Kempf) with

reference to the radial positions. At a given advance coefficient, the effects of Reynolds number and cavitation hysteresis are negligibly small when propeller test is made at sufficiently

Department of Marine Technology in this area. In the following a brief outline and summary of the findings of this research, which will improve the lack of knowledge associated with this important

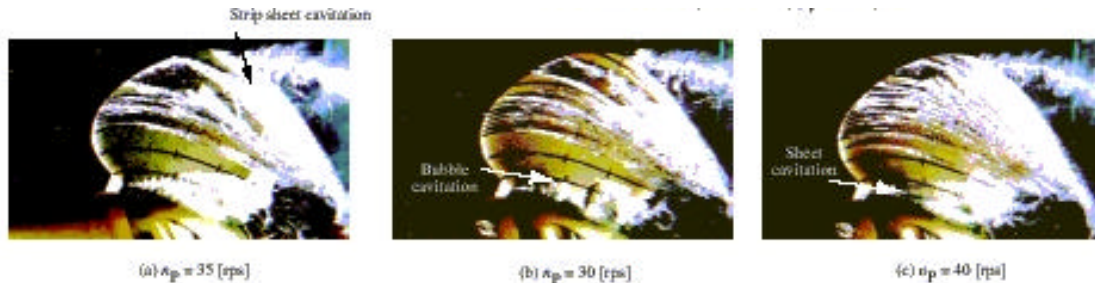


Fig.2. Cavitation patterns on suction side of blade (M.P.No.411); $J = 0.916$; $\sigma_V = 1.021$; $\delta = 6^\circ$

large Reynolds number (above the solid lines).

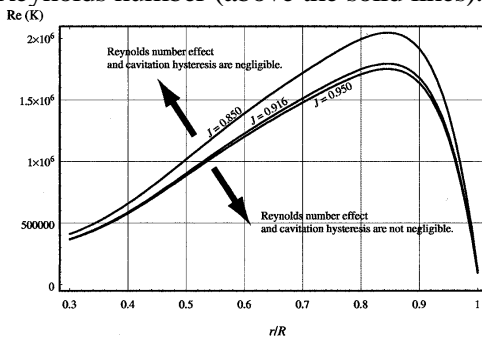


Fig.3: Reynolds number (Kempf); Each line represents 2 % thrust-down due to cavitation hysteresis at a given J .

Model propeller test should be made under condition which are free from the effect of Reynolds number and cavitation hysteresis. In addition, a criteria for cavitation pattern should be focused on so that reliable experimental results can be obtained.

The Importance of the Effect of Free-Stream Turbulence on the Inception of Cavitation of Marine Propellers

by E. Korkut, M. Atlar, University of Newcastle upon Tyne and A. Y. Odabasi, Technical University of Istanbul

INTRODUCTION

In Section 10 of their report to the ITTC, the Propulsion Committee conclude that "...It is not possible to quantify the influence of turbulence and blade roughness and research in this area is needed." I totally agree with their conclusion and pleased to report on a recently completed postgraduate research completed at the

topic, is presented.

Scale effect phenomena in the inception of cavitation and noise of marine propellers are the main problems in predicting the inception of cavitation and noise from model testings of propellers, particularly in cavitation tunnels. The factors contributing to the phenomena are mainly associated with the viscous nature of the flow, dynamics of bubble and effects of the gravity (ITTC, 1987). Although the main emphasis of the Cavitation Committee of the 21st ITTC (1996) and the Propulsion Committee of the 22nd ITTC (1999) has been on the effects of the bubble dynamics, there is also another factor affecting the phenomena, in particular viscous scale effects-called free-stream turbulence- which should be investigated systematically. Within this context, in order to make a further contribution into the state-of-the-art understanding of the scale effect phenomena in the inception of cavitation and noise of marine propellers and improve the prediction methods, a postgraduate research programme has been recently completed (Korkut, 1999). Early results of the investigation were presented in Korkut et al. (1998). Due to the requirements for sophisticated seeding mechanism and measuring equipment, a thorough investigation into the effect of the bubble dynamics has been excluded for the time being in this research study. However, the effect of the dissolved gas content has been included in the tests and its effect has been explored as one of the main variables contributing to the inception phenomena.

EXPERIMENTAL SET-UP AND TEST CONDITIONS

Experiments were carried out in three groups at the Emerson Cavitation Tunnel (ECT), which has a large rectangular test section with the cross-section dimensions of 1.22 m by 0.81 m (BxH). The first group tests involved the mapping of the free-stream turbulence characteristics of the tunnel water under the effect of varying levels of free-stream turbulence. The second group was the cavitation inception measurements of a rectangular planform hydrofoil under the effect of systematically varying levels of the free-stream turbulence and leading edge roughness applied at the leading edges of the foil. The third group included the similar cavitation inception measurements with a model propeller under the effects of the same parameter as well as dissolved gas content.

Free-stream turbulence levels of the tunnel at the test section were varied by using three different size of wire meshes attached to a hydrofoil support frame, which was located at a distance of 827 mm from the vertical plane where the flow measurements were taken. The flow measurements in the axial and transverse directions were taken using two-dimensional DANTEC LDA facility at a grid area of 350 mm x 380 mm in the measuring plane over a range of the tunnel water speed (1-7 m/s). See Table 1 for the mesh sizes used and the results of the free-stream turbulence intensity at $U=4$ m/s. Details of the measurements and analysis for the turbulence intensity levels can be found in (Atlar and Korkut, 1997).

Table 1. Mesh sizes used in tests and results of free-stream turbulence measurements at $U=4$ m/s

Turbulence generator type	Cell size (BxHxD) in mm	Free-stream turbulence intensity (%)
Base Frame	-	3.273
Largest-sized mesh	25.4 x 25.4 x 1.0	3.752
Medium-sized mesh	12.7 x 12.7 x 1.0	3.958
Finest-sized mesh	6.36 x 6.36 x 1.0	4.466

The hydrofoil used for the cavitation inception measurements was a rectangular planform foil ($c = 250$ mm x $b = 300$ mm), which had a cross-

section of NACA66-004, $a=0.8$ (modified) mean line, as shown in Figure 1. The model propeller was 5 bladed, right-handed and moderate skew Meridian type propeller with a diameter of 240 mm which can be seen in Figure 2. In order to alter the boundary layer characteristics of both test bodies, carborundum was used as the artificial roughness element. For the hydrofoil, the carborundum grains were applied over a narrow strip with a beam, which was equal to a 4% of the chord length, at the leading edge and both sides of the foil by using a polyurethane varnish as a glue. The similar exercise was also carried out for the model propeller by using an adhesive resin. The sizes of the roughness heights applied were 35, 60 and 100 μ m.

During the hydrofoil tests, the angle of attack of the hydrofoil was set to five different values, which were -4° , -3° , -2° , 5° and 6° . Relatively large values were preferred to prevent the high vacuum and tunnel velocities, which made observations difficult. By using the above set up and test procedure, the inception measurements of the foil were taken for four different turbulence levels, (typical results of the turbulence levels at $U=4$ m/s shown in Table 1), four different levels of roughness and five different angles of attack. During these tests, the dissolved gas content level was kept at about 35% while the Reynolds number based on chord length varied between 0.6 to 1.3×10^6 . Because of the physical limitations of the cavitation tunnel, the hydrofoil had to be hanged vertically from the lid of the tunnel at the top. This orientation coupled with a relatively thicker cross-section of the hydrofoil prevented to measure a clear inception of the tip vortex cavitation. This was because that the foil section near the stock had a maximum thickness, which was nearly double the maximum thickness of the original cross-section due the strength requirements. This triggered early inception of the cavitation at the top, which was further complicated by the combined boundary layer of the lid and the foil. As a result, it was not possible to record a realistic tip vortex cavitation. Under this circumstance, it was only possible to record the inception for the sheet cavitation at a suitable reference line, which was marked on the foil outside the fillet area, as shown in Figure 1, at a distance of 140 mm from the top. Since the cavitation always developed from the top of the foil, the progress of the cavitation was allowed until the reference line. As soon as the cavitation extent

reached the reference line the corresponding condition was recorded as the inception point for the sheet cavitation at that level.

On the other hand, the test procedure for the inception of the propeller was such that the tunnel flow velocity, U , was kept at 4 m/s. The tunnel static pressure was adjusted to a constant value and the rotational speed of the propeller was initially increased until a visual appearance of tip vortex cavitation was observed. The rotational speed was then decreased until the tip vortex cavitation was just flushing (intermittent) at the tip of the propeller and this condition was accepted as the onset of “**unattached**” tip vortex cavitation. In addition to the unattached form of the cavitation, three more stages of the cavitation were observed and associated inception points were recorded. These phases were observed following the observation of the unattached tip vortex cavitation such that: in the first stage, the tip vortex cavitation “**attached to the one blade only**”; in the second stage, the tip vortex cavitation “**fully attached to all blades**”; and in the third stage, the cavitation was allowed to extend up to $0.8R$ radius in the form of “**sheet cavitation**”. Under the earlier defined set up conditions, the cavitation inception measurements were taken for the above described four stages of the cavitation for varying levels of free-stream turbulence and roughness at two different levels of the dissolved gas content, which were 20% and 44%.

DISCUSSION OF TESTS RESULTS

Foil Tests

Figures 3(a) and 3(b) show the results of the inception measurements of the sheet cavitation for varying levels of the free-stream, which are represented by the turbulence intensity(%), and for varying levels of roughness height, $k(\mu\text{m})$ respectively. In these figures, the inception number, σ_i , was defined based on the free-stream velocity, U , which was recorded by the tunnel’s pitot facility, as:

$$\sigma_i = \frac{P_{st} - P_v}{\frac{1}{2}\rho U^2} \quad (1)$$

where P_{st} is the static pressure at the reference point, P_v is the saturated vapour pressure and ρ is density of the water.

As shown in Figure 3(a), the inception numbers display a fairly linear increase with increasing level of the free-stream turbulence intensity over the entire range of the angle of attack except for -4° . On the other hand, there is a clear increase in the inception number with increasing roughness level up to $60 \mu\text{m}$, beyond which the inception number decreases with increasing the roughness size (Figure 3(b)).

Although the results are not included in this paper, further inception measurements were taken under the combined effects of the roughness and free-stream turbulence. The trend in these measurements was similar to those obtained in the isolated measurements (Korkut, 1999).

Based upon the trends described above and bearing in mind the exceptional inconsistency recorded at -4° of the angle of attack and at the maximum roughness height, there seems to be similar trend in the influence of the two different mechanisms, which are the free-stream turbulence and leading edge roughness, on the inception measurements. This is rather interesting because although the nature of the two mechanisms are different, both can influence the boundary layer characteristics on the foil surface and hence the inception with a reasonably similar trend.

Propeller Tests

Figures 4(a) through 4(d) show the results of the inception measurements of the tip vortex and sheet cavitation of the propeller for varying levels of the free-stream turbulence at differing levels of the dissolved gas content. In these figures, the free-stream turbulence is represented by the turbulence intensity(%) and the dissolved gas content ratio is represented by α_D/α_S . In the same figures, the inception number, σ_i , was defined according to the mean cavitation number based on resultant or relative velocity, V_R , as:

$$\sigma_i = \frac{P_{st} - P_v}{\frac{1}{2}\rho V_R^2} \quad (2)$$

where $V_R = \sqrt{U^2 + (0.7\pi ND)^2}$, N is the rotational speed of the propeller and D is the diameter of the propeller.

Depending upon the type of the cavitation stages observed, which are defined earlier, σ_i ,

σ_{TVIB} , σ_{TVAB} and σ_{SC} denote the inception numbers of the unattached tip vortex, the tip vortex attached one blade only, the tip vortex fully attached to all blades and the sheet cavitation respectively.

As far as the effect of the free-stream turbulence is concerned, there seems to be a linear trend for the unattached tip vortex cavitation at both levels of the dissolved gas content which is shown in Figure 4(a). While the free-stream turbulence level is increased, the inception number also increases. For the stages towards the sheet cavitation shown in Figures 4(c) and 4(d), the results do not demonstrate the same trend as observed for the stage of the unattached tip vortex cavitation. As the free-stream turbulence level is increased, the cavitation number increases until a critical value of the free-stream turbulence level, beyond which it appears to be insensitive to the change in the turbulence level. These findings are observed at the low level of the dissolved gas content. The difference in the trends between the inception characteristics of unattached tip vortex cavitation and the other stages perhaps can be related to the development of bubble, such that the bubble at the stage of the unattached tip vortex cavitation shows different characteristics than at the growth and collapse stages of the bubble (the stages towards the sheet cavitation). This implies that cavitation process should be investigated separately at each stage due to the different behaviour of the bubble at different stages.

The figures also display that the clear effect of the dissolved gas content on the inception of cavitation. An increase in the level of dissolved gas content causes a considerable increase in the cavitation number of the unattached tip vortex at each level of the free-stream turbulence. However, this trend changes with the stages of cavitation towards the sheet type indicating the importance of the combined effect of the free-stream turbulence and dissolved gas content.

Although further tests involving the combined effects of the roughness and free-stream turbulence have been carried out, the results of these tests are not included in this paper due to the space limit. However, these results also confirmed the effectiveness of the two mechanisms, on the inception of cavitation, particularly the effect of free-stream turbulence (Korkut, 1999).

PRACTICAL USE OF THE TEST RESULTS

The analyses of the measurements with the propeller, which also include the tip vortex cavitation, display useful trends for the effects of the turbulence and roughness (Korkut, 1999). These analyses provide further support on the similar type of influence of the free-stream turbulence and roughness affecting the boundary layer and hence inception of cavitation as partly observed in the foil tests. Therefore, it will be very interesting if there will be any meaningful correspondence, which can be devised through further analysis of the experimental data, between the level of free-stream turbulence and that of blade roughness height for the similar values of the inception measured. The confirmation and applicability of such a relationship could be extremely attractive providing an alternative mechanism for the turbulence stimulation, which is more sound and practical to compare to the cumbersome leading edge roughness technique.

Therefore, the inception measurements obtained with the propeller tests were further analysed and presented in Figures 5(a) through 5(d). In these figures, x-axis presents the relative integral length scale, $\Delta\Lambda_g$, which basically represents the turbulence level, while Δk is the relative roughness height. The expression of “**relative**” is preferred since there is a need for a reference turbulence level, which should be known, and $\Delta\Lambda_g$ is defined relative to this value. Based on the same analogy, Δk should be defined relative to a reference roughness level, which should be known.

In constructing the above figures, firstly the inception values, σ_i , which are obtained from the tests with varying values of the free-stream turbulence, are plotted against $\Delta\Lambda_g$ values and best curves fitted to these data. Secondly, the similar exercise is carried out for σ_i against Δk values based on the roughness tests. Using these two sets of plotting, the values $\Delta\Lambda_g$ and Δk , which induce the same inception number, σ_i , are plotted in Figures 5(a) through 5(d) for various stages of the cavitation at the low level of gas content.

As shown in these diagrams, there is rather linear relationship between the two parameters for the unattached tip vortex cavitation while this trend gradually changes from the linear to non-linear although the pattern of the curves are reasonably well behaved. Once again, the effect of the

dissolved gas content appears to be an important parameter influencing the pattern of these curves.

The practical value of the above diagrams can be justified on the basis that somehow cumbersome technique of the turbulence stimulation using artificial roughness on the blade surface can be replaced with a more sound way of changing the level of turbulence in the free-stream using a suitable turbulence generator. This type of diagrams will be very useful for facilities, which have long history with the roughness technique but to swap this technique with the turbulence generators in the free-stream, to establish their confidence in the use of latter technique.

It is also important that the systematic nature of the data presented in the paper, in the most plausible sense, can provide a basis for developing an extrapolator to be used for predicting the inception of cavitation on full-scale propellers if it can be combined with a semi-empirical model. Although the development of such extrapolator will require comprehensive correlation with model test measurements and information on the full-scale turbulence level, a pilot semi-empirical model has been developed by Korkut based on the test data presented here and Lighthill's rule (Korkut, 1999; Korkut et al., 1999).

CONCLUSIONS

Within the scope and limits of the systematic investigation carried out in this study, it is concluded that:

The free-stream turbulence has been confirmed to be one of the most important factors contributing to the scale effect phenomena beside other factors.

Based upon the analysis of the experimental measurements, there are similarities in the trends of the effect of the free-stream turbulence and that of the leading edge roughness on the inception of cavitation.

The previous conclusions suggest that it may be worthwhile to consider suitable turbulence generating techniques instead of the leading edge roughness techniques for more efficient turbulence stimulation on the propeller blades.

REFERENCES

Atlar, M. and Korkut, E., 1997, "Emerson Cavitation Tunnel Inflow Characteristics Based on

2-D Laser Doppler Anemometry Analysis", Department of Marine Technology Report, University of Newcastle upon Tyne, Report No: MT-1997-001.

ITTC, 1987, "Cavitation Committee Report", 18th International Towing Tank Conference, Kobe, Japan.

ITTC, 1996, "Cavitation Committee Report", 21st International Towing Tank Conference, Trondheim, Norway.

ITTC, 1999, "Cavitation Committee Report", 22nd International Towing Tank Conference, Seoul, South Korea and Shanghai, China.

Korkut, E., 1999, "An Investigation into the Scale Effects on Cavitation Inception and Noise in Marine Propellers", Ph.D. Thesis, University of Newcastle upon Tyne, UK.

Korkut, E., Atlar, M. and Odabasi, A.Y., 1998, "Effects of Free-Stream Turbulence on Cavitation Inception of Marine Propellers", ASME Fluids Engineering Division Summer Meeting: Cavitation and Multiphase Flow Forum, Paper No: FEDSM98-5056, Washington D.C., USA.

Korkut, E., Atlar, M. and Odabasi, A.Y., 1999, "On the Viscous Scale Effects in Cavitation Inception of Marine Propellers", 3rd ASME/JSME Joint Fluids Engineering Conference, Symposium on Cavitation Inception, Paper No: FEDSM99-7297, San Francisco, California, USA.

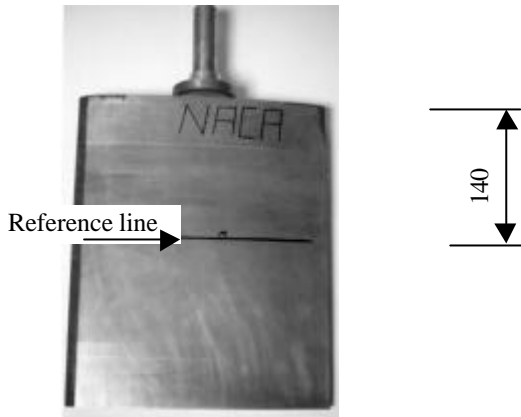


Figure 1. A general view of the rectangular planform foil with 35 μm roughness showing the marked reference line

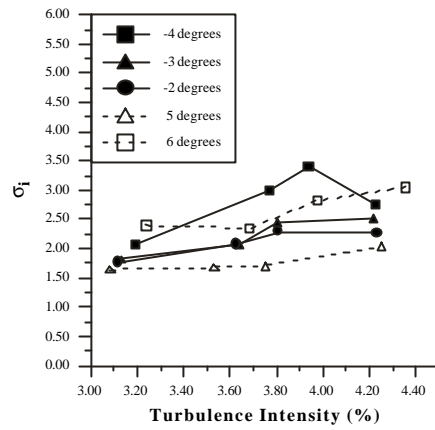


Figure 2. Model propeller used in tests

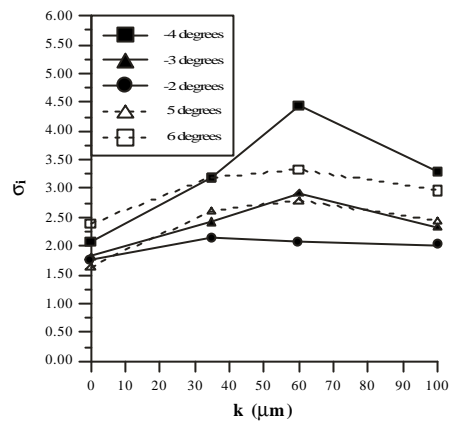


Figure 3. Comparison of cavitation inception numbers for varying angle of attack of NACA foil against: (a) free-stream turbulence level; (b) roughness height

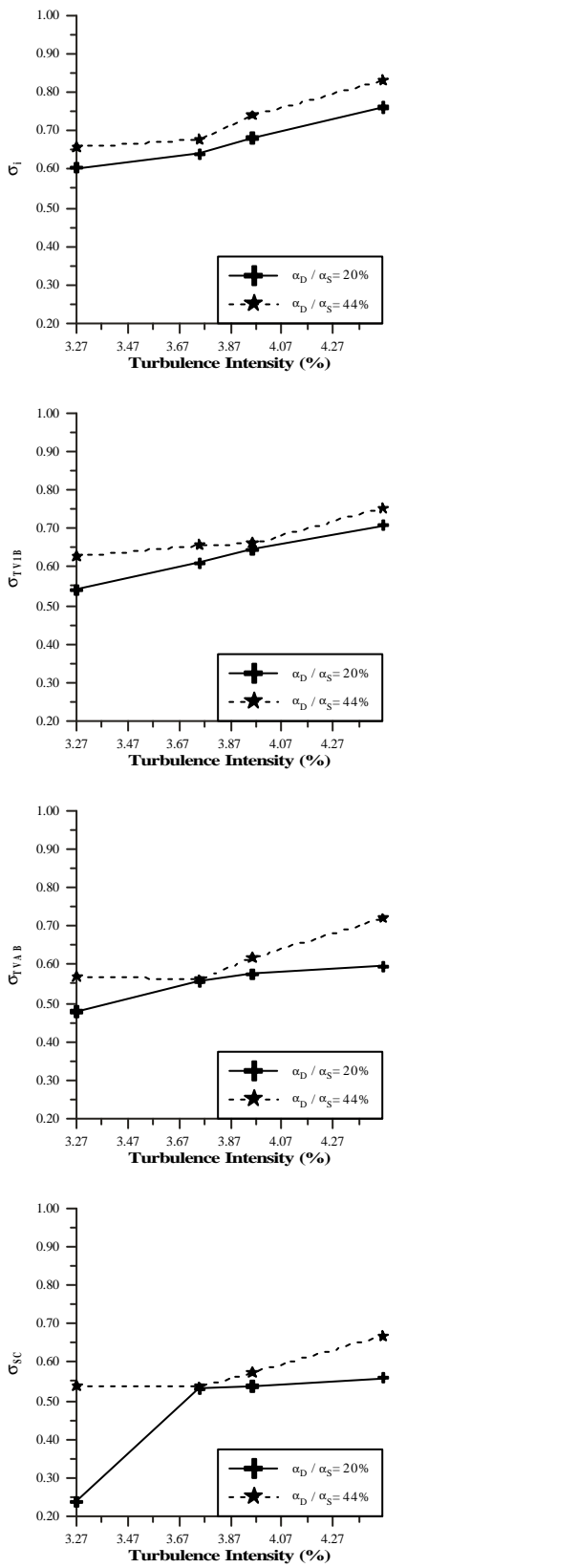


Figure 4. Comparisons of inception number of: (a) unattached tip vortex; (b) tip vortex attached to one blade only; (c) tip vortex fully attached to all blades; (d) sheet cavitation, against level of free-stream turbulence

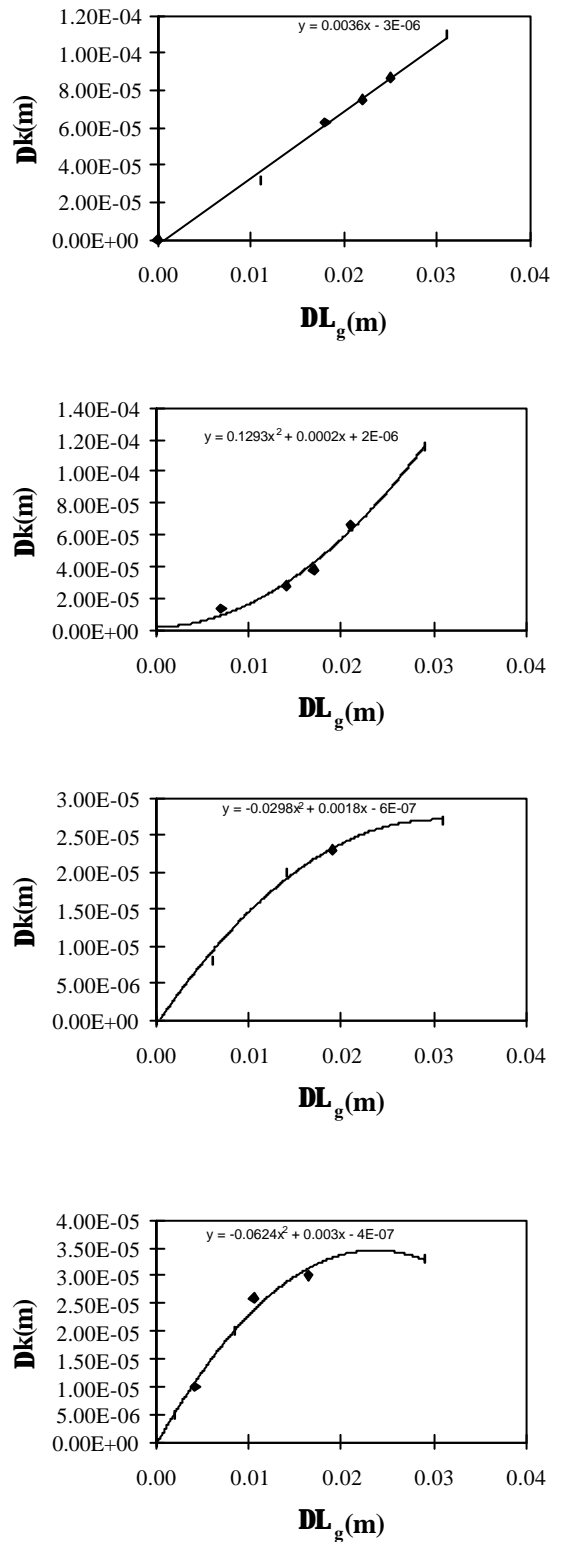


Figure 5. Plots of Δk against $\Delta \Lambda_g$ for: (a) unattached tip vortex; (b) tip vortex attached to one blade only; (c) tip vortex fully attached to all blades; (d) sheet cavitation, at $\alpha_D / \alpha_S = 20\%$

II Committee Replies

Reply of ITTC Propulsion Committee for Flat Plate Friction Formulae to Dr. Grigson

Dr. Grigson has put forward some challenging problems concerning the development and verification of the correctness of the formulation of the flat plate friction, which is still a basic element of the extrapolation of model experiments.

The Propulsion Committee does not share Dr. Grigson's viewpoint that the validity of the ITTC-1957 line is that of the Schoenherr line. The Committee is not convinced that the departure from reality is located in the high-Reynolds range where ITTC-1957 and the Schoenherr line agree. The disagreement between the two formulations at model Reynolds numbers, also for the 6 metre models at merchant Froude numbers, suggests that here a source of errors could well be present, the ITTC-line apparently being at a too high level and it being too steep. Inconceivably low form factors on small models and Dr. Grigson's own conclusions about the form factor variation in the results of geosim experiments corroborate this observation.

Dr. Grigson suggests, and he is right in doing this, that the introduction and verification of any other alternative to the ITTC-1957 formula would eventually become a matter for decision by authorisation. The Committee is convinced that the work of Dr. Grigson in this area should deserve full attention and that his formulation of the flat plate drag, condensed in 2 easy-to-handle formulae, could well form the basis for a new-generation flat-plate formulation.

Implementing a drastic change in the tools and related empirical coefficients used by the whole community of towing tanks is like changing some wheels in a clockwork which must be kept running! However sound the development of the alternative formulations may be, the Committee holds the opinion that anyhow, prior to introducing a major change in the basic elements of extrapolation of model test results, a thorough statistical verification of its claimed higher accuracy in model-to-ship extrapolation is needed on a large enough independent sample of good correlation data. This statistical verification should prove that the alternative is significantly better, indeed.

This verification, which has still to be made, should probably be similar as the basic procedure adopted in the development of the ITTC-1978 method by which it was shown that the dispersion in the correlation data diminished when a superior element was introduced in the extrapolation. Of course, such a vast exercise would involve the determination of new form factors and, hence, it is regarded a substantial task.

Reply of ITTC Propulsion Committee for the 1978 ITTC Performance Prediction Method to Mr. Bowden

The Committee agrees with Mr. Bowden that it is scientifically unsound to attempt to derive form factors using the 1957 ITTC line.

The last three paragraphs in the above reply of the Committee to Dr. Grigson will also address Mr. Bowden's comments.

Reply of ITTC Propulsion Committee for US Navy Database of Speed Powering Trials to Dr. Jensen

Physical reasons can be put forward that the three factors, resistance scaling, interaction effects, and scaling of propeller open water curves, in addition to the surface quality may contribute to the fact that smaller C_A values are needed nowadays than in the 1960's and 1970's. Without examining the original data of Karafiath in detail the Committee would not like to try to estimate the relative importance of the three factors.

Reply of ITTC Propulsion Committee for Hardy's Formula for Viscosity to Dr. Strasser

The Committee is aware that the two formulae for viscosity contained in the ITTC-1978 method constitute an approximation of the actual data presented and adopted at the ITTC in 1963. The approximation for fresh water for temperatures in the range 9-25 degrees C is excellent, the maximum departure being less than 0.5 per cent. The approximation of the viscosity in the ITTC-1978 method for standard salinity sea water is quite reasonable over the range of temperatures from 10 to 30 degrees C, the maximum deviation being a little over 1 per cent in viscosity. Nevertheless, the use of the tabulated values and Hardy's formula is to be preferred for consistency reasons. The departure in predicted propulsive power by using the ITTC-1978 formulae instead



of the data adopted in 1963 will be less than 0.2 per cent for temperatures in the indicated ranges for typical model experiments.

Reply of ITTC Propulsion Committee for the Propulsion Database and the 1998 Workshop on RANS/Panel Methods to Dr. Liu

The Propulsion Committee agrees with Dr. Liu that the abstracts should be included in the bibliography. The compilation of the bibliography required so large an effort that the abstracts could not be included in the bibliography. The Committee doubts whether it would be worthwhile to add abstracts to the oldest references.

The Propulsion Committee feels that the theme for the next workshop of comparative calculations could be two fold, (i) to investigate the progress since the previous workshop, (ii) to investigate new features in the codes made possible by advances in the state-of-the-art. The tasks for the 23rd ITTC Propulsion Committee have already been specified. The tasks for the 24th ITTC Propulsion Committee will be specified at the 23rd ITTC Main Meeting. Possibly a workshop of comparative calculations could profitably be organised every fifth or sixth year.

Dr. Liu suggests that a benchmark document should be used for defining the input data for the calculations and the comparison of the results. The Committee agrees with this idea. There was some confusion in transferring and interpreting the propeller geometry and onset flow data in the 1998 Workshop. The best way to avoid such confusion is to use a standard benchmark document.

It is quite true that the prediction accuracy of RANS and panel codes is at its best at the design point of the propeller especially with regards to K_Q . From the point of view of practical propeller design, good prediction accuracy at the design point is a prime requirement. Therefore, the first conclusion (Section 7.5#1) is to be considered in the sense of "accurate for practical design task".

Reply of ITTC Propulsion Committee for Developments in Panel Methods to Dr. Bosschers

The Propulsion Committee agrees with Dr. Bosschers that the flow aligned grid approach is a useful method to calculate the circulation and

pressure distributions in the tip region more accurately. However, in the context of the 1998 Workshop it would be difficult to judge which computational result is the most accurate because the experimental data were not available for the three test propellers. Therefore, the pressure in the tip region was not compared in the Workshop.

The second point of Dr. Bosschers' discussion is that a suitable grid for blade and wake should be provided to avoid grid problems. The purpose of the 1998 Workshop was the comparative calculation of different RANS/Panel methods including the grid generation approach for the blade and wake. The grid generation approach for the blade and wake is very important to obtain accurate results and therefore should be considered in the comparative calculation. The optimum grid is likely to depend on the specific mathematical and physical models of a code such as the turbulence model of RANS methods, the flow aligned grid concept of panel methods, the geometry of the real vortex structure, etc. The Committee feels that a simple grid should not be specified in a comparative calculation. Certainly it is instructive and useful to perform comparative calculations with a predetermined grid or paneling, particularly when testing and developing a code.

Reply of ITTC Propulsion Committee for Panel Methods and Inflow Velocity of Random Fluctuations to Dr. Bulgarelli

The Committee recalls a paper by Sevik (1968) that presented an analysis method for the response of a propulsor to random velocity fluctuations. As a special application case of his theory Sevik predicted the force fluctuations on a propeller of low solidity having blades of high aspect ratio and operating in a homogeneous isotropic field.

Reply of ITTC Propulsion Committee for the Performance of Propellers in Various Conditions such as for Ships when Turning, Accelerating, Decelerating, Backing or Operating in Waves to Dr. van Terwisga

The conclusions of the Propulsion Committee for Task 6 were as follows:

- The unsteady vortex lattice method seems to be a promising propeller analysis tool for accelerating or decelerating ships.
- The time-accurate RANSE method will be the appropriate analysis tool for the complicated flow under backing.

Generally unsteady panel methods or time-accurate RANSE codes should be used for a propeller operating under the conditions of Task 6 of the 22nd ITTC Propulsion Committee.

In the Committee Report the Committee reviewed two papers where good correlation was reported for the quasi-steady analysis (Chevalier et al., 1995; Jiang et al., 1991). In their application case Jiang et al. considered only open water steady crashback (+ V_S , -n). The quasi-steady approach proposed by Chevalier (et.al.) is only related to the wake input to the propeller calculation for the case of ship operation in a seaway. For the case considered, the wave encounter frequency was low compared to the propeller rotation frequency. The wake was assumed to be frozen or fixed at any instant, in which propeller unsteady forces are calculated.

Reply of ITTC Propulsion Committee for the Definition of the Term "Cavitation Performance" and the Use of "Steep" Density Distribution to Prof. Kuiper

As was also pointed out by Dr. Liu the propulsor community needs to pay more attention to exact definitions and clear use of terminology. The term "cavitation performance" is to be used only when there will be no confusion with regards to its meaning. Possibly in most cases a qualification to the term "cavitation performance" will do. In the case of pressure fluctuations the wording could be "induced pressure performance".

ITTC technical committees and ITTC Quality Systems Group have been assigned the task to provide new terminology in response to advances in hydrodynamics. Ultimately, it is the responsibility of the researcher writing a report or a paper to define the terminology in such a way that there will be no scope for misunderstanding.

The conclusion of the Committee was that it is difficult to compare cavitation inception data from different research organisations because of the different ways of defining cavitation inception point. In this respect a steep density distribution is believed to result in an improvement. Even though it is very difficult to produce a steep density distribution, it is good to keep in mind that it is a goal to be aimed at. The effect of electrolysis is somewhat similar to that of the steep density distribution.

Reply of ITTC Propulsion Committee for the Criteria for Cavitation Patterns on Propeller Models to Dr. Kawanami, Dr. Ukon, and Dr. Kudo

The test described is a uniform flow experiment, in which the propellers operate at close to ideal angles of attack, at very small cavitation numbers. For these designs, cavitation extends from leading edge to trailing edge, and beyond the trailing edge. This type of cavitation is very different from typical merchant ship applications, where blades pass through large wake deficits.

The Committee agrees with the discussers conclusions as to the importance of Reynolds number in the initiation, growth and collapse of thin, full chord cavities. It will be the task of the next Propulsion Committee to review the Quality Manual procedures for cavitation pattern tests. Reviewing procedures for high speed propellers would be therefore be recommended.

Reply of ITTC Propulsion Committee for the Effect of Free Stream Turbulence on the Inception of Cavitation of Marine Propellers to Dr. Korkut, Dr. Atlar and Prof. Odabasi

The contribution, in fact the paper, of Dr. Korkut, Dr. Atlar and Prof. Odabasi forms a valuable supplement to Task 8 of the 22nd ITTC Propulsion Committee. In the paper the authors concluded that the free-stream turbulence is one of the most important factors contributing to scale effect phenomena and that there are similarities in the trends of the effect of the free-stream turbulence and that of the leading edge roughness on the inception of cavitation.

In Task 8 the Committee was specially asked to review the developments in the effects of turbulence and propeller blade roughness on cavitation behaviour. The Committee did not find any recent references addressing this topic. The first paper of the discussers on this topic was published in 1997. It was unfortunate that the Committee did not get a copy of this report.

A general point is that it would be of mutual benefit for the Committee and researchers, if researchers sent their laboratory reports to the technical committees for information. Otherwise it is often difficult to get hold of laboratory reports that get a limited distribution.



III Errata

In Section 4.6 Streamlined Appendages on page 26 " $\text{Beta}=\text{C}_{\text{FM}}/\text{C}_{\text{FS}}$ " should read " $\text{Beta}=\text{C}_{\text{FS}}/\text{C}_{\text{FM}}$ ".

In Section 4.7 Non-Streamlined Appendages on page 27 "with the possibility of deriving the increase in form factor from $\Delta\text{C}_{\text{TM}}/\Delta\text{C}_{\text{FM}}$. Here, $\Delta\text{C}_{\text{TM}}$ is the change in appendage drag coefficient over the tested speed range when the model frictional coefficient varies by $\Delta\text{C}_{\text{FM}}$ " should read "with the possibility of deriving the increase in form factor from $\Delta\text{C}_{\text{APPM}}/\Delta\text{C}_{\text{FM}}$. Here, $\Delta\text{C}_{\text{APPM}}$ is the change in appendage drag coefficient over the tested speed range when the model frictional coefficient varies by $\Delta\text{C}_{\text{FM}}$ ".

IV References in the Replies of ITTC Propulsion Committee

Sevik, M., 1968, "The Response of Propulsors to Turbulence", 7th SNH, Rome, 25-30 August 1968, pp. 291-313.